

Spring 1993

Application of adaptive bone remodelling theory to the motion segments of lumbar spine: a theoretical study

Gopi Seenivasan

Copyright © 1993 Gopi Seenivasan Posted with permission of the author.

This thesis is available at Iowa Research Online: <https://ir.uiowa.edu/etd/5699>

Recommended Citation

Seenivasan, Gopi. "Application of adaptive bone remodelling theory to the motion segments of lumbar spine: a theoretical study." MS (Master of Science) thesis, University of Iowa, 1993.
<https://doi.org/10.17077/etd.80s70cmr>

Follow this and additional works at: <https://ir.uiowa.edu/etd>

Part of the [Biomedical Engineering and Bioengineering Commons](#)

APPLICATION OF ADAPTIVE BONE REMODELLING THEORY TO THE MOTION
SEGMENTS OF LUMBAR SPINE: A THEORETICAL STUDY

by
Gopi Seenivasan

A thesis submitted in partial fulfillment of the requirements for the Master of
Science degree in Biomedical Engineering in the Graduate College of
The University of Iowa

May 1993

Thesis supervisor: Professor Vijay K. Goel

Engineering
T1993
.S453
cop. 2

Graduate College
The University of Iowa
Iowa City, Iowa

CERTIFICATE OF APPROVAL

MASTER'S THESIS

This is to certify that the Master's thesis of

Gopi Seenivasan

has been approved by the Examining Committee for the
thesis requirement for the Master of Science degree in
Biomedical Engineering at the May 1993 graduation.

Thesis committee: _____
Thesis supervisor

Member

Member

To my parents and friends

ACKNOWLEDGEMENTS

I would like to extend my sincere appreciation and gratitude to my advisor, Professor Vijay K. Goel for his continued confidence, advice and patience throughout this project. I also appreciate and extend my thanks to the thesis committee members, Professors Joon B. Park and Krishnan B. Chandran for offering their time and expertise for this thesis.

I extend my sincere thanks to the ICAEN computing facility and more specifically to the one connected to the Department of Electrical Engineering for its 24 hour access.

I also express my thanks to Stephany and other office staff of the Department of Biomedical Engineering for their support throughout my stay at the University of Iowa.

I am thankful to my friends for their help and time in several occasions during this thesis work.

TABLE OF CONTENTS

	Page
LIST OF TABLES.....	vii
LIST OF FIGURES	viii
CHAPTER	
I. INTRODUCTION.....	1
1.1 Background.....	1
1.2 Objective of Present Study.....	3
1.3 Outline of the present study.....	5
1.3.1 Two-Dimensional FE Models.....	6
1.3.2 Three-Dimensional FE Model.....	6
1.4 Thesis Arrangement.....	6
II. REVIEW OF LITERATURE.....	8
2.1 Adaptive remodelling theories.....	8
2.1.1 Strain theory of adaptive elasticity.....	9
2.1.2 Strain Energy Density theory of adaptive remodelling.....	12
2.1.3 Theory of Self Optimization.....	18
2.2 Other remodelling Studies.....	21
2.3 Comparison of Parameters as stimulus of bone adaptation.....	26
2.4 Remodelling related study on spine.....	27
2.5 Conclusions.....	28
III. METHODS.....	29
3.1 Remodelling theory used in the present work.....	29
3.1.1 Mathematical formulation.....	29
3.2 The Finite Element Models.....	31
3.2.1 Two Dimensional models.....	31
3.2.1.1. One motion segment Model.....	32
3.2.1.2. Two motion segments model.....	32
3.2.2 Three Dimensional FE model.....	39

	Page
3.3 Remodelling studies on 2D FE Models.....	39
3.3.1 Prediction of Normal shape and Structure - Type I study.....	39
3.3.1.1 Force and constraint conditions.....	39
3.3.1.2 FEM analyses.....	40
3.3.1.3 FORTRAN programs.....	40
3.3.1.4 The Schematic of the remodelling iterative sequence.....	44
3.3.2 Adaptive remodelling following nucleotomy - Type II study.....	48
3.4 Remodelling Study on 3D FE model.....	51
3.4.1 Prediction of Normal shape and Structure - Type I study.....	51
3.4.2 Remodelling study following Partial Nucleotomy -Type II study.....	54
3.4.3 Study of bone remodelling induced by stress shielding - Type III study.....	56
3.5 Summary.....	58
IV. RESULTS AND DISCUSSION.....	59
4.1 Different cases of adaptive remodelling study conducted.....	59
4.2. Results of adaptive remodelling study type I.....	59
4.2.1 Results of 2-dimensional 1 motion segment model.....	59
4.2.1.1 Discussion of the results.....	61
4.2.2 Results of 2-dimensional two motion segments model.....	68
4.2.2.1 Discussion of the results.....	68
4.2.3 Results of 3-Dimensional two motion segments model.....	69
4.2.3.1 Discussion of Results.....	74
4.3 Results of adaptive remodelling study type II.....	78
4.3.1 Results of 2D one motion segment model(type II study).....	79
4.3.1.1 Discussion of results.....	79
4.3.2 Results of 2-dimensional two motion segments model.....	83
4.3.2.1 Discussion of results.....	84
4.3.3 Results of 3-Dimensional two motion segments model.....	89
4.3.3.1 Discussion of results.....	89
4.4 Results of adaptive remodelling study type III.....	92
4.4.1 Discussion of results.....	93
4.5 General discussion on the studies and the results.....	96
4.5.1 Comparison of the three different models.....	97
4.5.2 Limitations.....	98
4.5.3 Usefulness and importance of the present study....	99

	Page
V. CONCLUSIONS.....	101
5.1 Present Study.....	101
5.2 Future work.....	102
APPENDIX I. PROGRAM FORT-I.....	104
APPENDIX II. PROGRAM FORT-II.....	117
APPENDIX III. PROGRAM FORT-III.....	134
REFERENCES.....	147

LIST OF TABLES

Table		Page
3-1	Details of 2-dimensional one motion segment FE Model.....	34
3-2	Details of 2-dimensional two motion segments FE Model....	36
3-3	Details of 3-dimensional two motion segments FE Model....	37
4-1	Summary of remodelling studies conducted.....	60

LIST OF FIGURES

Figure	Page
1-1. Vertebral bodies of 2 motion segments of spine.....	4
2-1. Comparison of theoretically remodelled surface of the sheep radius following ulnar ostectomy with the experimental results.....	11
2-2. Apparent density distribution in the proximal femur.....	14
2-3. Shape remodelling caused by different stems.....	15
2-4. Remodelling tendency in the presence of lazy zone.....	17
2-5. Remodelling solutions for single loading case.....	20
2-6. Remodelling solutions for multiple loading case.....	20
2-7. Predicted density distributions for the model with intimate bone/implant contact and for the model with a proximal gap.....	22
2-8. Predicted peri-acetabular density distribution achieved with multiple loads and single load.....	24
2-9. Shape optimization of pedicular bone screw.....	25
3-1. 2-dimensional, 1 motion segment finite element model.....	33
3-2. 2-dimensional, 2 motion segments finite element model.....	35
3-3. 3-dimensional, 2 motion segments finite element model.....	38
3-4. Schematic diagram showing computations of $U^i(t)$ for an external surface node 'i' of the cortical bone.....	42
3-5. Schematic diagram for remodelling iterative sequence.....	46
3-6. Flow chart showing the computations for Type I study.....	47
3-7. The initial 2-dimensional models with nucleotomy for the Type II study.....	49

Figure	Page
3-8. The flow chart showing the computations for Type II study.....	50
3-9. The initial 3-dimensional 2 motion segments model with partial nucleotomy for Type II study.....	55
3-10. 3-dimensional, 2 motion segments finite element model with stabilizer plate and a partial nucleotomy.....	57
4-1. External remodelling of 2D, 1 motion segment: Type I study	64
4-2. Distribution of Young's Modulus and Density, after internal remodelling of 1 motion segment model, Type I study.....	66
4-3. Total strain energy and Volume of 1 motion segment, Type I	67
4-4. External remodelling of 2D, 2 motion segment: Type I study.....	70
4-5. Distribution of Young's modulus and Density, after internal remodelling of two motion segments model: Type I study.....	71
4-6. TSE and Volume for the vertebrae of 2 motion segments, Type I....	72
4-7. External remodelling of 3D, 2 motion segments: Type I study.....	75
4-8. Distribution of Young's modulus and Density, after internal remodelling of 3D, 2 motion segments model: Type I study.....	76
4-9. Change of TSED with iterations on the 3D model, Type I	77
4-10. External remodelling following Nucleotomy of 2D, 1motion segment model: Type II study.....	80
4-11. Internal remodelling following Nucleotomy of 2D, 1motion segment model: Type II study.....	81
4-12. TSE and Volume of 1 motion segment model, Type II study.....	82
4-13. External remodelling following Nucleotomy of 2D, 2motion segment model: Type II study.....	85
4-14. Internal remodelling following Nucleotomy of 2D, 2motion segment model: Type II study.....	86
4-15. TSE and Volume of 2 motion segments model, Type II	87
4-16. External remodelling following partial nucleotomy of 3D 2motion segment model: Type II study.....	90
4-17. Change of TSED with iterations on the 3D model, Type II.....	91

Figure	Page
4-18. External remodelling following fixation of stabilizer plate on the partially nucleotomized 3D, 2 motion segments model: Type II study	94
4-19. Change of TSED with iterations on 3D model with plate, Type III ..	95
A-1. The local changes in SED at surface nodes.....	146
A-2. The local changes in SED of cancellous elements.....	146

CHAPTER I

INTRODUCTION

1.1. Background

Bone being a living tissue is known to respond to changes in loads over time. Both the inner(trabecular) structure as well as the shape of the bone adapt to the new loading environment. The adaptive tendency of the bone was first expressed by Wolff J., as early as 1869 after a series of careful observations, and is commonly known as Wolff's law of bone remodelling. The law states that a relationship exists between stress transfer and architecture in bones, and that bone is able to adapt its structure to the actual stress patterns. In other words that bone in the first place is an optimal structure relative to its mechanical requirements and secondly that bone is able to maintain an optimal configuration relative to alternative mechanical requirements. The alternative mechanical requirements or abnormal stress fields may be caused by changes in loading, creation of injury, external reinforcements, prosthetic replacements and degenerative changes due to aging. As a result of these altered stress patterns bone would engage in the process of remodelling whereby the local bone mass is adapted to the new environment.

The need for understanding and predicting the exact nature of remodelling behaviour of bone arises as a consequence of the following clinical reasons.

- 1) To improve and understand the long-term success of the orthopaedic surgical treatments involving implants ranging from reinforcement plates, stabilizing rods to several kinds of prosthetic replacement surgery such as Total Hip Arthroplasty. These

implants tend to cause altered stress fields which would result in the external(shape) and internal(structure) remodelling of the treated bone. In the altered stress field the stress levels in the bone adjacent to the implant would change(normally decrease) as part of the load is transferred through the implant and this may cause

- a) thinning of cortical bone thickness
- b) osteoporosis (abnormal rarefaction of cancellous bone)
- c) altered external shape of the bone

These could substantially weaken the bone and lead to failure in the long-term. By predicting these remodelling behaviour of bone the adverse changes in the bone may be countered by proper modifications in the implant design or the surgical procedures.

2) To predict and control the abnormal occupational biomechanical stress induced remodelling in the bones.

3) To predict age related degenerative change induced remodelling of bone such as the formation of osteophytes in the vertebral bodies associated with the disc degeneration and to employ treatment procedures to counter the effects of the remodelling.

Thus quantitative prediction of adaptive changes of bone, both internal and external, are essential towards attaining improved results in the surgical treatments.

Even though Wolff's law states the adaptive nature of bone, it could not be directly employed for the quantitative predictions of bone remodelling. Recently several researchers have developed remodelling theories involving mathematical descriptions for the quantitative prediction of the adaptive behavior of the bone.^[3,4,7,15] Different mechanical parameters which change their values under altered loading environments were employed in these remodelling theories as factors which act as stimulus for the adaptive remodelling process. Even though identification of the specific mechanical objectives or parameters that reliably stimulate the adaptive response under varied(or abnormal) stress fields is still elusive,(inspite of many morphological and experimental studies) some

parameters such as the Maximum Principal Stress, Strain Energy Density, etc. seem to govern adaptive bone responses better than others.^[3] To date, the research work in this area has largely focused on qualitative replication of a few generic remodelling patterns of direct clinical interest, although there is clearly great potential for advances in quantitatively accurate remodelling predictions.

Several researchers have applied these remodelling theories with one or more mechanical parameters governing adaptive bone responses to some specific cases such as

- a) the prediction of the trabecular architecture of femur to verify that bone is an optimal internal structure^[4,5,15]
- b) to reproduce the bone morphology of the natural acetabular region ^[22]
- c) to study the bone remodelling process following implant surgeries such as Total Hip Arthroplasty, Total Knee Replacement and those involving unbonded, press fit hip stems^[15,16]

These remodelling studies have been carried out as computer simulation procedures, in combination with the Finite Element Method of stress analysis applied to the appropriately developed models representing the respective bones. These predictions were found to be in agreement with the experimental results to a reasonable extent.

1.2 Objective of present study

The present work is aimed at applying the theory of adaptive bone remodelling for studying the processes of shape(external) and structural(internal) remodelling of a spinal motion segment. The shape and structure of the vertebra are highly intricate and is one of the main load transferring structures of the human body. Figure-1 shows vertebral bodies of two motion segments of spine^[1]. The vertebral body is made up of dense cortical outer

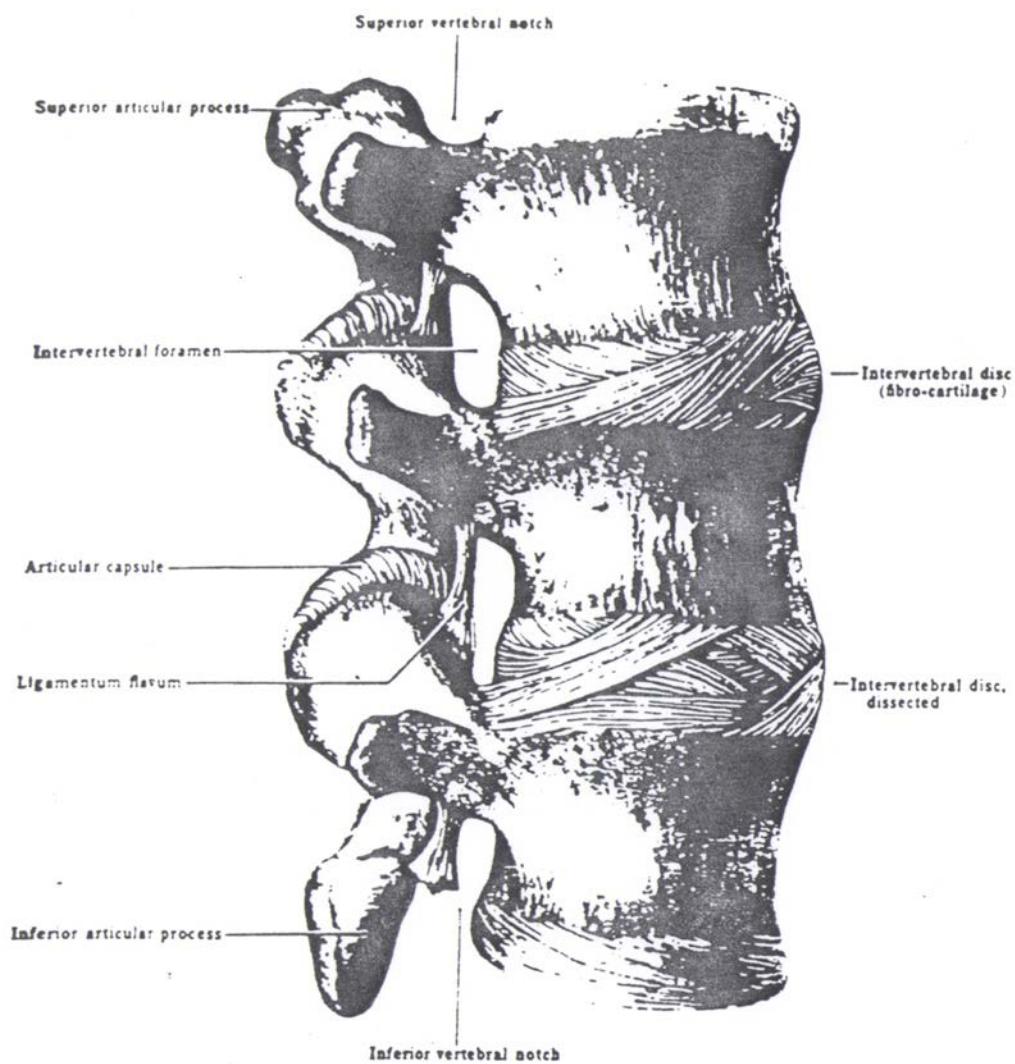


Figure 1-1. Vertebral bodies of 2 motion segments of spine^[1]

shell and trabecular cancellous bone within. The disc consists of annulus fibrosus and nucleus pulposus.

In addition to the function of transmitting the loads, the human spine also protects the spinal cord, which is of paramount importance for the muscular activities. Owing to these important functions any damage created on the vertebral column due to injury, overloading or defects caused by age related degeneration have to be treated to restore its normal function.

The use of spinal implants in surgery ranging from plates and screws to intervertebral rods to restore the stability of the vertebral column is ever increasing. There are also age related degenerative changes occurring in the spinal column such as degeneration of disc, rarefaction of cancellous bone, etc. The presence of spinal implants or any degenerative defects in the vertebral bodies would alter the stress field. As a result of this abnormal stress field the vertebral bone mass undergoes remodelling process involving shape and structural changes to optimize for the new environment.

The prediction of the adaptive bone remodelling behaviour of the vertebral body under the above mentioned conditions becomes highly important in order to understand the effects of surgery and age over time. This has created the motivation for the present study of predicting the adaptive bone remodelling behaviour of a spinal motion segment.

1.3 Outline of the present study

The adaptive bone remodelling theory with Strain Energy Density (SED) as the parameter governing the adaptive bone responses for both internal (structure) and external (shape) is used for studying the remodelling behaviour of the vertebral body of spinal motion segment. The study is carried out on 2-Dimensional and 3-Dimensional, simplified finite element models of the motion segments without posterior elements and ligaments.

1.3.1 Two-Dimensional FE models

Two dimensional FE models have been developed for one motion segment and two motion segments of the lumbar spine to study the adaptive remodelling behaviour. The study involves a.) Application of the adaptive remodelling theory to predict the optimized shape and structure under normal conditions (Type I study). This study will test the hypothesis that the vertebral body as a bone in the first place is an optimal structure by itself. Secondly, b.) prediction of remodelling behaviour leading to the osteophytic growth as a result of abnormal stress field induced by nuclectomy (Type II study). The nuclectomy was simulated by removing the elements representing the nucleus pulposus of the FE Model of the motion segments.

1.3.2 Three-Dimensional FE model

A 3-dimensional FE model was developed for the two lumbar motion segments for studying the adaptive remodelling behaviour. The study involves a.) application of the remodelling theory to arrive at the optimized shape and structure under normal loading conditions to verify the optimal nature of the vertebral body as a bone (Type I study). Secondly b.) prediction of remodelling behaviour leading to the osteophytic growth as a result of abnormal stress field induced by partial nuclectomy (Type II study). The partial nuclectomy was simulated by removing part of the elements forming the nucleus pulposus. Thirdly c.) prediction of adaptive remodelling behaviour leading to shape changes following the attachment of a plate to the vertebral bodies after partial nuclectomy (Type III study).

1.4 Thesis arrangement

The thesis is arranged in 5 chapters including the introduction. The Chapter 2 deals with the literature and explains the motivation and direction for the present work undertaken. Chapter 3 explains the methodology, the development of different finite element

models of spinal motion segments and the different FORTRAN programs developed and used for the remodelling study. In Chapter 4 the results of different adaptive remodelling studies conducted on different models are presented. Detailed discussion on the results are also included in this chapter. Chapter 5 reviews the objectives achieved and also discusses limitations of the study. The guidelines and directions for the future work on the remodelling study of spinal motion segments are also included.

CHAPTER II

REVIEW OF LITERATURE

2.1 Adaptive remodelling theories

Even though Wolff's law states the adaptive remodelling nature of the bone it could not be directly employed for the quantitative predictions. It does not mathematically relate the stress related mechanical parameters to the remodelling behaviour of bone. Motivated by the need for the quantitative prediction of adaptive remodelling of bone, several researchers have attempted to develop remodelling theories, involving mathematical descriptions, relating the altered stress fields to the remodelling behaviour of the bone. These theories in general are amenable to the computer simulation procedures in combination with the finite element method of stress analysis. These theories have been employed for the quantitative prediction of adaptive remodelling of bone. Different mechanical parameters which change their values under altered loading environments have been employed in these remodelling theories as factors which act as stimulus for the adaptive remodelling process.

The adaptive remodelling of bone, as mentioned in the introduction, includes both external and internal remodelling. The external remodelling deals with the change of shape of the bone. The internal remodelling deals with the change in the property of the cancellous bone, namely the Young's modulus, E , and in turn the density, ρ , as these two properties are related to each other (equation 2.9 gives the relation between E and ρ).

Different theories and associated experimental studies performed by the researchers are reviewed in the following section. It is of importance to mention here that these theories range from simple to complex based the type of loading conditions considered and the use of one or more mechanical parameters influencing the remodelling behaviour. The theories are presented in the order of increasing complexity.

2.1.1 Strain theory of adaptive elasticity

Cowin et al developed the theory of adaptive elasticity to explain the remodeling behavior of cortical bone.[7,8] This theory primarily attempts to describe the adaptive nature of the bone from one loading configuration to another, rather than predicting the optimal structure of the normal bone. In this theory it is assumed that the cortical bone tissue has a site-specific natural or homeostatic equilibrium strain state. A change of load, or, an abnormal actual strain state will stimulate the bone tissue to adapt its mass in such a way, that the equilibrium strain state is again obtained. The rate of adaptation is coupled to the difference between the equilibrium and actual strain rates. The internal and the surface(external) remodelling are separately modeled by the authors as follows. The elastic modulus(related to density) is made to adapt according to

$$\frac{dE}{dt} = A_{ij}(e_{ij} - e_{ij}^0) \quad (2.1)$$

where

E is the local modulus of elasticity, e_{ij} is actual strain tensor, e_{ij}^0 is the equilibrium strain tensor, and A_{ij} is the matrix of remodelling coefficients.

For the external remodelling the bone is assumed to add or remove material on the periosteal and endosteal surfaces, stimulated by the strain state at those surfaces, according to the following equation.

$$\frac{dX}{dt} = B_{ij} (e_{ij} - e_{ij}^0) \quad (2.2)$$

where X is a characteristic surface coordinate perpendicular to the surface. B_{ij} is a matrix of coefficients for external remodelling.

The first application of the theory of surface remodelling was to highly idealized models of mid section of a long bone in the shape of right circular concentric cylinders resembling a thick walled pipe. Cowin and Firoozbakhsh have analytically determined the remodelled shape of the hollow cylinder subjected to constant compressive loads.^[9] Hart et al have determined the remodelled shape for the above problem using finite element method [13,14]. Their predictions indicated that both the endosteal and periosteal surfaces moved as a result of remodelling.

Cowin and Hart have applied the surface remodelling theory to actual bone shape adaptation processes and established preliminary values for the remodelling rate parameters from the results of animal experiments performed earlier by different researchers that induced net bone remodelling in the animals. They include experiments by Jaworski involving disuse atrophy in young and old beagles, experiments by Woo et al in young pigs involving increased exercise activity which resulted in the net bone deposition on both endosteal and periosteal bone surfaces of the femora, and experiments by Lanyon et al in sheep involving ulnar ostectomy on their right limb while the left forelimb was used as control.^[17,19,27] Figure 2-1 compares the theoretically predicted remodelled surface of the sheep radius following the ulnar ostectomy with the experimental results. The theory could predict the surface remodelling behaviour of the radius reasonably well.

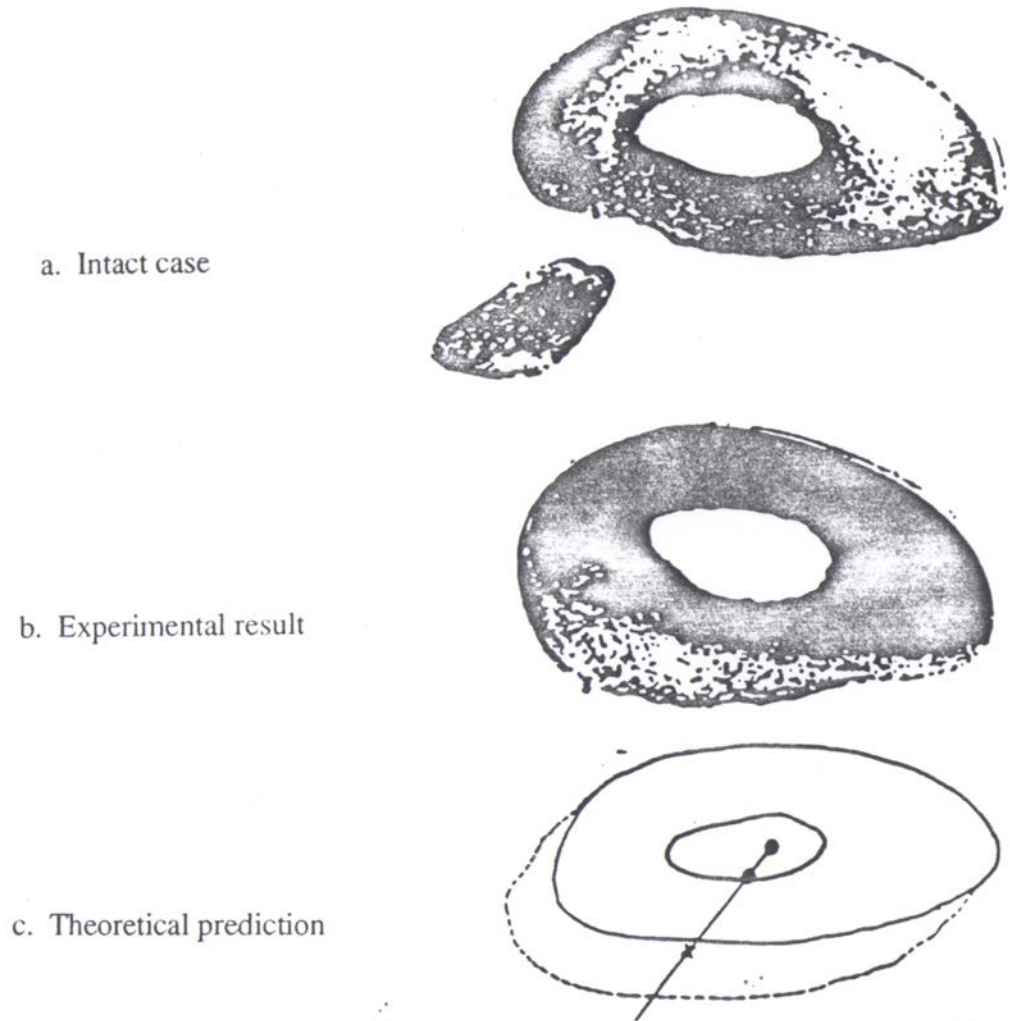


Figure 2-1. Comparison of theoretically remodelled surface of the sheep radius following ulnar osteotomy with the experimental results.^[8]

2.1.2 Strain Energy Density theory of adaptive remodelling

Huiskes et al developed an alternative formulation of adaptive bone remodelling theory which uses the Strain Energy Density (SED) as the feed-back control variable to determine the adaptive external and internal remodelling of bone to alternative functional requirements, whereby homeostatic SED distribution was assumed as the remodelling objective.[15] The remodelling theory was used in conjunction with a two dimensional finite element model.

The Strain Energy Density, SED is defined as Strain energy per unit volume at any region inside a stress field and can be written as,

$$U = \frac{1}{2} e_{ij} \cdot \sigma_{ij} \quad (2.3)$$

where σ_{ij} is the local stress tensor and e_{ij} is the strain tensor. The difference between the actual SED, U , and a site-specific homeostatic equilibrium SED, U_n , is assumed as the driving force for adaptive activity. The mathematical formulation of the theory can be written for Internal remodelling as,

$$\frac{dE}{dt} = C_e (U - U_n) \quad (2.4)$$

and for external remodelling as,

$$\frac{dX}{dt} = C_x (U - U_n) \quad (2.5)$$

where

$$\begin{array}{ll} \frac{dE}{dt} & \text{-rate of change of elastic modulus, E,} \\ \frac{dX}{dt} & \text{-rate of surface growth} \end{array}$$

C_e, C_x -remodelling rate coefficients

The above equations are transformed into finite difference formulations as follows

For internal remodelling

$$\Delta E = \Delta t C_e \{ U^i(t) - U_n^i \} \quad (2.6)$$

$i = 1, n$ where n is the number of elements

For external remodelling

$$\Delta X = \Delta t C_x \{ U^i(t) - U_n^i \} \quad (2.7)$$

$i = 1, m$ where m is the number of surface nodal points considered.

ΔE -change in the elastic modulus in one time step

ΔX -growth of the surface nodal point normal to the surface

Δt -period of one time step

The constants C_e and C_x determine the remodelling rate. As the values of these constants were not well established they were given arbitrary values. Hence only the final result of the remodelling process was considered realistic.

The authors applied internal remodelling simulation model to the classical problem of predicting density distribution in the proximal femur. The density of the bone was related to the Young's modulus as $E = 3790 \rho^3$. The initial FE model of the proximal femur had an uniform density distribution, and hence uniform elastic modulus. The elastic modulus was subjected to an upper bound of $E = 2.5 * E_{04}$.

Figure 2-2 shows the resulting apparent density distribution predicted in the proximal femur. The result had shown some similarity to the actual bone density distribution in the femur and the result compared well with those of Carter et al.[4]

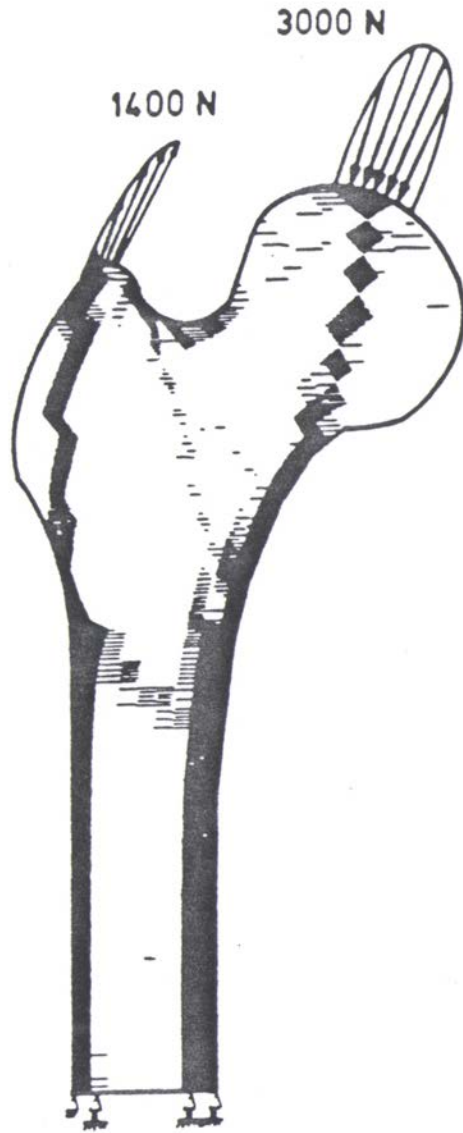


Figure 2-2. Apparent density distribution in the proximal femur^[15]

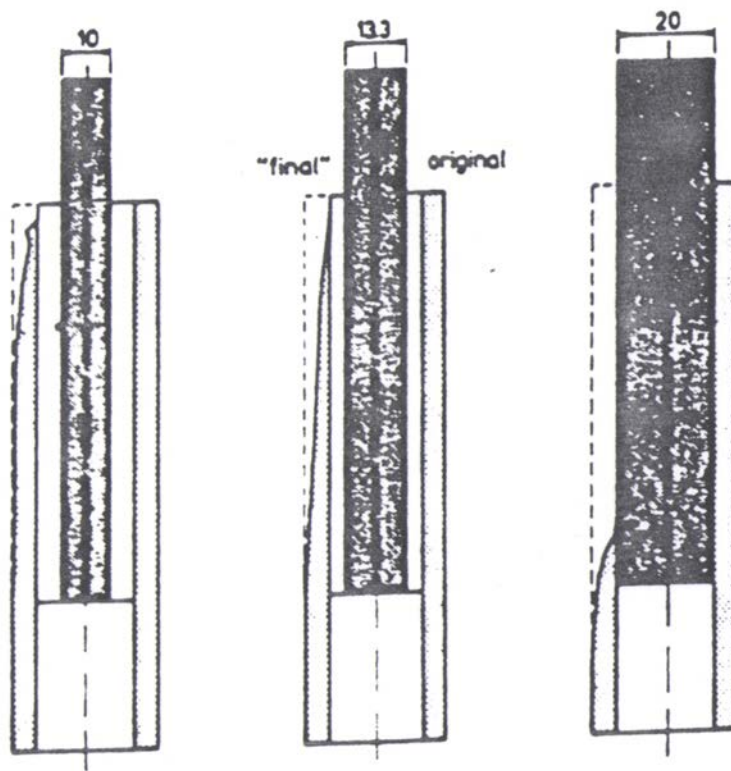


Figure 2-3. Shape remodelling caused by different stems^[15]

The above remodelling procedures were also applied to investigate the relation between stress shielding and adaptive external remodelling around an intramedullary prosthesis. A 2-Dimensional FE model was used to represent the intramedullary fixation. The internal and external remodelling were simulated separately. In the remodelling process it was assumed that bone adapts to the actual SED, after implantation, by remodelling its shape and density in such a way that the pre-implantation, homeostatic SED, U_n was obtained. In the case of internal remodelling the difference between the actual SED and the homeostatic SED of each element is used as a feed back signal to change the elastic modulus. In the case of external remodelling the SED in the surface nodal points is used to iteratively adapt the external surface.

The adaptive external remodelling process for the fixed intermediate stem is illustrated in Figure 2-3. As a consequence of the implantation of the stem, the SED at the surface of the bone is reduced relative to the natural value, U_n , in particular at the proximal side. The remodelling procedure makes the bone reach a homeostatic SED configuration after a wedge-formed volume of about half the cortex has resorbed.

The remodelling theory suggested by Huiskes in its alternate form takes into account an assumed 'lazy' behaviour of bone and incorporates certain threshold level(s) before the bone starts remodelling due to changes in the SED levels(U) compared to the homeostatic SED levels(U_n). Figure 2-4 shows the remodelling nature in the presence of the lazy zone. However, no study was conducted using this lazy zone by the authors.

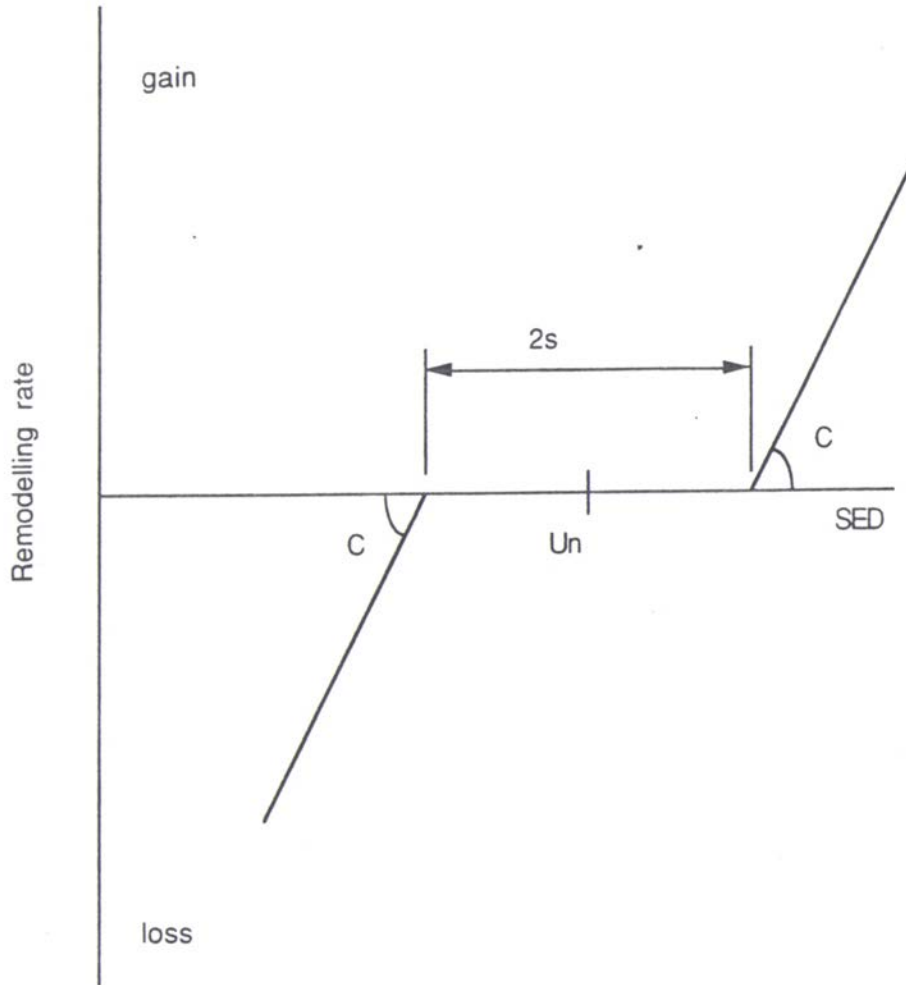


Figure 2-4. Remodelling tendency in the presence of lazy zone

2.1.3 Theory of self optimization

Fyhrie and Carter proposed a single optimization principle in which bone anisotropy (trabecular orientation) and apparent density (internal remodelling) are adjusted to optimize a function based on strength and stiffness criteria.^[4] This principle was implemented using finite element bone remodelling technique to predict the bone density distribution in the femoral head and neck when a loading condition representing the single-limb-stance phase of gait was applied. The remodelling revealed a density distribution which was consistent with that found in the normal femoral head.

Later Carter et al expanded the single load approach for predicting bone density to encompass the multiple-loading history of the femoral bone over a specified time period.^[6] In this approach the bone loading histories for an average day are characterized in terms of stress magnitudes or cyclic Strain Energy Density and the number of loading cycles. In other words the feed back control variable used is the effective stress derived from the Strain Energy Density. Relationships between local bone apparent density and loading history were developed which assume that bone mass is adjusted in response to the strength and energy considerations.

Carter et al hypothesized that the local apparent density of cancellous bone could be approximated by the relationship

$$\rho = K \left[\sum_{i=1,c} n_i \sigma_i^m \right]^{(1/2 m)} \quad (2.8)$$

where the daily loading history has been summarized as c discrete loading conditions and subscript "i" designates a specific loading condition, n = number of loading cycles.

σ = continuum model cyclic peak effective stress (scalar quantity)

ρ = apparent density

K and m are constants.

The effective stress is related to the Strain Energy Density as follows

$$\sigma_{\text{effective}} = \sqrt{2 E U}$$

where,

E = continuum model elastic modulus

U = continuum model Strain Energy Density

The relation between the elastic modulus and the apparent density of cancellous bone is given by,

$$E = 3790 \rho^3 \quad (2.9)$$

In the process of solving for the bone morphology the bone was considered to be isotropic and homogeneous structure in which the apparent density and modulus would subsequently vary as the remodelling process was carried out.

Initial properties of bone

$$E = 1000 \text{ MPa}$$

$$\rho = 0.64 \text{ g/cc}$$

The Strain Energy Density and the effective stress were calculated for each loading case. The remodelling was carried out for single and multiple loading histories and the resulting bone density distribution was predicted. Figure 2-5 shows the remodelling solutions for single loading case. Figure 2-6 shows the remodelling solutions for the multiple -load- direction stress history. The solutions have shown the consolidation of the

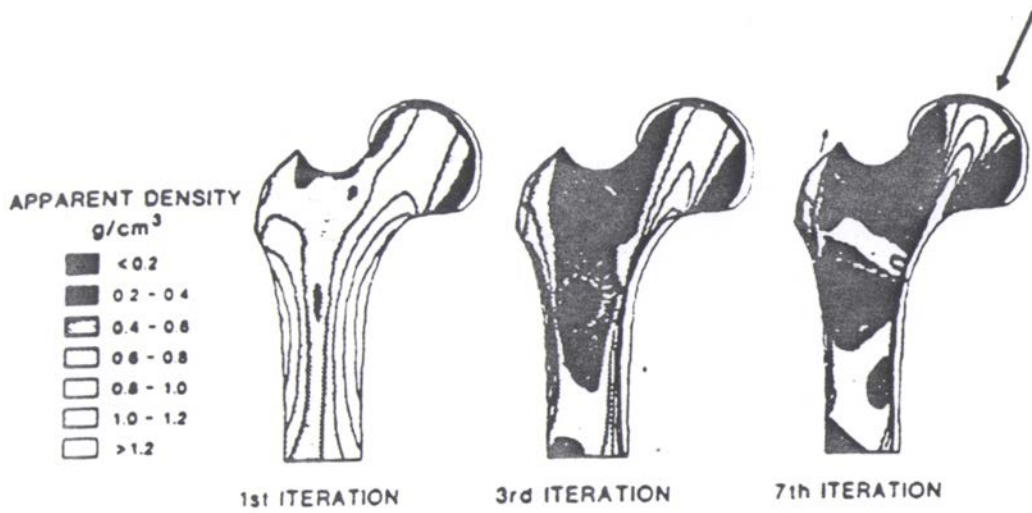


Figure 2-5. Remodelling solutions for single loading case^[4]

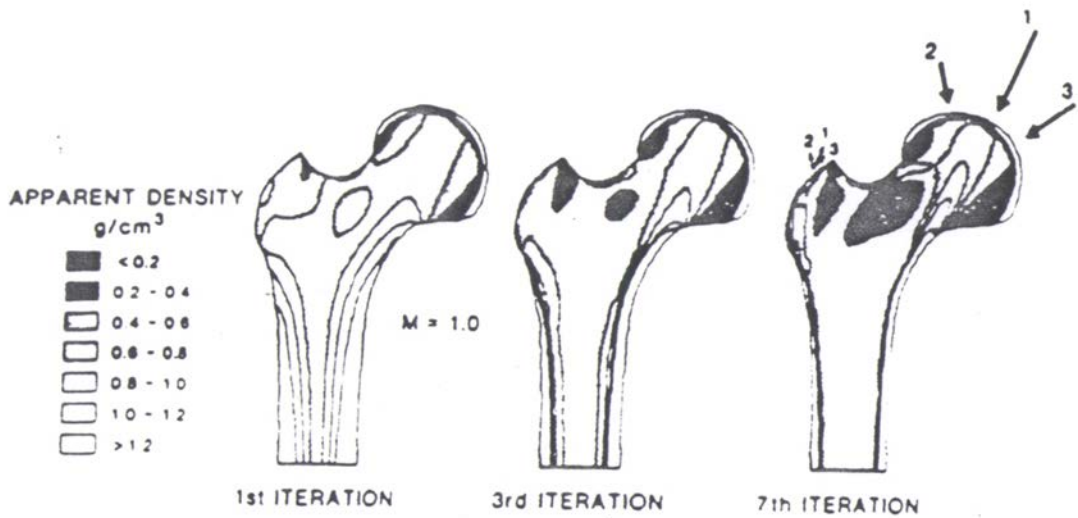


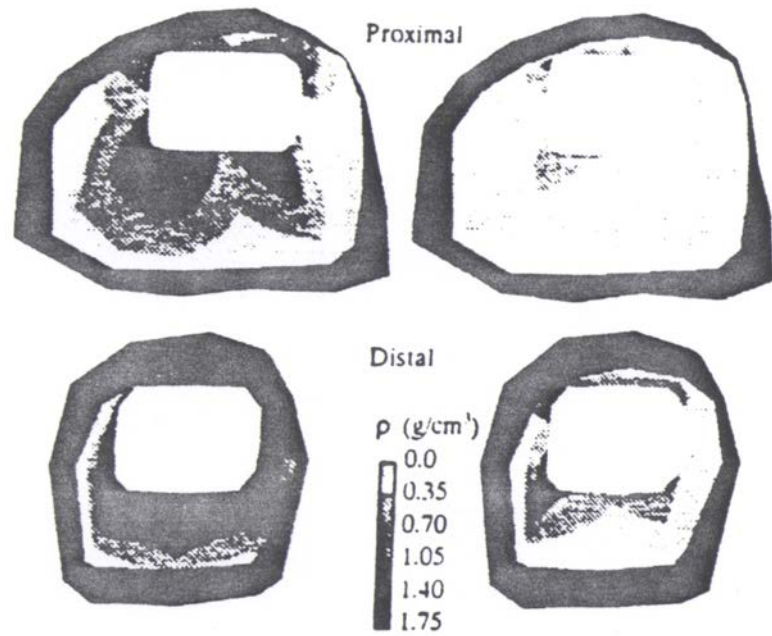
Figure 2-6. Remodelling solutions for multiple loading case^[4]

bone density which created a dense cortical diaphysis and a strong column of trabecular bone in the femoral head. The results were found comparable to that of the actual femoral bone architecture. It is important to note that the bone remodelling works carried out by Carter et al based on their theory of self optimization were mainly devoted to the prediction of bone morphology in long bones namely femur and not on the shape or external remodelling.

2.2 Other remodelling studies

Brown et al have carried out an extensive remodelling study with the objective of identifying the most reliable mechanical parameters governing the adaptive responses of bone.^[3] They formulated a complementary experimental- analytical approach, using an animal model with a well controlled mechanical environment combined with finite element modelling. They selected functionally isolated turkey ulna, for the loading could be completely characterized and the periosteal adaptive responses subsequently monitored and quantified after four and eight weeks of loading. Known loads were input into a 3D, linearly elastic FEM of the ulna. The FEM was validated against a normal strain-gaged turkey ulna, loaded *invivo* in an identical fashion to the experimental ulnae. They compared 24 candidate mechanical parameters to the quantified adaptive responses, using statistical techniques. The results suggested the Strain Energy Density (SED), tensile principal stress, and longitudinal shear stress as the parameters most likely related to the initiation of the remodelling response.

Huiskes et al^[16] have carried out simulation and experimental validation of bone remodelling around unbonded, press fitted hip stems. Two 3-D FE models were used one representing the immediate post operative configuration of the operated side, the other representing the control side. The same loads were assumed for the operated and the control configurations. The feed back control variable used for the remodelling simulations



a. Intimate bone/implant contact

b. Proximal gap

Figure 2-7. Predicted density distributions for the model with intimate bone/implant contact and for the model with a proximal gap^[16]

is the Strain Energy Density. The external and internal remodelling processes were carried out simultaneously. The results of the simulations were in agreement with those of the experimental ones, 2 years post operatively. Figure 2-7 shows the predicted density distributions for the cases of a.) model with intimate bone/implant contact and b.) model with a proximal gap.

Levenston [22] et al have employed a time dependent bone remodelling technique to reproduce the bone morphology of the natural acetabular region. Two alternative load histories on the acetabular surface were considered. The first corresponded to the single limb-stance phase of gait.. The second included additional load cases corresponding to peak loads during stair climbing and two more extreme activities such as rising from a chair. Initial homogeneous distribution of density throughout the model was assumed. The SED was used as the remodelling stimulus. Remodelling process was carried out by incrementally modifying the density and material properties of each element based on the combined stimulus(SED) from the total assumed load history. Figure 2-8 shows the periacetabular density distribution achieved with single and multiple loads.

Mattheck [24] et al carried out shape optimization study on the pedicular screw which is used in combination with an internal fixator for the transpedicular fixation of instabilities or fracture occurring in the spinal column. The optimization study was carried out in order to reduce the stress concentrations created by the screw having deep-thread profile with sharp flanks. The von Mises stress was used as the feedback control variable with objective of attaining homogeneous von Mises stress distribution. Figure 2-9 shows the shape of the optimized screw in comparison with the non-optimized one.

Thus in the recent past a number of theories for the quantitative prediction adaptive bone remodelling have been proposed and applied to the bone models, mostly finite element models, representing the structure and shape of the bones with appropriate loading

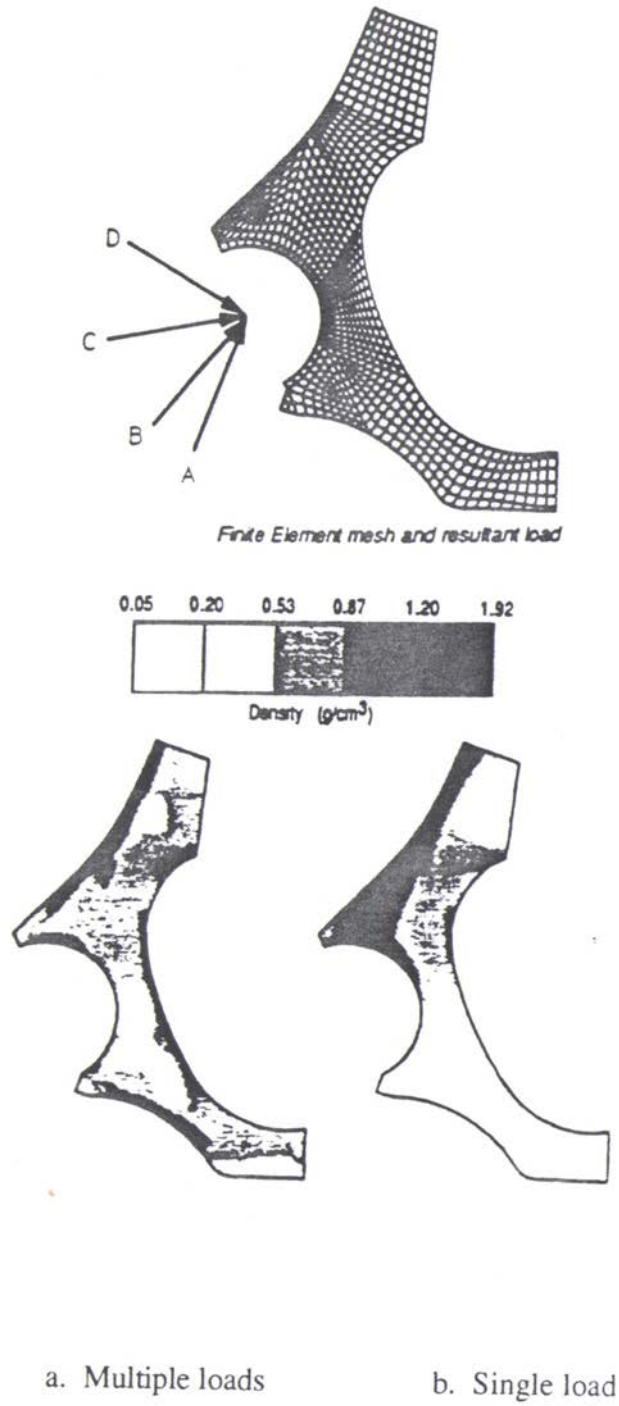


Figure 2-8. Predicted peri-acetabular density distribution achieved with multiple loads and single load [22]

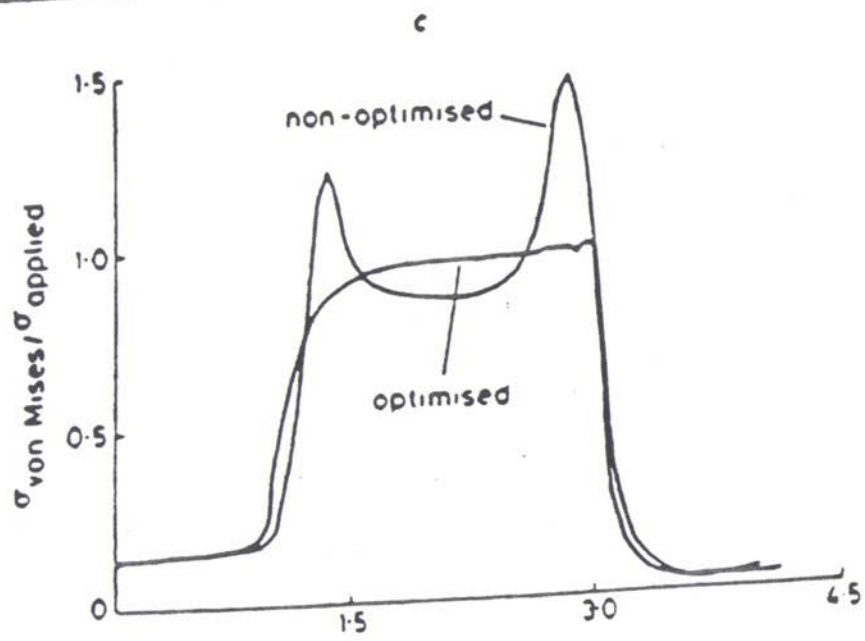
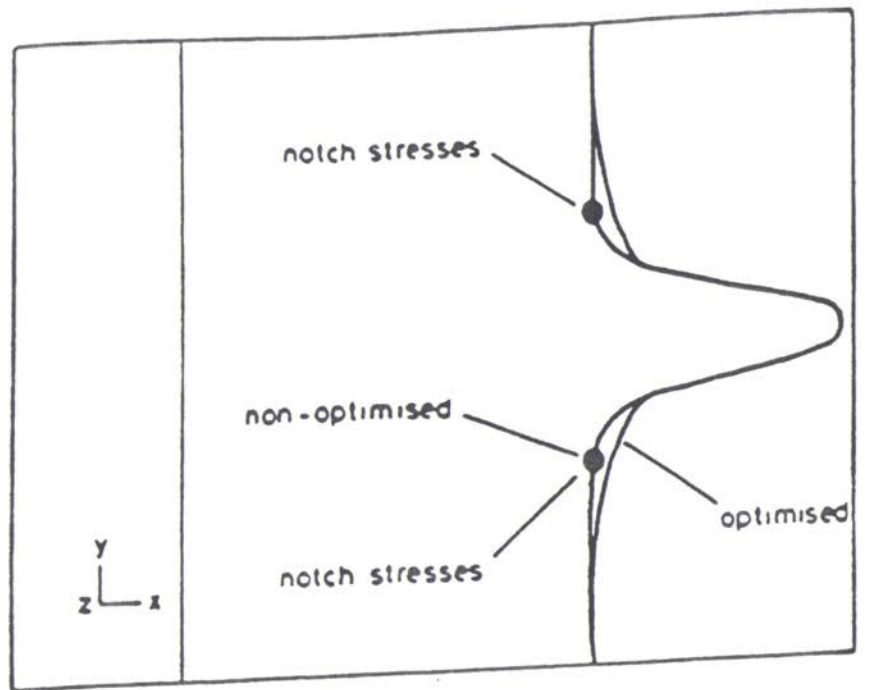


Figure 2-9. Shape optimization of pedicular bone screw^[24]

configurations. As mentioned earlier most of these bone remodelling prediction studies are applied to the long bones such as femur and ulna. The models were able to predict the bone morphology of the femur as an optimized structure(internal remodelling) and some models,namely by Huijkes and Brown were able to predict the post operative bone adaptation involving bone growth or absorption(external remodelling).

2.3 Comparison of parameters as stimulus of bone adaptation

Even though numerous remodelling theories, with different mechanical parameters as stimulus of bone adaptation, have been applied to study the remodelling behaviour of bone, the identification of the specific mechanical parameters that reliably stimulate the adaptive response under varying conditions remain elusive. It is possible certain parameters are more representative as a stimulus than the others under different conditions. Large quantum of research work involving experiments combined with the model analyses is required before identifying most representative parameters of stimulus for the adaptive response of bone.

In any case it is possible to compare the different parameters that have been used in the past by different researchers. The candidate parameters for comparison are Strain Energy Density, Principal Strain, Principal Stress and Effective Stress(derived from the SED). Cowin et al have used principal strain as the stimulus and applied to their adaptive remodelling theory. Effective stress is used as the remodelling objective by Carter et al for multiple loading history study on the prediction of femoral bone morphology. Strain Energy Density have been widely used by different authors namely Huijkes, Carter, Levenston and Brown for the prediction of both internal and external remodelling of bone. Principal stress was used as by Brown et al in the process of identifying the reliable parameters stimulating the adaptive bone response. Among these parameters the Strain Energy Density was stated to be a better reliable as suggested by different authors

namely, Huiskes, Brown, Tissakt, Carter, from the outcome of their studies. The use of SED is also more preferential because it is the representation of both basic mechanical parameters of stress as well as strain. As a result of this SED has been chosen to be the feed back control variable in the present work of application of adaptive remodelling theory to predict the remodelling behaviour of spinal motion segments.

2.4 Remodelling related study on spine

Lee et al have studied the osteophyte formation which are the secondary reactive process to primary degenerative changes of the spinal motion segments.[20] They hypothesized that osteophytes are formed purposefully to restabilize unstable motion segments that are caused by primary degenerative changes and that the size, shape and location of these osteophytes are, therefore, precisely determined by the nature of the primary instability. The authors conducted an in-vivo experimental study on thirteen coonhounds by dividing them into 3 groups and creating the following instabilities through surgery.

- a.) anterior annular incision and nucleotomy(Group I, n=3)
- b.) anterior nucleotomy and vertebral endplate decortication(Group II, n=5)
- c.) anterior nucleotomy, endplate decortication and insertion of an eccentrically placed spacer, 1 cm diameter elastomeric cylindrical rod.(Group III, n=5).

After the sacrifice of the animals after 3 months post-operatively the lumbar spinal motion segments were harvested and tested for mechanical stability under compressive and torsional loading. They found vertebral osteophyte formation in Group III and increase in stiffness compared to other groups and normal group(with no surgical instability) and demonstrated that vertebral osteophytes function in the restabilization of experimentally induced instability.

2.5 Conclusions

Different theoretical adaptive bone remodelling studies involving mathematical formulations and FE stress analysis, and the related experimental studies available in the literature have been reviewed. In general the theoretical prediction studies of bone remodelling are yet to attain considerable accuracy and a large quantum of information from experimental results exploring different possible remodelling situations are very much essential towards achieving that goal. Use of the right mechanical parameter for the right type of bone as the stimulus for the remodelling requires a huge body of research information from experiments. Nevertheless these theoretical prediction studies are the steps in the right direction towards accurate prediction of bone remodelling behaviour.

A large proportion of the theoretical adaptive bone remodelling studies were applied to bones that have simpler shape and structures such as femur, ulna and radius. The studies on intricate bone structures such as vertebral bodies of spinal motion segments are not available in the literature, except for a very few experimental studies on osteophytic formation and related studies. Nevertheless the bone remodelling studies on the spinal motion segments are very much essential considering the importance of stability of spine. This is the motivation for undertaking the present theoretical study of adaptive remodelling on spinal motion segments using FEM analysis. However, taking into account the above discussed problems such as the intricacy of the shape and structure of the vertebral bodies, and the preliminary nature of available adaptive remodelling methods of study, a step by step approach is imperative. As a first step simplified models of spinal motion segments without the posterior elements were subjected to the adaptive bone remodelling process. Based on the results obtained and the problems encountered during the process of the study, future directions and methods could be arrived at.

The Finite Element models developed and the methods used for the adaptive bone remodelling study on the spinal motion segments are presented in the next chapter.

CHAPTER III

METHODS

3.1 Remodelling theory used in the present work

In the present study the adaptive remodelling theory suggested by Huiskes et al, with Strain Energy Density (will hence forth be referred as SED) as the parameter governing the adaptive bone response, has been employed. The adaptive bone response in the present study include both internal and external remodelling behaviour of the vertebral body of the spinal motion segments. It is important to note here that in the present study the bone is assumed not to exhibit any lazy zone ($s=0$) during the process of remodelling. This assumption makes the remodelling behaviour of the bone be in linear relationship with the remodelling driving force.

3.1.1 Mathematical formulation

As mentioned earlier in section 2.2.3, for the present theory of adaptive remodelling, the driving force for the adaptive activity is the difference between the site specific homeostatic SED, namely U_n , and the actual SED at that site under abnormal stress field conditions. The mathematical formulation of the theory can be coupled with the corresponding finite element formulation of the spinal motion segment model as follows.

Internal remodelling

$$\frac{dE}{dt} = C_e (U - U_n) \quad (3.1)$$

where,

$\frac{dE}{dt}$	-	rate at which the elastic modulus, E, of the cancellous bone change during the period of adaptation
C_e	-	remodelling rate coefficient for elastic modulus
U	-	actual SED at an internal element of the FE model representing the cancellous bone
U_n	-	the site specific homeostatic SED at that element

External remodelling

$$\frac{dX}{dt} = C_x (U_i - U_n) \quad (3.2)$$

where

$\frac{dX}{dt}$	-	rate at which the surface of cortical bone grows perpendicular to the surface it self.
C_x	-	is remodelling rate coefficient for surface growth
U_i	-	is actual SED at a surface node of the FE model representing the cortical bone, which is computed as the average of the SEDs of the cortical elements connected by that node and the SEDs of the cancellus elements adjacent to them
U_n	-	is the site specific homeostatic SED at that node

The above rate equations are transformed into finite difference formulations using Newtons forward difference technique as follows.

For internal remodelling

$$\Delta E = \Delta t C_e \{ U^j(t) - U_n^j \} \quad (3.3)$$

$j = 1, n$ where n is the number of cancellous bone elements

Δt - constant time step between remodelling iterations

ΔE - change in the elastic modulus in one time step

For external remodelling

$$\Delta X = \Delta t C_x \{ U^i(t) - U_n^i \} \quad (3.4)$$

$i = 1, m$ where m is the number of surface nodal points

ΔX - change in the location of the surface nodal point

The constants C_e and C_x determine the remodelling rate. As the values of these constants are not well established they were given arbitrary values. Hence only the final result of the remodelling process is considered realistic. However, to insure stability of the iteration process, the time step Δt has been chosen adequately small. The chosen values for the products $\Delta t C_x$ and $\Delta t C_e$ are given below.

$$\Delta t C_x = 0.300 \text{ mm}^4/\text{J}$$

$$\Delta t C_e = 5.000 \text{ mm}$$

3.2 The Finite Element Models

Appropriate 2D and 3D finite element models of spinal motion segments were developed. Finite element stress analysis was carried out using these models. The SED values required in the remodelling equations were obtained through these analyses. The details of the FEM models developed for the remodelling studies are explained below.

3.2.1 Two Dimensional models

Two dimensional FE Models for one motion segment and two motion segments of the lumbar spine with simplified vertebral bodies were developed in order to carryout stress analysis.

3.2.1.1. One motion segment Model

The 2D finite element model for one motion segment of lumbar spine is shown in Figure 3-1. The dimensions of the model were selected from the finite element model for one motion segment of lumbar spine developed by Goel et al [23]. The model contains 2 successive vertebral bodies separated by the vertebral disc. The vertebral body has been modelled as having straight external edges without any curved shape. The vertebral body consists of dense but thin cortical outer shell and spongy cancellous bone in the interior. The disc consists of annulus fibrosus and nucleus pulposus. The type of elements and material properties selected for representing different constituents making up the motion segments and other details of the FE model are given in Table 3-1. [23] A total of 559 nodes and 180 elements were used in the FE model. The commercial finite element software package ANSYS was used for the analysis.

3.2.1.2. Two motion segments model

The two motion segments finite element model is shown in Figure 3-2. The model contains 3 successive vertebral bodies of lumbar spine each separated by the intervertebral disc. The type of elements and material properties [23] selected for representing different constituents making up the motion segments and other details of the finite element model are given in Table 3-2. A total of 1059 nodes and 294 elements were used to develop the model. The commercial finite element software package of ANSYS was used for the analysis.

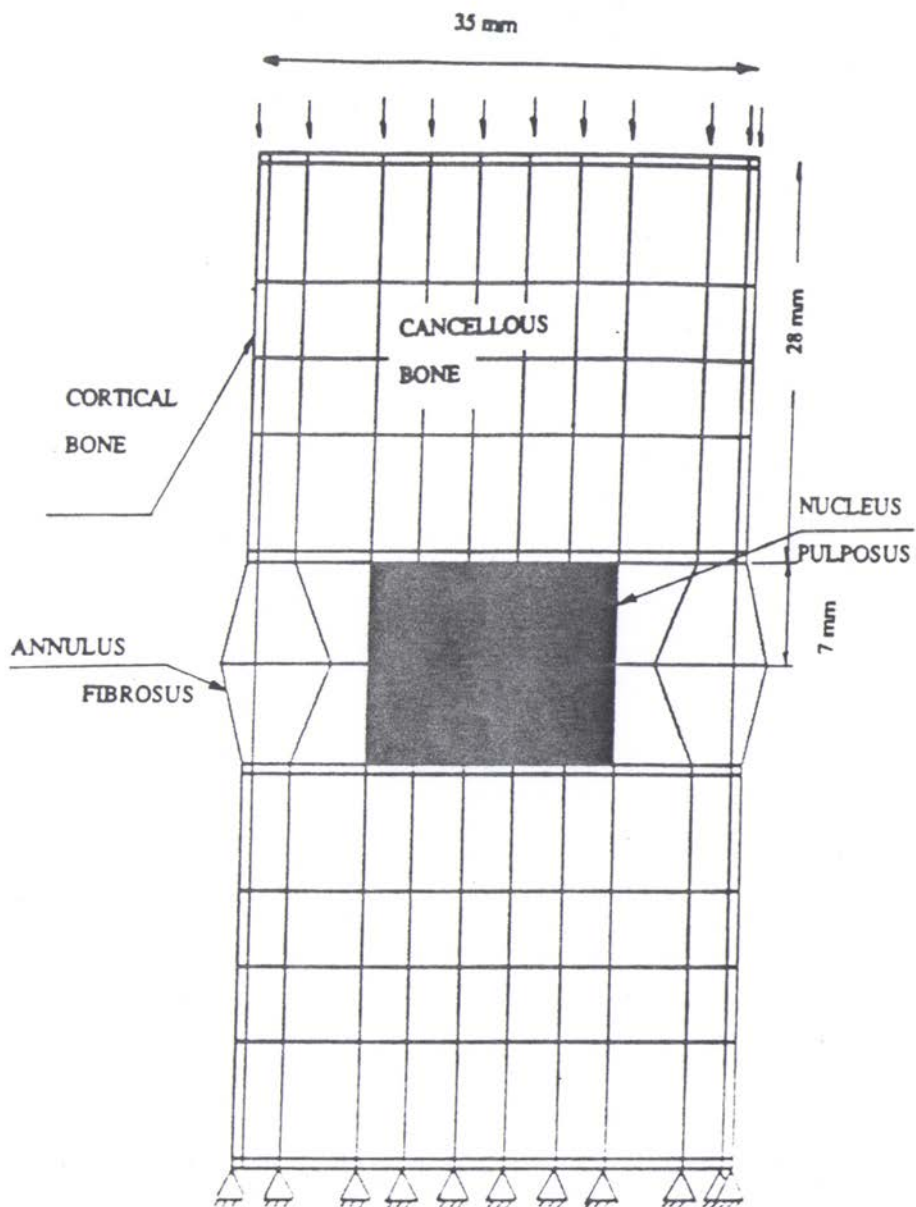


Figure 3-1. 2-dimensional, 1 motion segment finite element model

Table 3-1 Details of 2-dimensional one motion segment FE Model.

PART NAME	# OF ELEMENTS	ELEMENT TYPE (FEM software is ANSYS)	YOUNGS MODULUS E, MPa.	POISSON RATIO ν
Cortical bone	60	2-dimensional 8 nodal, Iso Parametric solid, STIFF 82.	12000	0.30
Cancellous bone	72	2-dimensional 8 nodal, Iso Parametric solid, STIFF 82.	100	0.20
Annulus (ground substance)	12	2-dimensional 8 nodal, Iso Parametric solid, STIFF 82.	4.2	0.45
Annulus fiber	24	Tension only element STIFF 10	175	
Nucleus Pulposus	12	2-dimensional 4 noded Fluid element, STIFF 50	1667.7*	

* Bulk Modulus of the fluid element

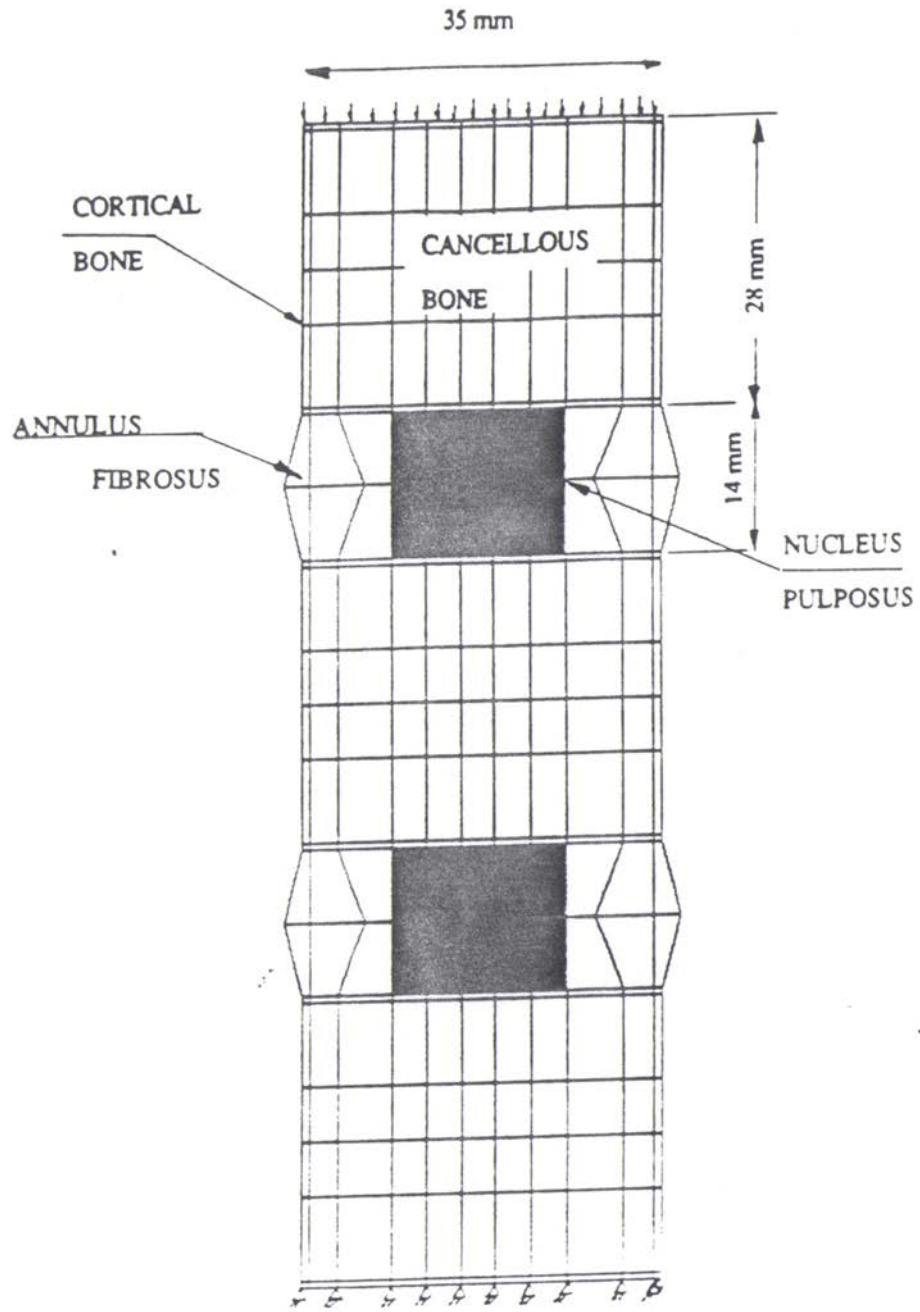


Figure 3-2. 2-dimensional, 2 motion segments finite element model

Table 3-2 Details of 2-dimensional two motion segments FE Model.

PART NAME	# OF ELEMENTS	ELEMENT TYPE (FEM software is ANSYS)	YOUNGS MODULUS, E, MPa.	POISSON RATIO, ν
Cortical bone	90	2-dimensional 8 noded, Iso Parametric solid, (STIFF 82)	12000	0.30
Cancellous bone	108	2-dimensional 8 noded, Iso Parametric solid, (STIFF 82)	100	0.20
Annulus (ground substance)	24	2-dimensional 8 noded, Iso Parametric solid, (STIFF 82)	4.2	0.45
Annulus fiber	48	Tension only element (STIFF 10)	175	
Nucleus Pulposus	24	2-dimensional 4 noded Fluid element, (STIFF50)	1667.7*	

* Bulk Modulus of the fluid element

Table 3-3 Details of 3-dimensional two motion segments FE Model.

PART NAME	NUMBER OF ELEMENTS	ELEMENT TYPE (FEM software is ABAQUS)	YOUNGS MODULUS E, MPa.	POISSON RATIO ν
Cortical bone	504	3-Dimensional, 8 nodal, linear displacement brick, C3D8.	12000	0.30
Cancellous bone	630	3-Dimensional, 8 nodal, linear displacement brick, C3D8.	100	0.30
Annulus (ground substance)	144	3-Dimensional, 8 nodal, linear displacement brick, C3D8.	4.2	0.45
Annulus fiber	96	Tension only element C1D2	175	0.3
Nucleus Pulposus	72	3-Dimensional, 8 nodal, linear - displacement brick, C3D8.	4.0	0.499
Metallic Plate (typeIII study of Remodelling only)	..13	3-Dimensional, 8 nodal, linear displacement brick, C3D8.	180000	0.3

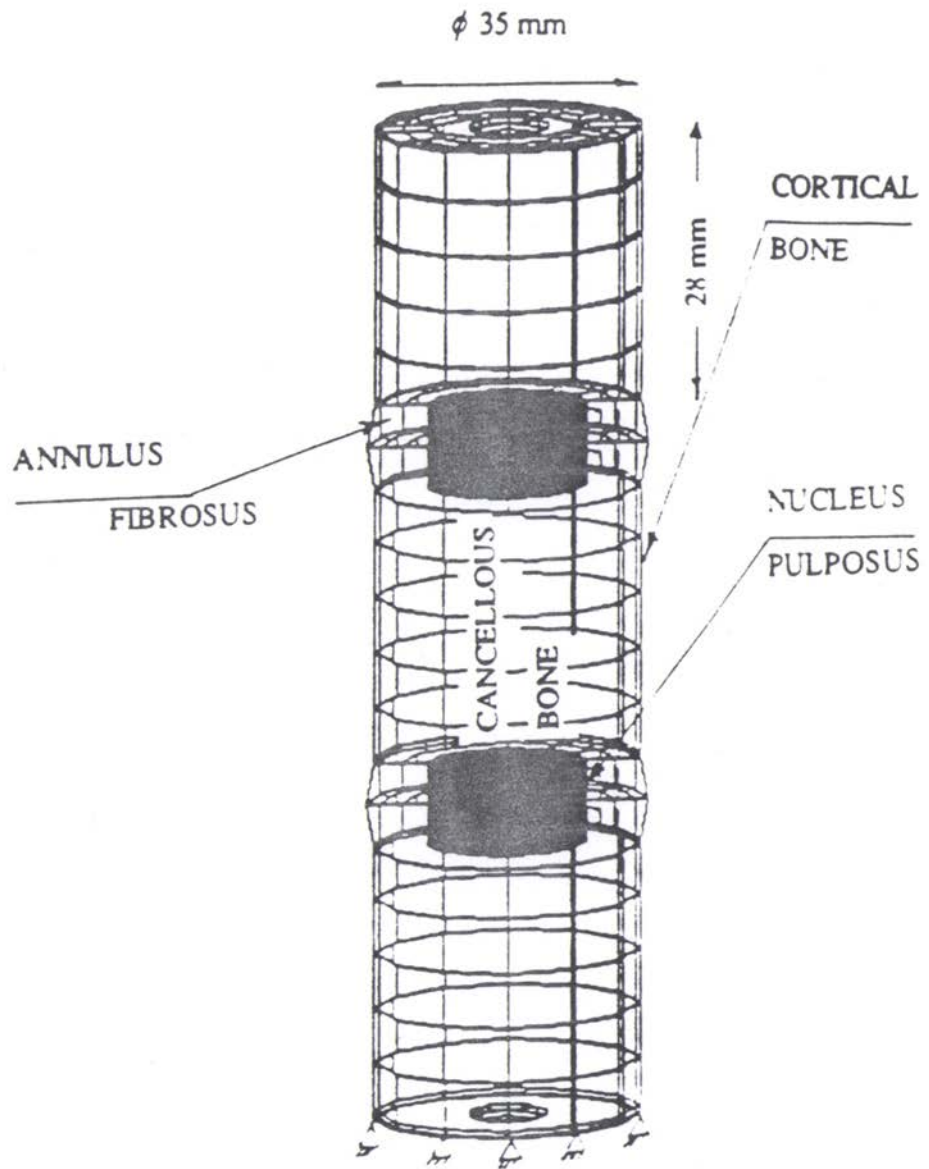


Figure 3-3. 3-dimensional, 2 motion segments finite element model

3.2.2 Three Dimensional FE model

A three dimensional finite element model of the two motion segments of lumbar spine was developed for studying the remodelling behaviour. The model has simplified representation of the vertebral bodies as 3 cylindrical segments separated by the intervertebral discs. Figure 3-3 shows the three dimensional FE model. The FE model was created using cylindrical coordinate system in order to facilitate the external remodelling computations and subsequent translation of external nodes. The type of elements, material properties^[21] selected for representing different parts making up the motion segments and other details of the 3D-FE model are given in Table 3-3. A total of 1586 nodes and 1446 elements were used in the model. The commercial finite element software package of ABAQUS was used for the analysis.

3.3 Remodelling studies on 2D FE Models

3.3.1 Prediction of Normal shape and Structure - Type I study

The type I study of remodelling which involves the prediction of normal shape and structure of vertebral body was carried out to test the hypothesis that bone by itself is an optimized structure. The optimal structure of bone implies that the external shape and internal trabecular architecture (Modulus of elasticity and density of the cancellous bone) of the bone, under normal loading conditions, are optimized to have minimum material and maximum effective use of bone material. Both the one motion segment and the two motion segments FE models of the vertebral bodies were subjected to the adaptive remodelling under axial compressive load conditions.

3.3.1.1 Force and constraint conditions

For the one motion segment model, a constant axial compressive load, in the form of pressure force, of 35 Newtons was applied at the top end plate of the superior vertebral

body of the model. All the nodes of the bottom end plate of the inferior vertebral body were completely constrained. For the two motion segments model, a constant axial compressive load same as that for the one motion segment model, in the form of pressure force of 35 Newtons was applied at the top end plate of the upper most vertebral body of the model. All the nodes at the bottom endplate surface of the inferior vertebral body of the model were completely constrained. Both the 2-dimensional FE models are assumed to have a unit thickness of 1 mm for the purposes of loading and stress analysis.

3.3.1.2 FEM analyses

Finite element stress analysis were carried out on these models using ANSYS(commercial FEM software), under the above specified force and constraint conditions. From the analysis the SED value and volume for each element were obtained. These values of SED and volume were the output of stress analyses of the initial models.

3.3.1.3 FORTRAN programs

These SED values were incorporated in the external remodelling equations 3.4 modified appropriately to the type I remodelling study, and the resulting movements of the external nodes of the vertebral bodies, ΔX and ΔY were computed using FORTRAN programs FORT I and FORT II(Appendices I and II)for the one and two motion segments respectively. These FORTRAN programs yielded new sets of nodes for the one and two motion segments as the result of first iterative step based on the above mentioned computations.

The equations 3.4 once again are given below for the purpose of explanation of the type I remodelling study.

$$\Delta X = \Delta t \ C_x \ \{ U^i(t) - U_n^i \}$$

$i=1,m$ where m is the number of surface nodal points

where

- ΔX - change in the location of the surface node normal to itself
 Δt - constant time step between iterations
 C_x - external remodelling rate coefficient
 $U^i(t)$ - SED of the external surface node i

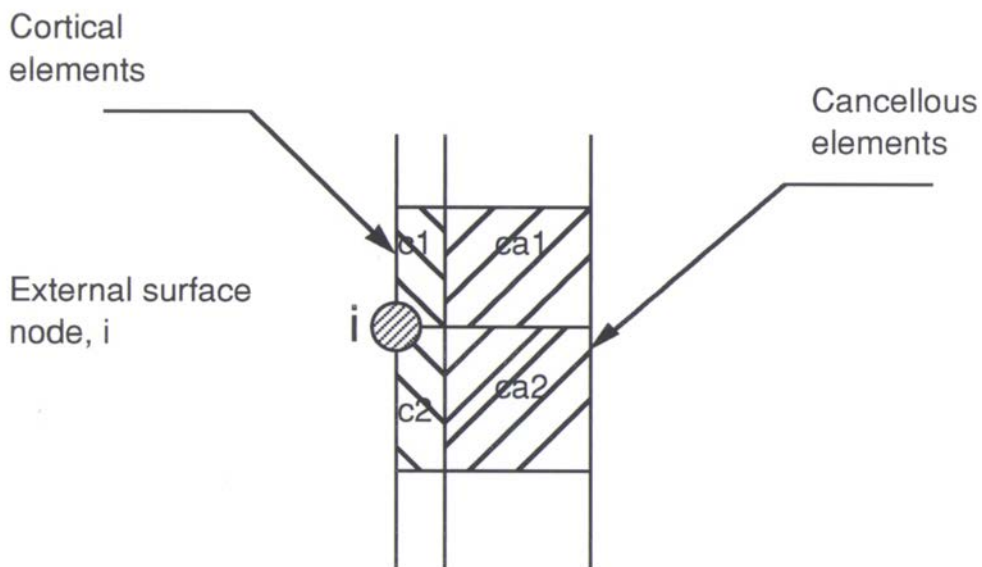
The term U_n^i which was described as the homeostatic SED value for the node i was replaced with a term U_{av}^i , which is the average of SED values of all the surface nodes for the case of type I study. This modification of the term from U_n^i to U_{av}^i was due to the reason that in this type I study, the remodelling was not due to any abnormal stress field conditions, but purely due to the nature of the bone to have an optimized shape and structure for the normal mechanical requirements from an arbitrary straight edged shape of the vertebral body. Thus the term homeostatic SED(U_n^i) of the remodelling equations did not exist for an arbitrarily chosen initial shape, and hence the term was replaced by average of SEDs of all the surface nodal points of the vertebral body. The modified external remodelling equation for the type I study is given below.

$$\Delta X = \Delta t C_x \{ U^i(t) - U_{av}^i \} \quad (3.5)$$

$i=1, m$ where m is the number of surface nodal points

- ΔX - change in the location of the surface node i , normal to itself
 Δt - constant time step between iterations
 C_x - external remodelling rate coefficient
 U_{av}^i - average of SEDs of all the external surface nodes computed for the time step t
 $U^i(t)$ - SED of the external surface node i .
 $\Delta t C_x = 0.300 \text{ mm}^4/\text{J}$

The SED of an external surface node i , namely $U^i(t)$ was computed for every external surface node according to the Figure 3.4 shown below.



$$\begin{aligned}
 \text{SED of Node } i &= U^i(t) \\
 &= \frac{\sum \text{SEDs of } c1, c2, ca1, ca2}{4} \\
 &= \left(\sum U_{e, \text{cort}} + U_{e, \text{canc}} \right) / 4
 \end{aligned}$$

where,

$U_{e, \text{cort}}$ - The sum of the SEDs of the cortical elements C1 and C2

$U_{e, \text{canc}}$ - The sum of the SEDs of the cancellous elements Ca 1 and Ca 2

Figure 3-4. Schematic diagram showing computation of $U^i(t)$ for an external surface node 'i' of the cortical bone.

The change in shape in one iteration step is caused by the small movement ΔX , perpendicular to the surface, of the external cortical bone of the vertebral body at all surface nodes, computed using the external remodelling equation. This ΔX is not the deposition or resorption of cortical bone but simple translational movement of the outer cortical bone towards or away from the inner cancellous bone.

The resulting modified FEM model, after one time step, with changed external shape was subjected again to the same force and constraint conditions and FEM stress analysis was carried out on the changed model. The subsequent SED values at different nodes and elements have been used again in the remodelling equation along with the new value for U_{av}^i for that time step and the changes ΔX for different external nodes, again been computed for the next time step. These results were again incorporated in the FE model and the iterations continued. The iterations were continued until, the total Strain Energy of the model is minimized for the same loading condition. At the end of these iterations the modified shape of the vertebral body was arrived at completing the shape adaptation for the normal loading conditions.

Once the external remodelling for shape optimization has been completed the internal remodelling, adapting the modulus of elasticity of the cancellous bone was carried out on the optimized model. The force and the constraint conditions were kept the same. FEM stress analysis was carried out on the model and the resulting SED values for the inner cancellous elements of the vertebral bodies were obtained. These SED values were employed in the internal remodelling equations 3.3 suitably modified for type I study and the resulting change in the modulus of elasticity ΔE for one time step was computed for all of the cancellous elements. The modification made in equation 3.3 was essentially that the term U_{n}^j , which was the homeostatic SED for the cancellous element j , was replaced with the average of the SEDs of all the cancellous elements namely U_{av}^j . The modified internal remodelling equations for type I study is given below.

$$\Delta E = \Delta t C_e \{ U_j(t) - U_{j_{av}} \} \quad (3.6)$$

$j = 1, n$ where n is the number of cancellous bone elements

where,

Δt - constant time step between remodelling iterations

ΔE - change in the elastic modulus cancellous element j

C_e - internal remodelling rate coefficient

$U_j(t)$ - SED of the cancellous bone element j

$U_{j_{av}}$ - average of SEDs of all the cancellous elements computed
for the time step t

The product of remodelling coefficient and the time step is given below.

$$\Delta t C_e = 5.000 \text{ mm}^4/\text{J}$$

These changes in the elastic moduli of the different cancellous elements have been incorporated in FE model and the resulting model was again subjected to the FEM stress analysis and the remodelling was carried out for the next time step using the resulting SED values of cancellous bone elements in the remodelling equations. The iterations were repeated until the total Strain Energy of the vertebral bodies were minimised.

3.3.1.4 The Schematic of the remodelling iterative sequence

As explained earlier the adaptive remodelling was carried out iteratively. The sequence of actions carried out in one iteration are schematically shown in Figure 3.5. Firstly FE stress analysis is carried out on the existing model. The FE stress analysis on the model yields the Strain Energy Density values and volumes of different constituent elements of the model for the type of loading and constraint conditions imposed on the

model. These SED values were fed into the appropriate FORTRAN program(FORT I for 1 motion segment and FORT -II for 2 motion segments model). The program incorporated SED values in the remodelling equations and computed the values of ΔX and ΔE depending on remodelling study performed, namely external or internal. The program also computed the total Strain Energy of the model. For the case of external remodelling the program used the ΔX values and determined the new coordinate values of the external nodes and rearranged internal nodes accordingly. For the internal remodelling case the program changed the Youngs modulus values of the cancellous bone elements using the ΔE values. The program yielded the new nodal coordinates of the model for the external remodelling and new Youngs modulus values of the cancellous bone for internal remodelling after one iterative step. The new resulting model was again subjected to FE stress analysis and the resulting SED values were fed to the FORTRAN program to continue the iterations. The iterations were terminated if the total Strain Energy computed by the program attained a minimum value. This was achieved by comparing the total Strain Energy of the new iterative step(TSEN) to the total Strain Energy of the old(TSEO) iterative step. For the 3 dimensional case the criteria used for the completion of iterations was the minimization of total strain energy density instead of TSE. This is due the nature of the FEM software used, namely ABAQUS, as it does not provide the element strain energy values but only provides the SED values.

The flow charts given by Figure 3-6 show the computations done by the FORTRAN programs during type I remodelling process for the external and internal remodelling.

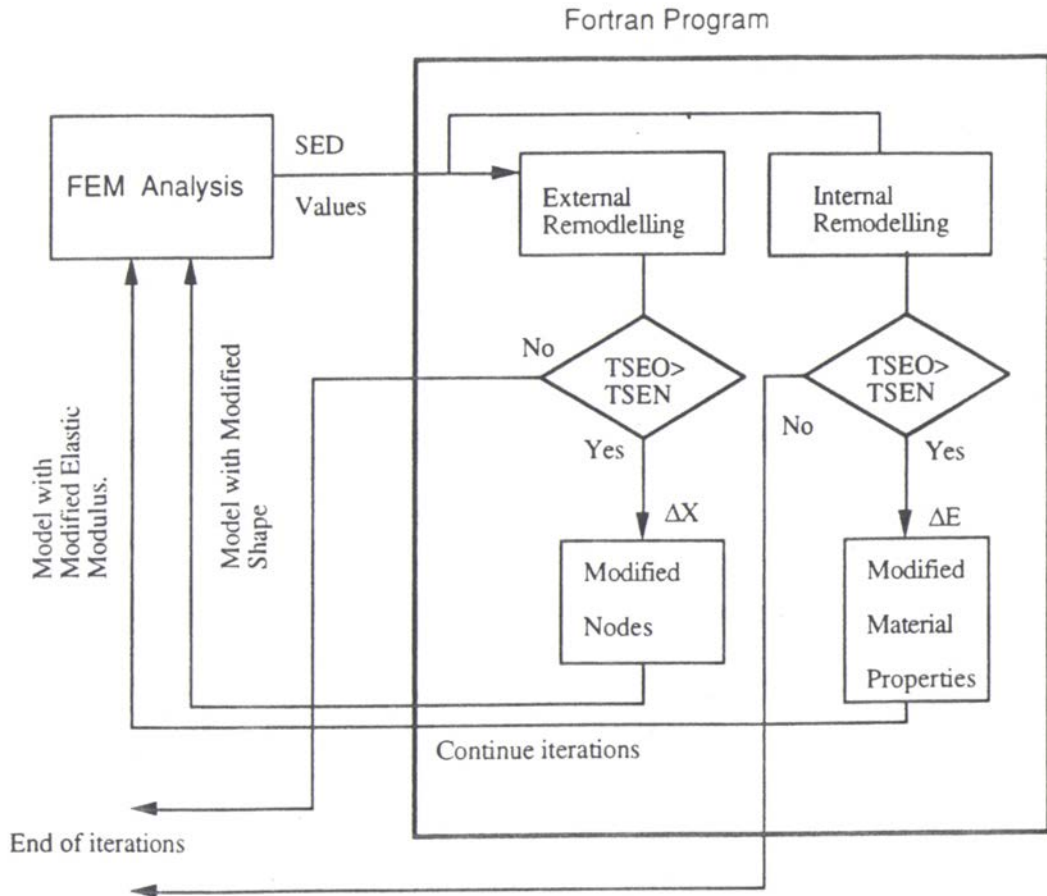
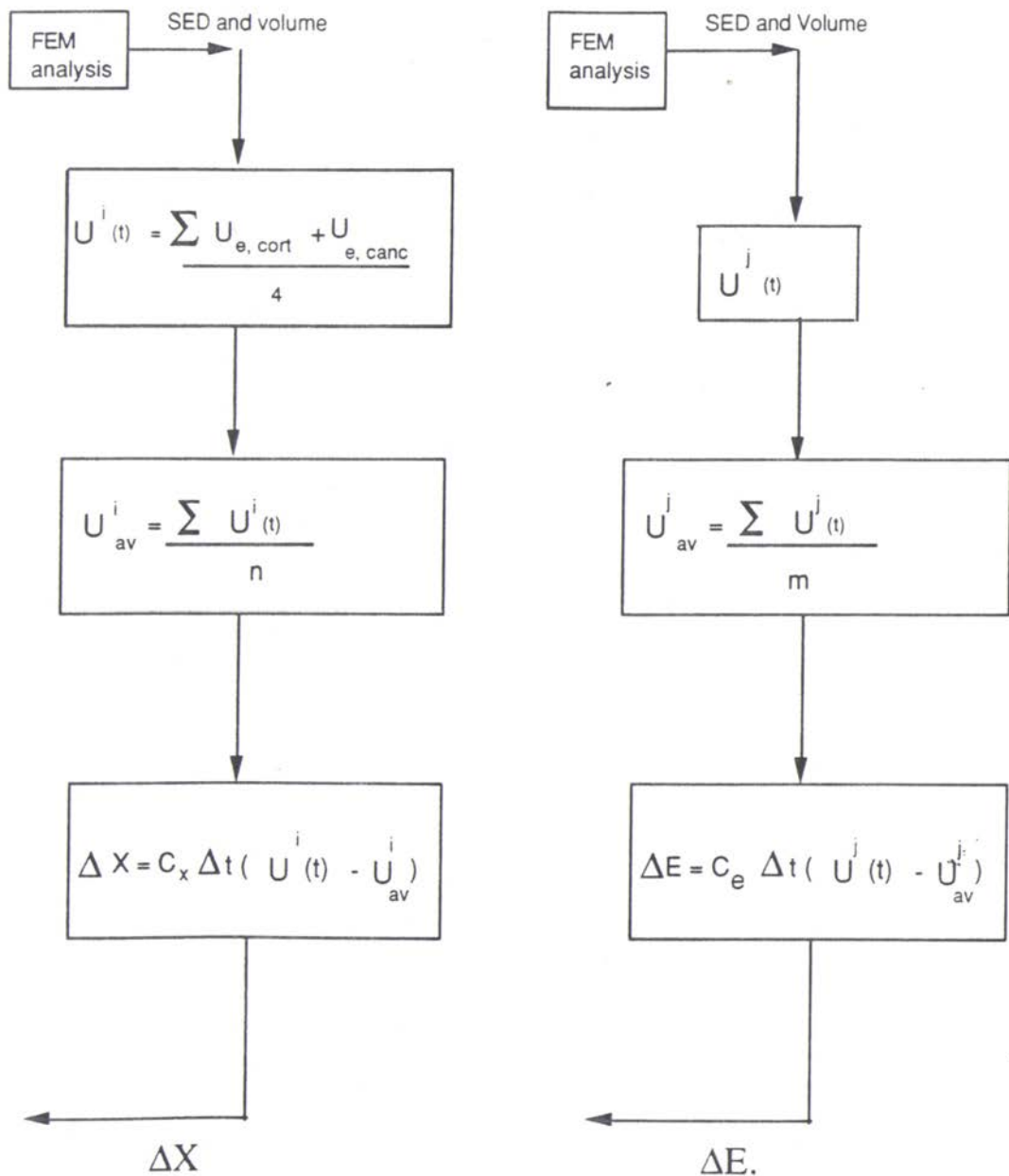


Figure 3-5. Schematic diagram for remodelling iterative sequence



a. External remodelling

b. Internal remodelling

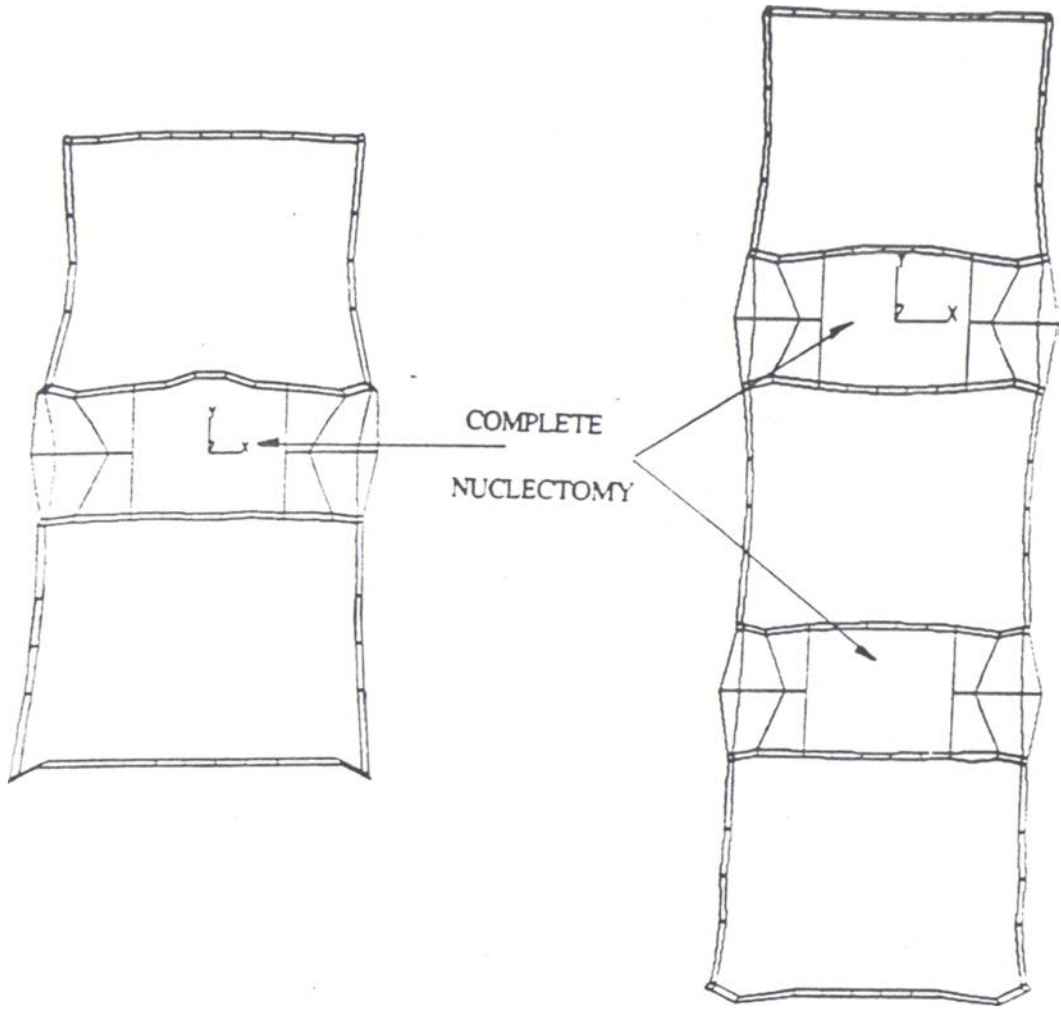
Figure 3-6. Flow chart showing the computations for Type I study

3.3.2 Adaptive remodelling following nucleotomy - Type II study

The optimized models of the 1 and 2 motion segments arrived through the above remodelling study were used as the initial FE models in this study of remodelling caused by nucleotomy. The elements forming the nucleus pulposus of the disc were removed from the models to simulate the nucleotomy. This could also be correlated to the real situation of age related degeneration of nucleus. Figure 3-7 shows the FE models following the nucleotomy.

For the type II study, the remodelling equations 3.3 and 3.4 were used directly without any modifications. This was due to reason that after performing the type I study the normal optimized models of one and two motion segments were made available and hence the homeostatic values of SEDs for different elements and nodes for the intact model through the FE analysis on them.

The nucleotomised models were subjected to the FE analysis. The modified stress field in the injured model induced the vertebral bone mass to adaptively remodel externally and internally in accordance with the remodelling equations. The SED values for different nodes and elements of the nucleotomized model were obtained from the FE analysis. The external and internal remodelling of the vertebral bodies were carried out using the remodelling equations 3.4 and 3.3 respectively by incorporating SED values under modified stress field for external surface nodes and internal cancellous elements. The homeostatic SED values (U_n) for the corresponding nodes and elements of the intact model were incorporated in the equations. The external remodelling was carried out first followed by internal remodelling. The programs FORT-I and FORT-II carried out the computations for remodelling parameters ΔX and ΔE . Figure 3-8 shows schematically the computations done by the FORTRAN programs FORT I and FORT II for the external and internal remodelling for the type II study.



a. One motion segment

b. Two motion segment

Figure 3-7. The initial 2-dimensional models with nucleotomy for the Type II study

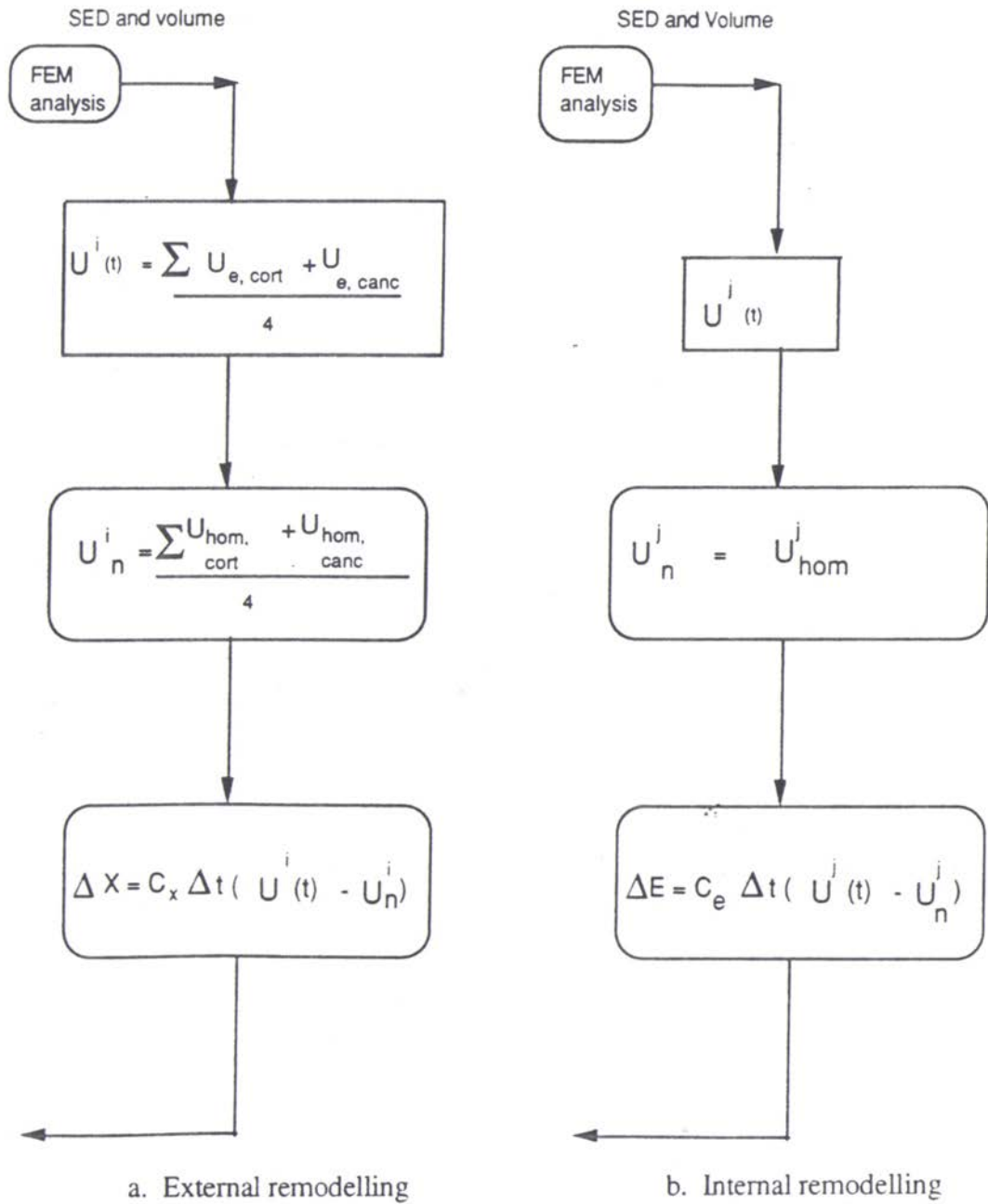


Figure 3-8. The flow chart showing the computations for Type II study

The terms $U_{\text{hom, cort}}$, $U_{\text{hom, canc}}$ and U_{hom}^j of Figure 3-8 are explained below.

$U_{\text{hom, cort}}$ - The homeostatic SED of the cortical elements of the intact model related to node i , of Figure 3-4.

$U_{\text{hom, canc}}$ - The homeostatic SED of the cancellous elements of the intact model related to node i , of Figure 3-4.

U_{hom}^j - The homeostatic SED of any cancellous element ' j ', of the intact model.

The shape and structure of the vertebral bodies of the 1 and 2 motion segments models resulting after this remodelling process due to nucleotomy is discussed in the following chapter.

3.4 Remodelling Study on 3D FE model

3.4.1 Prediction of Normal shape and Structure - Type I study

The remodelling study of prediction of normal shape and structure of vertebral body was carried out on the 3-dimensional FE model for the 2 motion segments of lumbar spine. The details of this 3D model are provided in section 3.2. In this model the vertebral bodies have straight cylindrical shape. This type I study was carried out to verify the tendency of the bone to have optimal shape and structure under normal loading environment.

The remodelling procedural sequence was exactly similar to one that was used for the 2D models. A compressive load of 950 Newtons in the form of pressure was applied at the top surface of the superior vertebral body. The nodes at the bottom surface of the inferior vertebral body were completely constrained.

FE stress analysis was carried out on the 3D model using ABAQUS(FEM Software). The shift to the ABAQUS FEM software from that of ANSYS, for the 3D

model, was due to the limited capability of ANSYS package available (can only handle problems having wave front less than 200). From the FE analysis the Strain Energy Densities for all the elements were obtained. A FORTRAN program FORT III (Appendix III) was developed to carry out the computations required for the external and internal remodelling for the 3D model.

The external remodelling was carried out first. The average of SEDs for the external surface nodes namely U^i_{av} for the vertebral bodies was computed. The homeostatic SED value U^i_n in the external remodelling equation 3.4 was replaced by the average SED value for the external surface nodes U^i_{av} . The external remodelling equations for the type I study on 3D model are given below.

$$\Delta R = \Delta t C_x \{ U^i(t) - U^i_{av} \}$$

$i=1, m$ where m is the number of surface nodal points

ΔR - change in the location of the surface node i , normal to itself

Δt - constant time step between iterations

C_x - external remodelling rate coefficient

U^i_{av} - average of SEDs of all the external surface nodes computed for the time step t

$U^i(t)$ - SED of the external surface node i .

$$\Delta t C_x = 0.300 \text{ mm}^4/\text{J}$$

For the nodes at the end plates,

$$\Delta Z = \Delta t C_x \{ U^i(t) - U^i_{av} \}$$

ΔZ - change in the location of the end plate surface node normal to itself

The changes for the first time step, in the positions of the external surface nodes, namely, ΔR for all the nodes on vertical surfaces, and ΔZ for the nodes on the horizontal surfaces(end plates) of the vertebral bodies were computed. These ΔR values represent the movement of the surface nodes on the vertical surfaces, either radially inwards or outwards from the cancellous bone of body. The ΔZ values represent the movement of the external horizontal surface nodes in the vertical direction towards or away from the inner cancellous bone. The required computations of ΔR and ΔZ have been carried out using the program FORT-III. The program also determined the altered nodal positions the interior nodes of the vertebral body, to match the movements of the surface nodes so that the interior elemental shapes are kept within the allowable limits of the FEM analysis. This completed the first iterative step for the external remodelling producing a resultant model for the next iterative step.

FEM stress analysis was carried out on the resultant model with changed shape and the SEDs for the different surface nodes and all the elements were determined from the analysis. These SEDs were again incorporated in the remodelling equations and the remodelling parameters ΔR and ΔZ were determined using the FORT III program. The iterations were terminated when the total Strain Energy Density of the vertebral bodies were minimized for the same loading conditions.

After the optimal shape have been arrived the model was subjected to internal remodelling. From the SED values obtained through the FEM analysis the average SED U_{av}^j of the cancellous elements of the vertebral bodies were computed. These SED values were incorporated in the internal remodelling equations for the 3D model. The equations are given below.

$$\Delta E = \Delta t C_e \{ U^j(t) - U_{av}^j \}$$

$i=1,n$ where n is the number of surface nodal points

- ΔE - change in the Young's Modulus of the cancellous element j
- Δt - constant time step between iterations
- C_e - internal remodelling rate coefficient
- U_{av}^j - average of SEDs of all the cancellous elements computed for the time step t
- $U^j(t)$ - SED of the cancellous element j .

the changes in the elastic moduli ΔE of the internal elements, for the first time step, have been computed using the FORT III program. The resultant model with changed cancellous bone properties is again put under FEM stress analysis and the remodelling process was repeated iteratively. The iterations were continued until the Total Strain Energy Density (TSED) attains a minimum value. The TSED instead of TSE was taken for consideration in the case of 3D model as the ABAQUS (finite element software) provides only the SED values and not the element strain energies. The results of the External and internal remodelling are shown and discussed in the following chapter.

3.4.2. Remodelling study following Partial Nuclectomy -Type II study

Adaptive shape remodelling study on the 3-Dimensional 2 motion segments was carried out following a partial nuclectomy. The right half of the nucleus as seen on the Figure3.9, of the superior intervertebral disc was removed from the 3D model. A partial nuclectomy instead of a total nuclectomy was conducted in order see clearly the difference in the remodelling behaviour between the left half and the right half of the vertebral bodies. Figure 3-9 also shows a cross sectional view of the superior intervertebral disc (cross section created by a horizontal plane passing through of the mid-plane of the superior intervertebral disc). The nucleus elements marked 1-9 were removed. The resultant model was subjected to FEM stress analysis. The partial nuclectomy of the disc caused the abnormal stress field which induced the remodelling process. The external

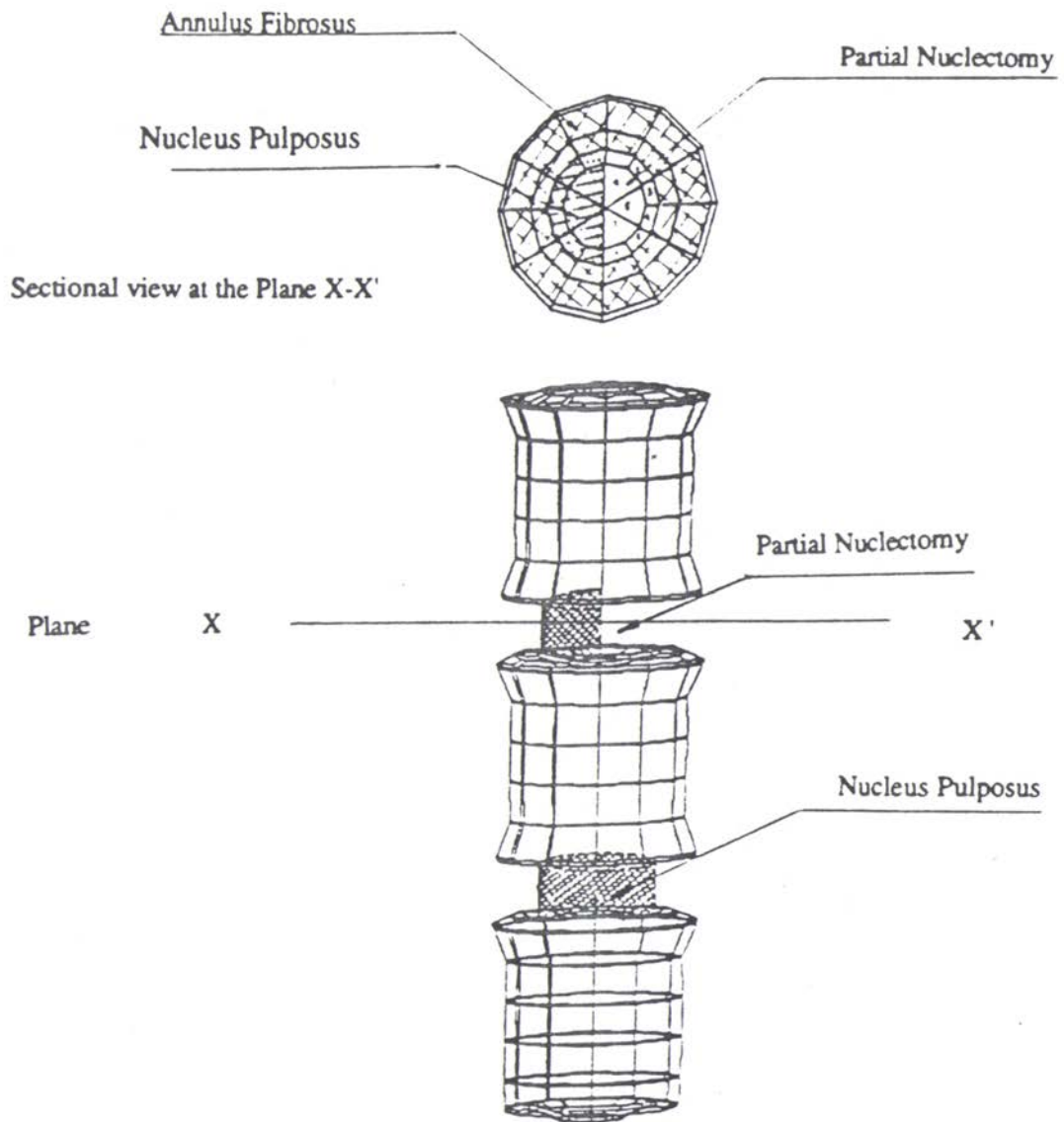


Figure 3-9. The initial 3-dimensional 2 motion segments model with partial nucleotomy for Type II study

remodelling(shape) was carried out using the FORTRAN program FORT-III in similar lines as one that carried out for the 2-Dimensional models. It is important to note that only the external remodelling was conducted for type II study on the 3D model. The results of the external remodelling study are discussed in the following Chapter.

3.4.3 Study of bone remodelling induced by stress shielding - Type III study

The use of 'stabilizer' plates to restore stability of spine is one of the surgical procedures. Here the remodelling study was carried out to study the effect of stress shielding induced by such a plate. The optimized 3D model of the 2 motion segments, obtained through the type I study was subjected to a partial nucleotomy on its superior intervertebral disc and was fitted with a plate across vertebral bodies sandwiching the disc. Fig 3.10 shows the FE model along with the plate. It is important to note that there were no screws used for fixing the plate. The plate was attached directly on to the cortical bone of the vertebral bodies. The use of the plate with out the screws for the remodelling study is justified from the point of view of the simplified nature of the model. The bone remodelling induced by the placement of the stabilizer plate was studied by applying the adaptive bone remodelling procedure to the modified model.

The external(shape) remodelling have been carried out using the appropriate adaptive remodelling equations. The SED values of the nodes and elements required in the equations were obtained from the FE analysis of the plate fitted model. The corresponding homeostatic SED values were obtained from the optimized intact model. The remodelling procedure was similar to the earlier remodelling studies. The remodelled shape and structure of the vertebral bodies are discussed in the following chapter.

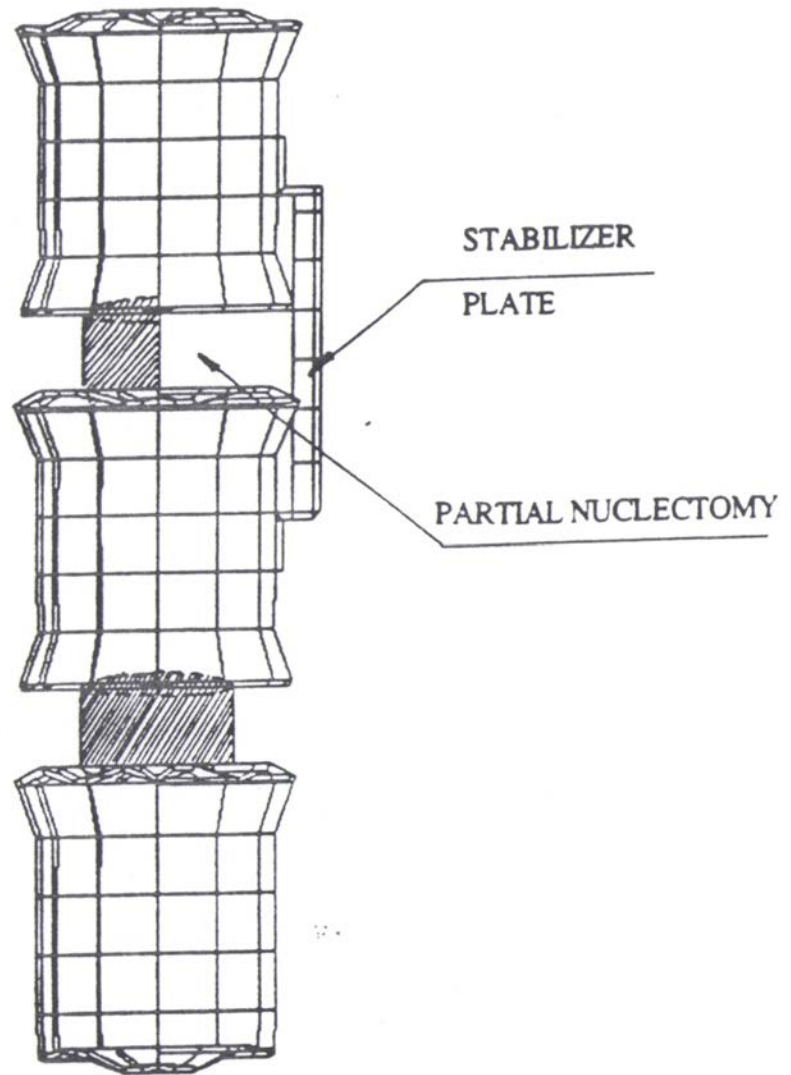


Figure 3-10. 3-dimensional, 2 motion segments finite element model with stabilizer plate and a partial nucleotomy

3.5 Summary

The methods employed and the finite element models used for the present study were described in detail in this chapter. It is essential to note that the FE models used to represent the spinal motion segments were simplified ones. The models do not include the posterior elements and ligaments. Only compressive loading is applied on the models. Three types of remodelling studies were carried out on these models. The finite element softwares ANSYS and ABAQUS were used for the stress analysis of the models. Three different FORTRAN programs were used for the application of adaptive remodelling theory, with SED as the stimulus for remodelling, on the models. The results of remodelling studies are presented and discussed in the following chapter.

CHAPTER IV

RESULTS AND DISCUSSION

The results of the various adaptive bone remodelling studies performed on 2 dimensional(1 and 2 motion segments) and 3-dimensional(2 motion segments) finite element models of the motion segments of spine are presented. The results of each individual case of remodelling study are presented in the following sections and the results are discussed in the respective sections. A general discussion on the whole set of remodelling studies is carried out at the end of this chapter. Before presenting the results of different cases of remodelling studies a brief summary of the remodelling cases that were dealt in the study is given below.

4.1 Different cases of adaptive remodelling study conducted

As mentioned in Chapter 3, three different finite element models of spinal motion segments were developed for studying the adaptive bone remodelling behaviour of the vertebral body. Two of them were two-dimensional and the third one was 3-dimensional. Table 4-1 summarises the different remodelling studies conducted.

4.2. Results of adaptive remodelling study type I

4.2.1 Results of 2-Dimensional 1 motion segment model.

The 2-Dimensional one motion segment FE model used in the study is shown in Figure 3-1. The details of this model are described earlier in section 3.2.1.1. It is

Table 4-1 Summary of remodelling studies conducted

Remodelling study type	Description of study	Finite element models used	Nature of remodelling
Type I study	remodelling study to verify the hypothesis that the vertebral body as a bone, by itself is an optimal structure	2D, one motion segment	external and internal
		2D, two motion segments	external and internal
		3D, two motion segments	external and internal
Type II study	remodelling study following full nucleotomy	2D, one motion segment	external and internal
		2D, two motion segment	external and internal
		3D, two motion segments model	only external
Type III study	remodelling following fixation of a stabilizer plate on the partially neclectomised model	3D, two motion segments model	only external

important to mention here that the vertebral bodies of the model have straight external edges and the cancellous bone on the interior of the vertebral body has a uniform modulus of elasticity of 100 MPa.

The adaptive remodelling study of prediction of optimal normal shape and structure of the vertebral body was carried out iteratively on this model in accordance with the procedure mentioned in the section 3.2.1. Figure 4-1 b shows the final shape of the vertebral bodies of the 2-Dimensional one motion segment model after the adaptive external remodelling. Figure 4-1a shows the initial shape of the model for the purpose of comparison. Figure 4-1c shows the sagittal section of a lumbar specimen.^[26] Figure 4-2 a and b show the distribution of modulus of elasticity and density respectively of the cancellous bone of the vertebral body of the model at the end of adaptive internal remodelling. The property values of namely Young's modulus and density for the cancellous bone in the initial model are 100 MPa and 0.297 g/cc respectively. Figure 4-3a and b show the changes in the value of the total Strain Energy(TSE)and volumes of the superior vertebra and the whole model respectively after every iterative step, as the remodelling was carried out . The changes of TSE and volumes during the external and internal remodelling are presented on the same Figure for the purpose of comparison. The local changes in SED at surface nodes during external remodelling is shown in Figure A-1 in Appendix I. Similarly the local changes in the SED of cancellous elements during internal remodelling is shown in Figure A-2 in Appendix I.

4.2.1.1 Discussion of the results

From Figure 4-1b it could be seen that the superior vertebral body remodels differently compared to the inferior one. This is attributed to the different nature of boundary conditions at the outer end plates of these vertebrae. The top endplate of the upper vertebral body has a constant pressure condition where as the bottom end plate of the

lower vertebra has constrained nodal conditions. The remodelled shape of the superior vertebral body resembles more closely the normal shape of a vertebral body of a lumbar motion segment of spine shown in Figure 4.1c. The inward curvature at the side and at the inferior end plate regions of the superior vertebral body resembles the actual one. There is no inward curvature of the top endplate. This is due to the boundary condition imposed at the top endplate which results in the unchanging uniformly distributed compressive load as a result of which there is no shape remodelling taking place in that region. The remodelled shape of the inferior vertebral body does not resemble that of the actual one due the constraint boundary condition imposed at the bottom end plate.

From the results of the shape remodelling of the 1 motion segment model it could be inferred that the boundary conditions influence greatly the remodelling pattern of the vertebral bodies. This is due to the reason that the boundary loading conditions may not be exactly similar to that one experienced by the vertebral end plates in the presence of a intervertebral disc. This is precisely the reason for extending the remodelling study to a 2 motion segments model in which there are three vertebral bodies and the loading conditions(boundary conditions) experienced by the middle vertebral body more closely resemble the loading conditions experienced by an actual vertebral body of the spinal motion segment.

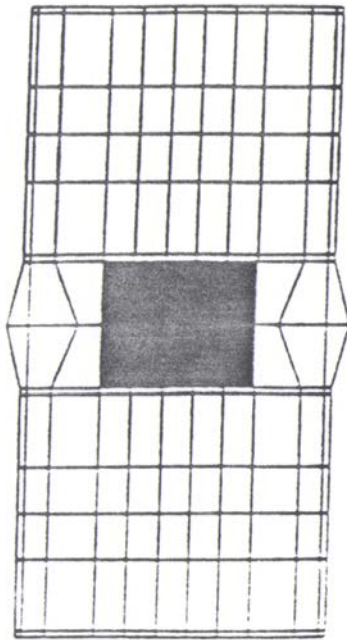
Coming to the results obtained through internal remodelling study on the one motion segment model, it could be seen from the Figure 4-2 a that there is difference in the nature of distribution of modulus of elasticity values between the upper and lower vertebral bodies. This again is attributed to the difference in the boundary loading conditions of these vertebral bodies. Nevertheless a general inference that the values are higher along the central core of the vertebral body compared to the lateral sides could be made from the distribution. This tendency is more clearly seen in the superior vertebral body. In order to

compare and validate the present results, a reference is made here to the experimental study conducted by Keller et al.^[18]

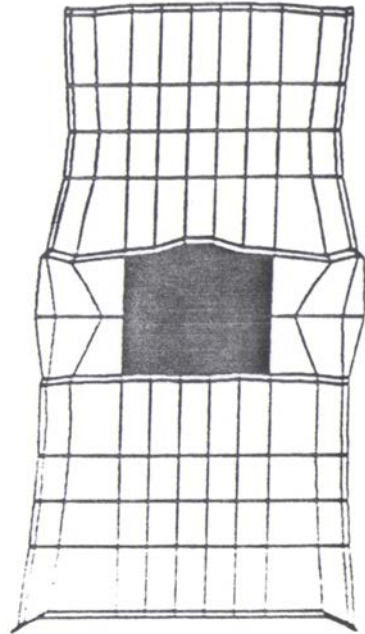
Keller et al have conducted experiments to find the regional variations in the compressive properties of lumbar vertebral trabeculae. They found that there was a tendency for the trabecular bone to be strongest in the center, just above the disc nucleus, and weakest in the peripheral region. This strength variation was especially noted among the specimens with less degenerated discs or intact discs. In the case of the degenerated discs, the compressive stress was more uniformly distributed over the entire disc plane. The trabecular bone strength was found to have similar uniform distribution.

The distribution of modulus of elasticity obtained in the present study compares reasonably well with the results obtained by Keller et al.^[18], despite the adverse influence of the boundary effects in the 1 motion segment model.

Fig 4.3a shows the change in the total Strain Energy of the superior vertebral body along with the changes in material volume. Figure 4-3b shows the change in the total Strain Energy of the whole model and its volume. The TSE(Total Strain Energy) of the superior vertebral body decreases along with the material volume. The optimized shape of the superior vertebral body has reduced(minimized as the result of remodelling)TSE as well as minimum material conditions. The remodelled shape of the inferior vertebral body does not have the minimized material volume as the volume has increased from 980 mm³ to 1100 mm³, due the effect of boundary conditions imposed at the bottom end plate. Even though the net remodelled shape of the superior vertebra does not exactly resemble that of an actual normal vertebral body the trend in the shape on the sides and at the inner endplate regions are in line with that of the actual one. Figure 4-3b shows the reduction in TSE along with the reduction in the volume of the whole model. Based on these results it is reasonable to expect better results in the case of the 2 motion segments model which are discussed in the following section.

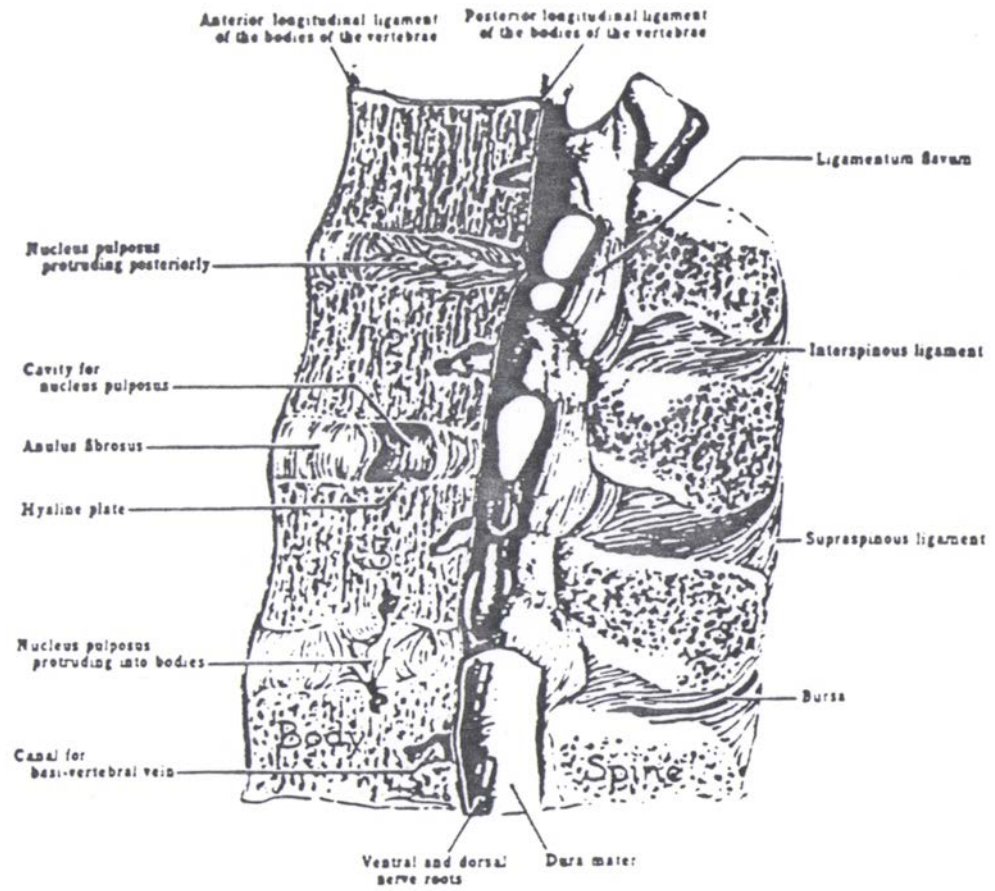


a. Initial model



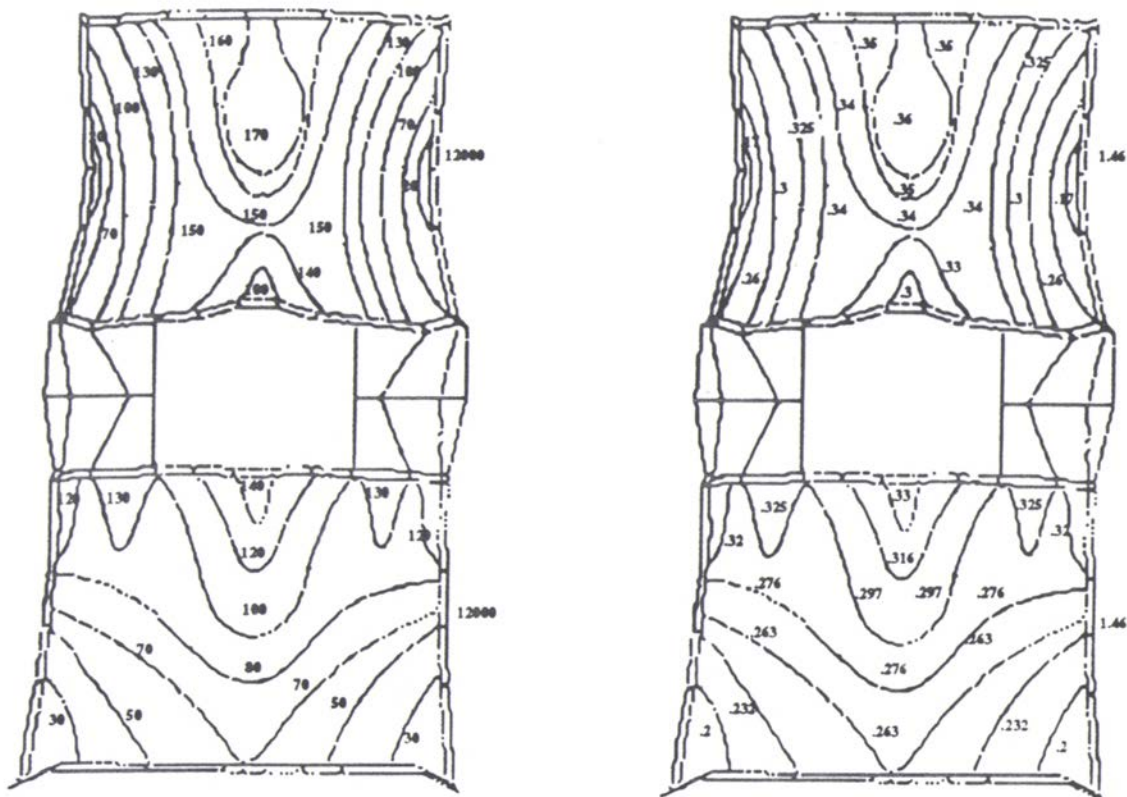
b. Final model

Figure 4-1. External remodelling of 2D, 1 motion segment: Type I study



c. Sagittal section of actual lumbar specimen^[1]

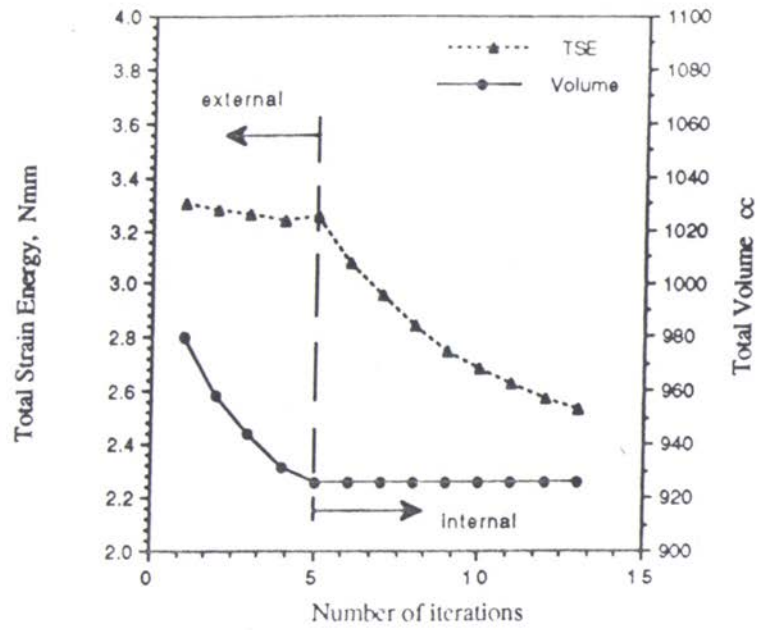
Figure 4-1. Continued



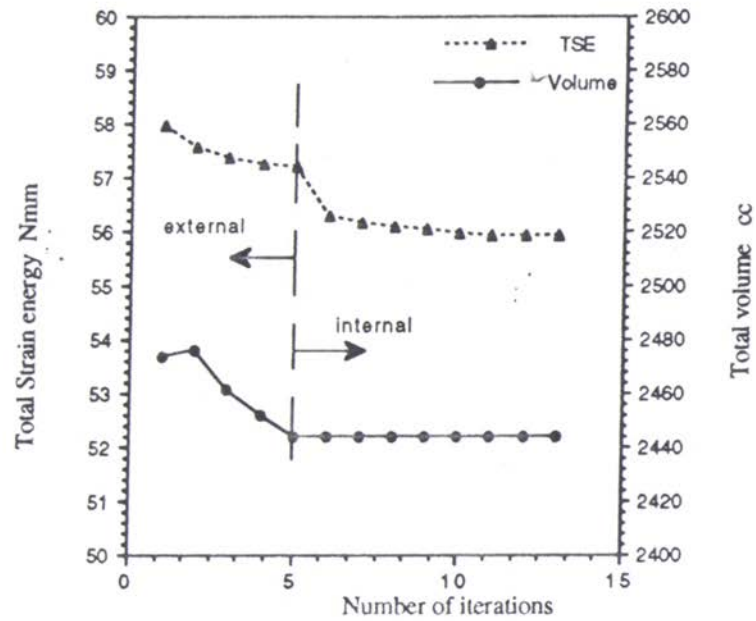
a. Young's Modulus, MPa

b. Density, g/cc

Figure 4-2. Distribution of Young's modulus and Density, after internal remodelling of 1 motion segment model: Type I study



a. Superior vertebra



b. Full model

Figure 4-3. Total strain energy and Volume of 1 motion segment, Type I

4.2.2 Results of 2-dimensional two motion segments model

The details of the 2-dimensional two motion segments FE model are described already in section 3.2.1.2. The two motion segments model was subjected to the same loading conditions as that of the one motion segment model. The results of type I study on this model are described below.

Figure 4-4b shows the final shape of the vertebral bodies of the 2-dimensional one motion segment model after the adaptive external remodelling. Figure 4-4a shows the initial shape of the model for the purpose of comparison. Figure 4-5 a and b shows the distribution of modulus of elasticity and density respectively of the cancellous bone of the vertebral body of the model at the end of adaptive internal remodelling. The property values of namely Young's modulus and density for the cancellous bone in the initial model are 100 MPa and 0.297 g/cc respectively. Figure 4-6a and b show the changes in the value of the total Strain Energy and volume of the superior and middle vertebral bodies after every iterative step, as the remodelling was carried out. Figure 4-6c show changes of the above variables for the whole model. The changes during the external and internal remodelling are presented on the same Figure for the purpose of comparison.

4.2.2.1 Discussion of the results

From the Figure 4-4b it could be seen that the remodelled shape of the middle vertebral body is much more close to that of the actual one(Figure 4-1c) compared to the results obtained from the 1 motion segment model. This is due to the more realistic stress conditions experienced by the middle vertebral body at the endplate regions and its isolation from the applied boundary conditions. Thus the stress pattern in the middle vertebral body resembles much more closely to that of an actual one. The body curvatures at the sides and the end plate regions are remarkably close to the actual one. Thus the prediction of optimized shape of the vertebral body of a spinal motion segment has yielded a satisfactory

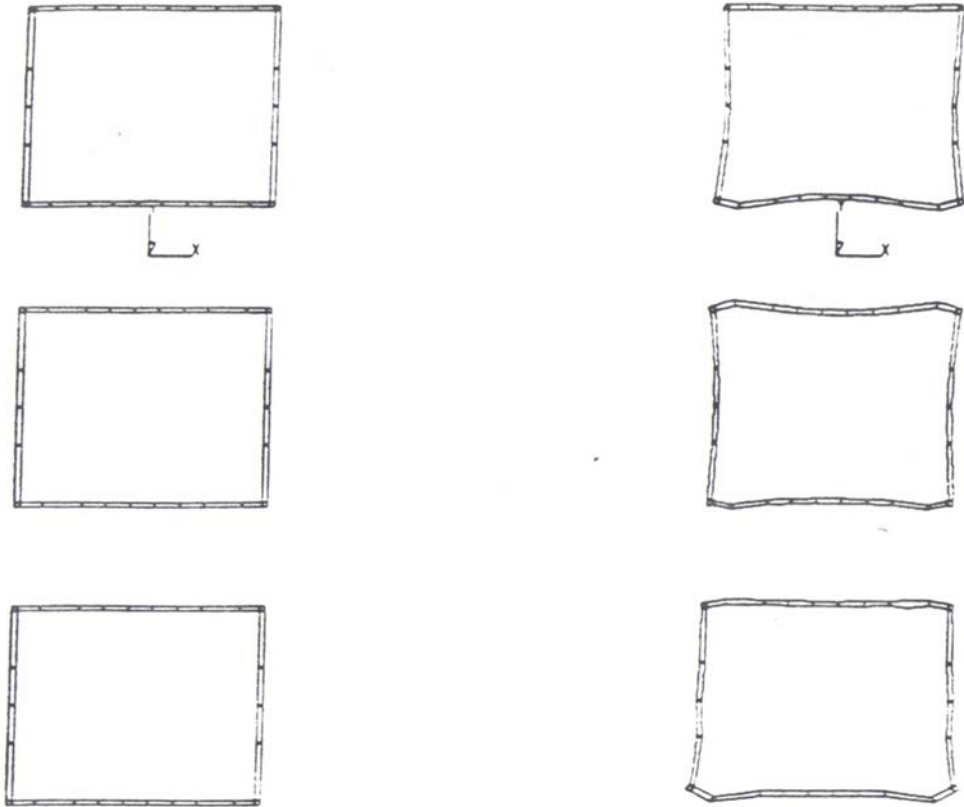
result in the case of 2 motion segments model. It is also important to note that the superior vertebral body also remodels in a satisfactory manner except at the top end plate region which is due absence of remodelling behaviour resulting out of the imposed boundary condition in that region.

Figure 4-5a shows the distribution of modulus of elasticity of the cancellous bone of the vertebral bodies obtained through the internal remodelling. The distribution of modulus of elasticity of the three vertebral bodies differ due the boundary effects. In general it is very clearly seen from the distribution that the central core region of the vertebral bodies have higher values and the lateral regions have lower values. The middle vertebral body which is isolated from the boundary effects, remarkably exhibits the tendency found out by Keller et al^[18] through their experimental investigation on distribution of compressive strength of the vertebral trabeculae. Thus the study of adaptive internal remodelling predicting the optimal trabecular structure of the vertebral body has brought out the normal observed property distribution of the vertebral trabeculae.

Figure 4-6a and b show the change in the total Strain Energy of the superior and middle vertebral bodies along with the changes in material volume. Figure 4-6c shows the change in the total Strain Energy and volume of the whole model. The TSE of the superior and middle vertebral bodies decrease along with the material volume as the remodelling proceeds. The optimized shapes of the superior and middle vertebral bodies have minimised (as the result of remodelling)TSE as well as minimum material conditions which are the optimisation criteria. The remodelled shape of the inferior vertebral body does not have a minimised volume as could be seen from Figure 4-4b due the boundary effects.

4.2.3 Results of 3-Dimensional two motion segments model

The details of the 3-dimensional two motion segments FE model are described already in section 3.2.1.2. The 3D two motion segments model was subjected to



a. Initial model

b. Final model

Figure 4-4. External remodelling of 2D, 2 motion segment: Type I study

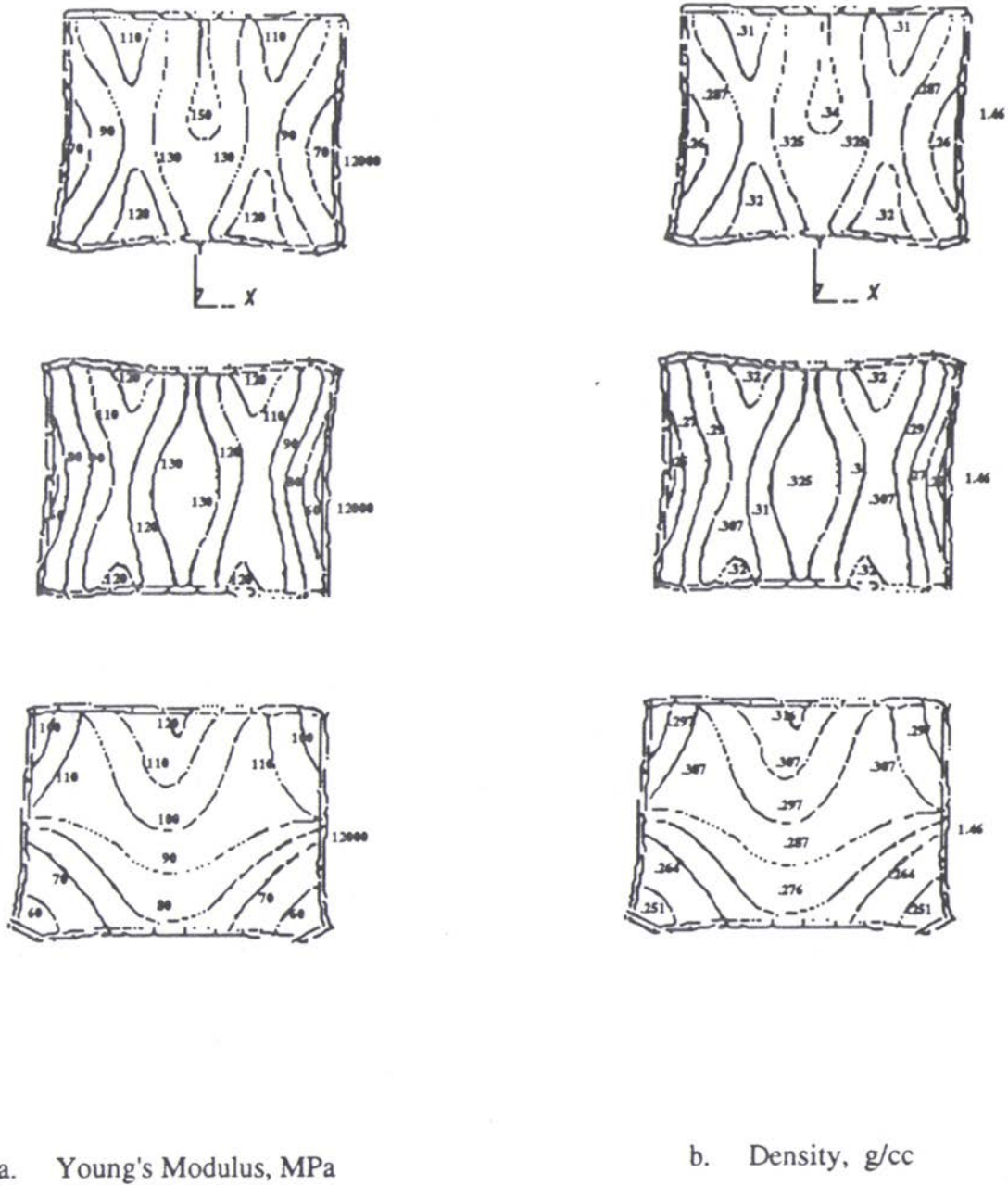
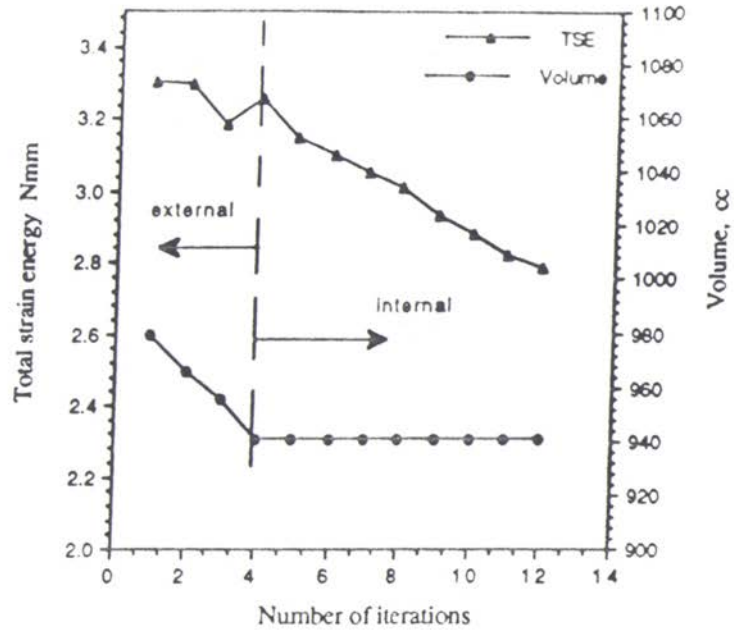
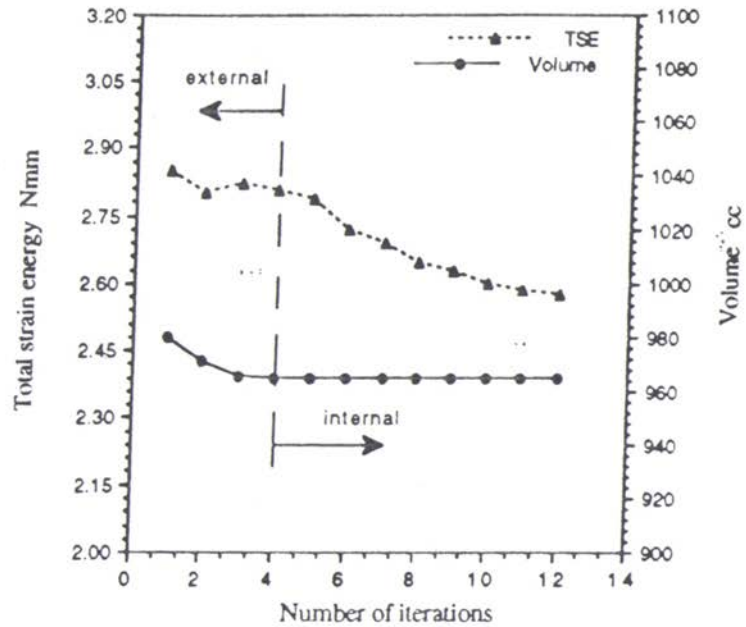


Figure 4-5. Distribution of Young's modulus and Density, after internal remodelling of 2 motion segments model: Type I study

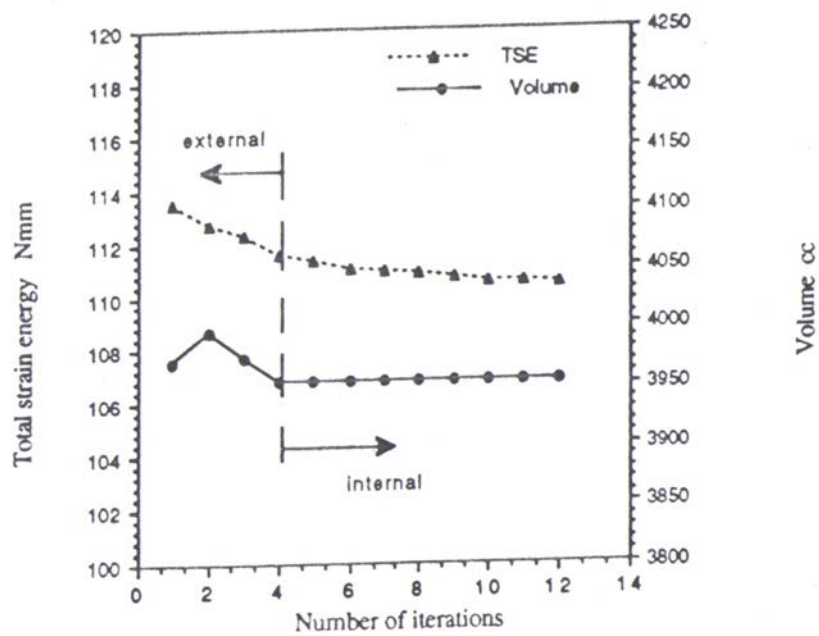


a. Superior vertebra



b. Middle vertebra

Figure 4-6. TSE and Volume for the vertebrae of 2 motion segments, Type I



c. Full model

Figure 4-6. Continued

uniformly distributed load of 950N (equivalent to that for the 2D models) at the top endplate of the superior vertebral body. The results of the type I study on the 3D model are described below.

Figure 4-7b shows the final shape of the vertebral bodies after the adaptive external remodelling. Figure 4-7 a shows the initial shape of the model for the purpose of comparison. Figure 4-8 a and b shows the distribution of modulus of elasticity and density respectively of the cancellous bone of the vertebral bodies of the model at the end of adaptive internal remodelling. The property values of namely Young's modulus and density for the cancellous bone in the initial model are 100 MPa and 0.297 g/cc respectively. Figure 4-9a show the changes in the value of the Total Strain Energy Density of the superior and middle vertebral bodies after every iterative step, as the remodelling was carried out. The changes during the external and internal remodelling are presented on the same Figure for the purpose of comparison. Figure 4-9b shows the changes of the above parameters for the whole model.

4.2.3.1 Discussion of Results

From the Figure 4-7b it could be seen that the remodelled shapes of the superior and middle vertebral bodies resemble that of an actual vertebral body. The shape of the middle vertebral body is more close to the actual one as the boundary effects are minimized due to the isolation from the boundary conditions. The inward curvatures in the lateral and at the endplate regions are similar to that of an actual one. The 3-dimensional model with the 2 motion segments has in fact brought out more closely the normal optimized shape of a vertebral body because of its 3D nature. The results obtained through the 3D model are more reliable as the model is a closer representation of the actual spinal motion segment. Thus the remodelled shape of the vertebral body obtained through the adaptive optimization



a. Initial model



b. Final model

Figure 4-7. External remodelling of 3D, 2 motion segments: Type I study

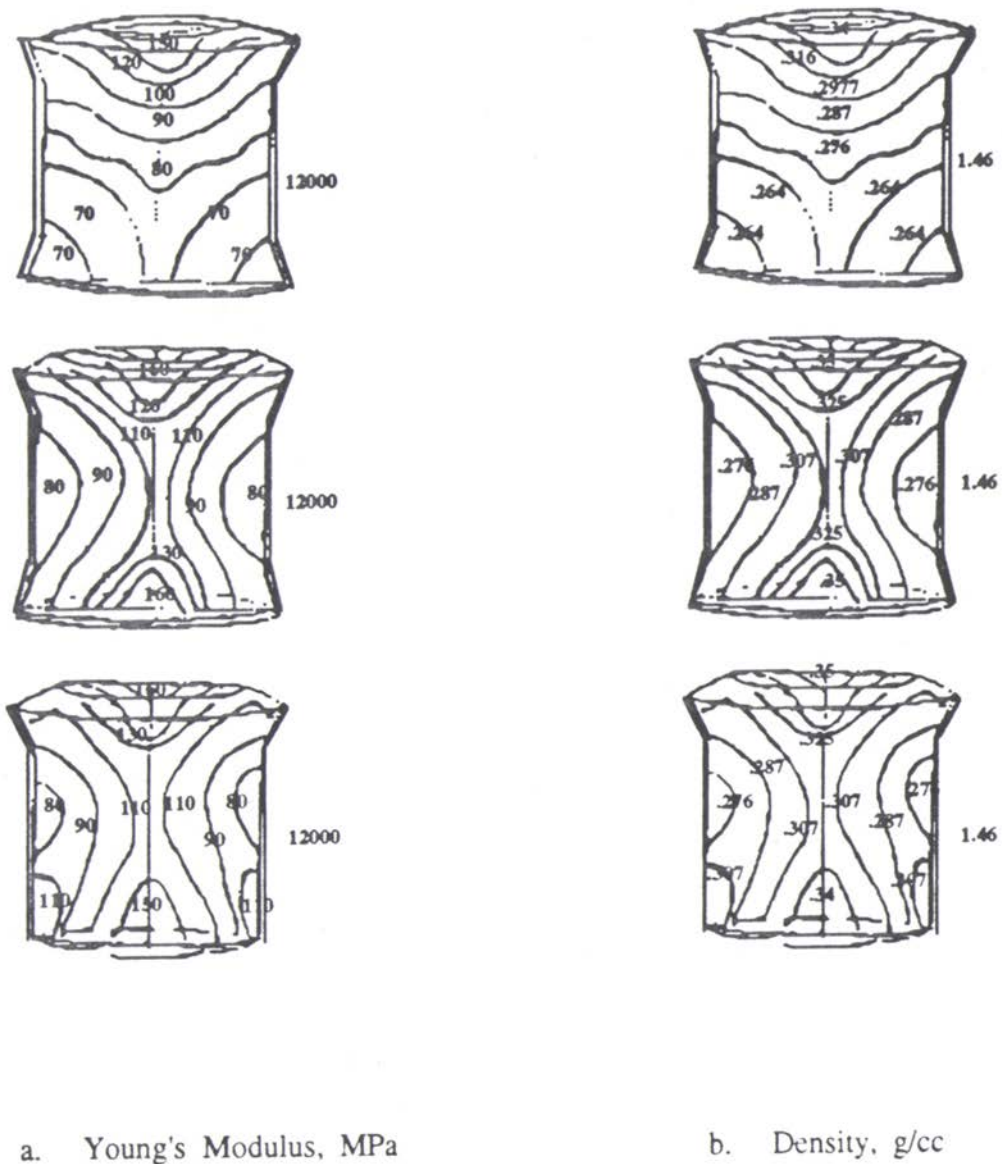
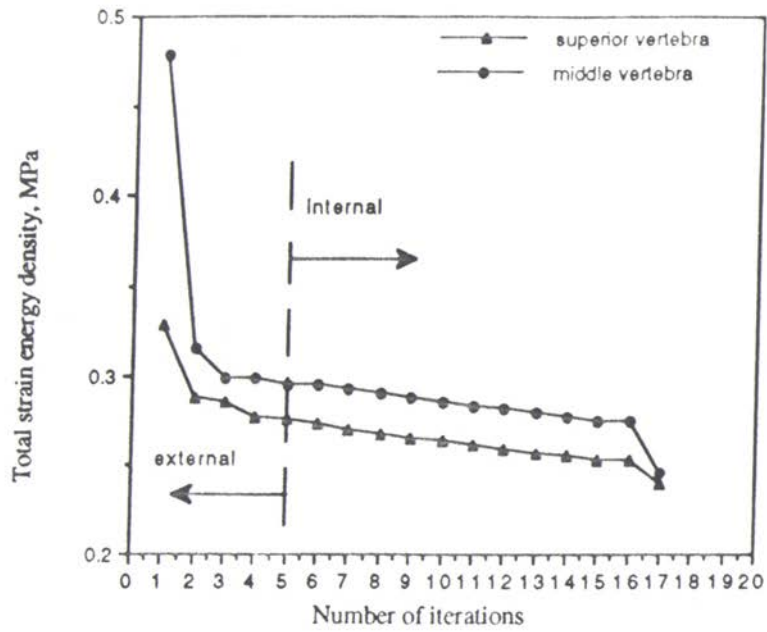
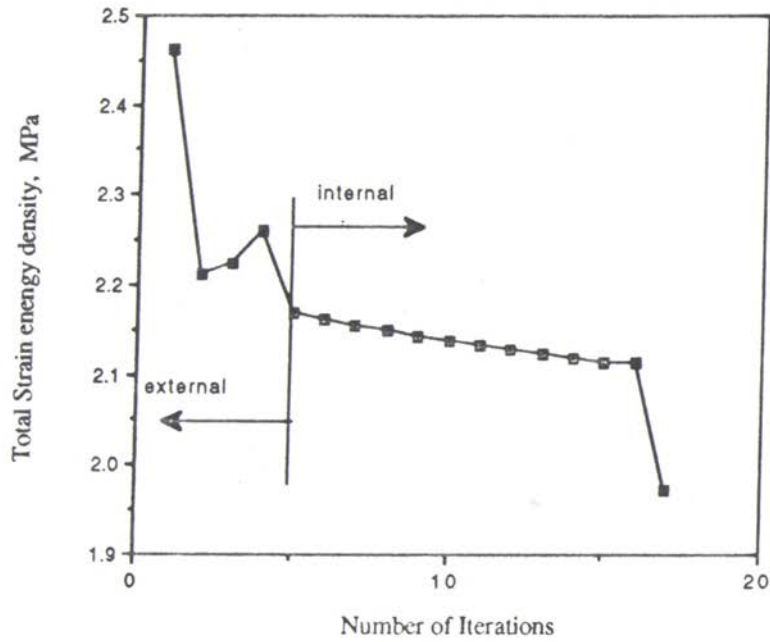


Figure 4-8. Distribution of Young's modulus and Density, after internal remodelling of 3D, 2 motion segments model: Type I study



a. Superior and middle vertebrae



b. Full model

Figure 4-9. Change of TSED with iterations on the 3D model, Type I

procedure closely resembles the actual normal vertebral body there by validating the Wolff's law that bone by itself has an optimized structure under normal conditions.

Figure 4-8a shows the radial distribution of the modulus of elasticity of the cancellous bone for the three vertebral bodies. It could be clearly seen that the central core region of the vertebral bodies have higher values of the modulus of elasticity and the lateral regions have decreased values. This nature is very clearly seen in the case of the middle vertebral body while the superior vertebral body also indicates the same nature of distribution. Thus the results are in close agreement with the experimental results of Keller et al. Even though inferior vertebra exhibits a slightly different distribution, the central region predominantly has higher values of the modulus, despite the influence of the boundary effects. Figure 4-9a shows the reducing trend of the TSED of the superior and middle vertebral bodies along the remodelling iterative sequence. The remodelling study of prediction of internal structure of vertebral bodies has brought out the optimized structure of the vertebral body under normal conditions.

4.3 Results of adaptive remodelling study type II

The adaptive remodelling study type II involves the prediction of adaptive remodelling behaviour of the vertebral body leading to the osteophytic growth. The remodelling is induced by abnormal stress field caused by the injury in the disc created by nucleotomy. All the three different motion segment models were included in this study. The 2-dimensional models were subjected to complete nucleotomy of their discs (for 2 motion segments model, both the discs), while the 3D model was subjected to a partial nucleotomy of its superior intervertebral disc while the inferior disc was kept intact. The right half of the nucleus as seen in the Figure 4-16a, was removed simulating a partial nucleotomy. Both external and internal remodelling were conducted on the 2-dimensional

model, while only shape remodelling study was performed on the 3D model. The results of this study are presented and discussed in the following sections.

4.3.1 Results of 2D one motion segment model(type II study)

Figure 4-10b shows the final shape of the vertebral bodies of 2-dimensional one motion segment model after the type II remodelling study. Figure 4-10a shows the initial model taken for the study, to facilitate comparison. Figure 4-11a and b show the remodelled distribution of modulus of elasticity and density respectively. Figure 4.12 a and b show the changes in the total Strain Energy and volume of the superior vertebral body and the whole model along the iterative sequence of remodelling.

4.3.1.1 Discussion of results

The type II remodelling study following nucleotomy on the 1 motion segment model brought out adaptively modified shape of the vertebral bodies shown by Figure 4-10b. Comparing the Figures 4-10a and b it could be noted that there is growth of the cortical bone at the two edges of the superior endplate region of the inferior body . A similar growth of the inferior end plate of the superior vertebral body at regions just interior to the edges. This type of growth of the endplate regions allows the transfer of load with minimum TSE. Even though the small growth of the of the cortical bone could be predicted by the above study, the total osteophytic growth has contributions from the other sources such as abnormally strained ligaments and the annulus fibrosus. The study also predicts the higher abnormal values of SED in the annulus fibrosus as a result of nucleotomy but the disc is not put through the adaptive remodelling procedure as it is outside the scope of the present work.

The adaptive internal remodelling results following the nucleotomy have yielded modified distribution of modulus of elasticity of the cancellous bone of the of the vertebrae. In the modified distribution there is no distinct high values in the central core region of the

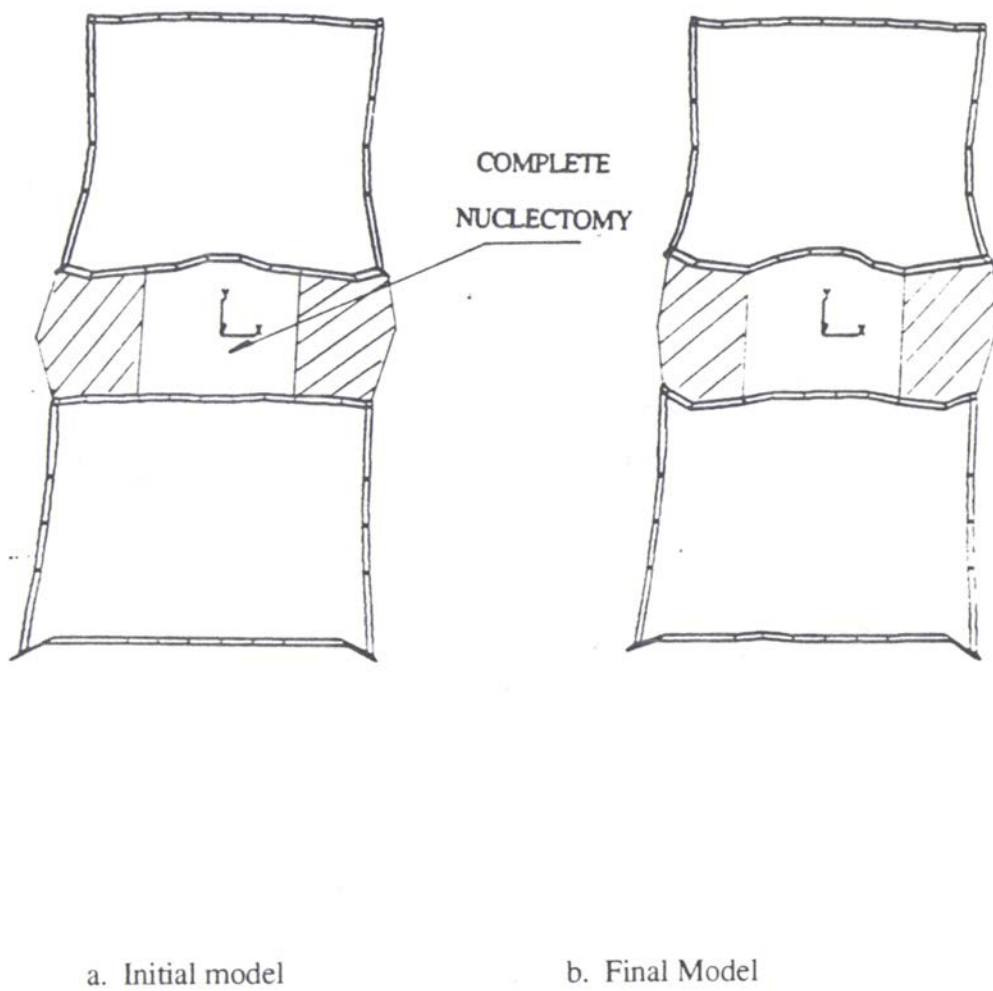
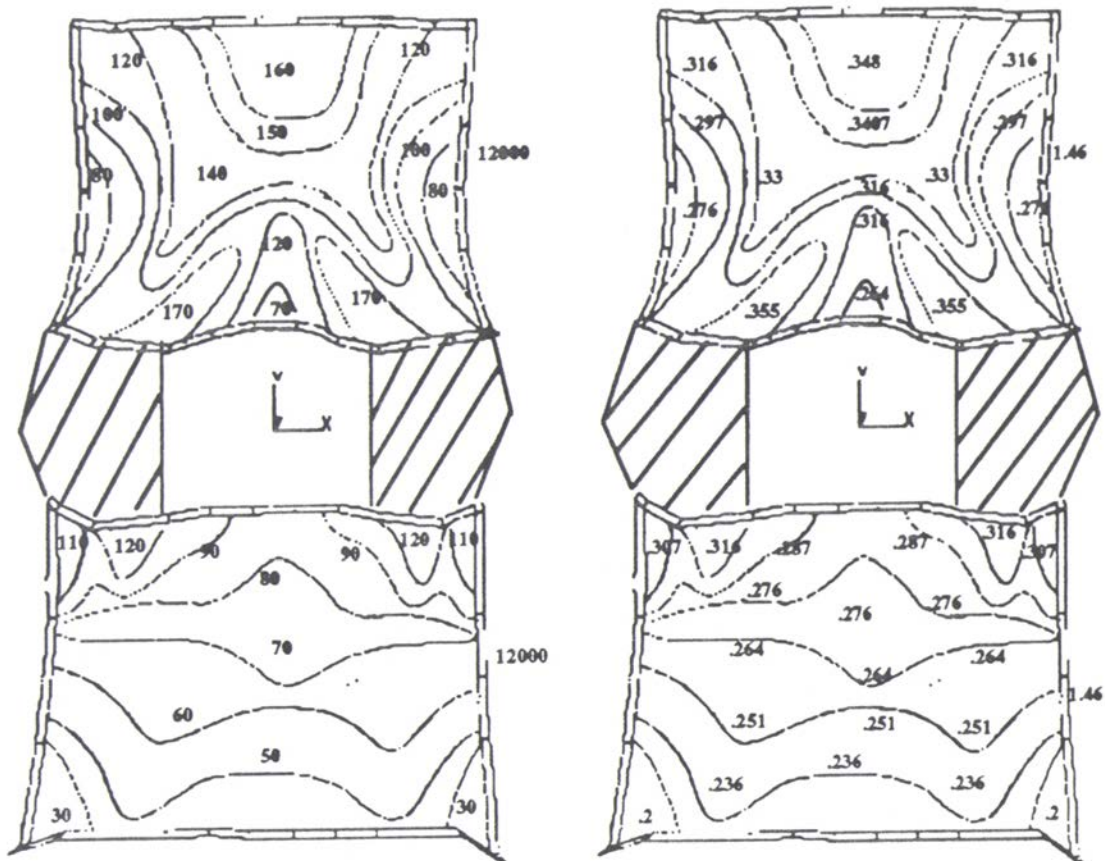


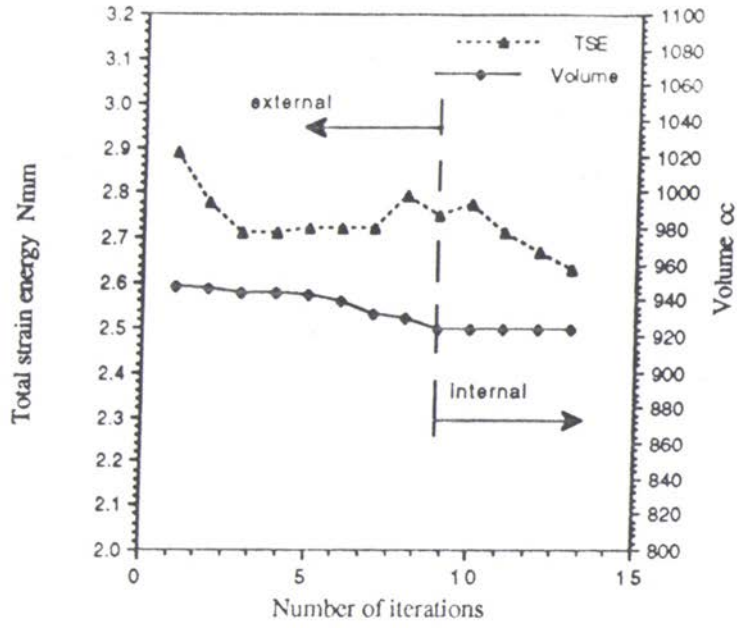
Figure 4-10. External remodelling following Nucleotomy of 2D, 1motion segment model: Type II study



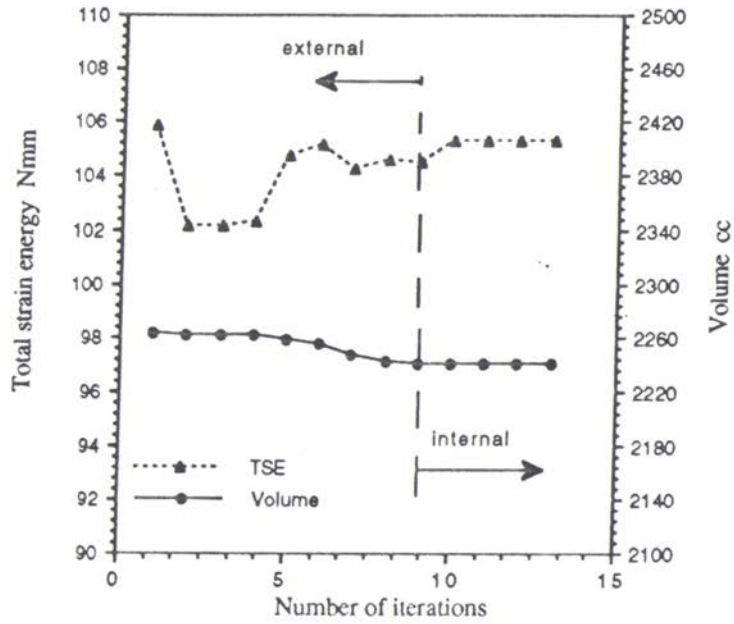
a. Young's Modulus, MPa

b. Density, g/cc

Figure 4-11. Internal remodelling following Nucleotomy of 2D, 1motion segment model: Type II study



a. Superior vertebra



b. Full model

Figure 4-12. TSE and Volume of 1 motion segment model, Type II study

vertebral bodies. The modulus values are more uniformly distributed within a plane passing parallel to the endplates at different heights of the vertebral bodies even though there is slight variation between different planes and reduction in values at the regions very close to the cortical bone. This kind of redistribution is in agreement with the Keller's experimental results which suggest that there is no strong central core of the vertebral trabeculae in the vertebral bodies of spinal motion segment with injured discs. From Figures 4-12a and b it could be seen that the adaptive remodelling following nucleotomy reduces the TSE and volume of the superior vertebral body and the whole model.

4.3.2 Results of 2-dimensional two motion segments model

In the type II study, the two motion segments model with the vertebral bodies having optimal shape and internal structure, obtained through the type I remodelling study, was modified to create total nucleotomy. The elements representing the nucleus pulposus of both the intervertebral discs were removed to simulate the nucleotomy. The resulting model was subjected to the same loading conditions as in the case of type I study (35 N uniformly distributed compressive load at the top end plate of the superior vertebral body) and the type II study was carried out on the model as explained in chapter 3. Figure 4-13b shows the final shape of the vertebral bodies of 2-dimensional two motion segments model after the type II remodelling study. Figure 4-13a shows the initial model taken for the study, to facilitate comparison. Figure 4-14a and b show the remodelled distribution of modulus of elasticity and density respectively. Figure 4-15a, b and c show the changes in the total Strain Energy of the superior and middle vertebral bodies and the whole model along the iterative sequence of remodelling.

4.3.2.1 Discussion of results

The type II remodelling study following nucleotomy on the 2 motion segments model brought out adaptively modified shape of the vertebral bodies shown by Figure 4-14b. Comparing the Figures 4-14a and b it could be noted that there is growth of the cortical bone at the two edges of the inner endplate region of the superior and middle vertebral bodies. The study also predicts the higher abnormal values of SED in the annulus fibrosus as a result of nucleotomy but the disc is not put through the adaptive remodelling procedure as it is outside the scope of the present work.

The adaptive internal remodelling results following the nucleotomy have yielded modified distribution of modulus of elasticity of the cancellous bone of the of the vertebrae. In the modified distribution there is no distinct high values in the central core region. In general the modulus values are more uniformly distributed with in a plane passing parallel to the endplates at different heights of the vertebral bodies, except in the regions very close to the end plates. Near the end plate regions the cancellous bone is stronger away from the central region(just above the position of nucleus pulposus), that is near the region of edges. This is due to the increase in the load transferred through the annulus fibrosus in the absence of the nucleus pulposus. In the case of the middle vertebral body the strength of the central core region is slightly lower than the lateral regions and this nature is opposite to the case with the normal intact disc. This kind of redistribution is in agreement with the Keller's experimental results which suggest that there is no strong central core of the vertebral trabeculae in the vertebral bodies of spinal motion segment with injured discs.

Figure 4-15a shows a reduction in the TSE of the superior vertebral body along with the reduction in the volume. Figure 4-15b shows reduction in the TSE of the middle vertebral body along with some increase in volume predicting the osteophytic type of growth. Figure 4-15c shows the reduction in the TSE along with a slight increase in the overall volume of the model.

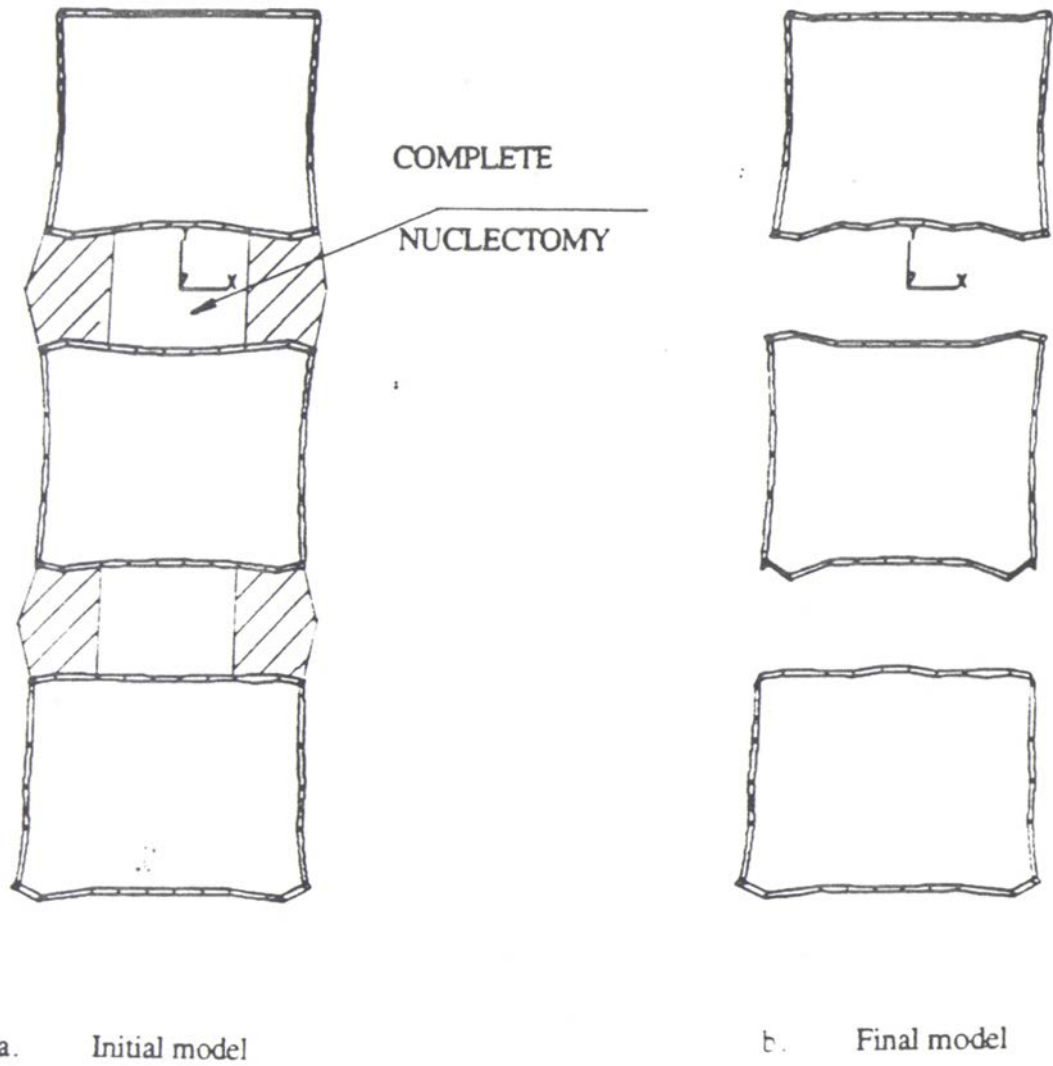


Figure 4-13. External remodelling following Nucleotomy of 2D, 2motion segment model: Type II study

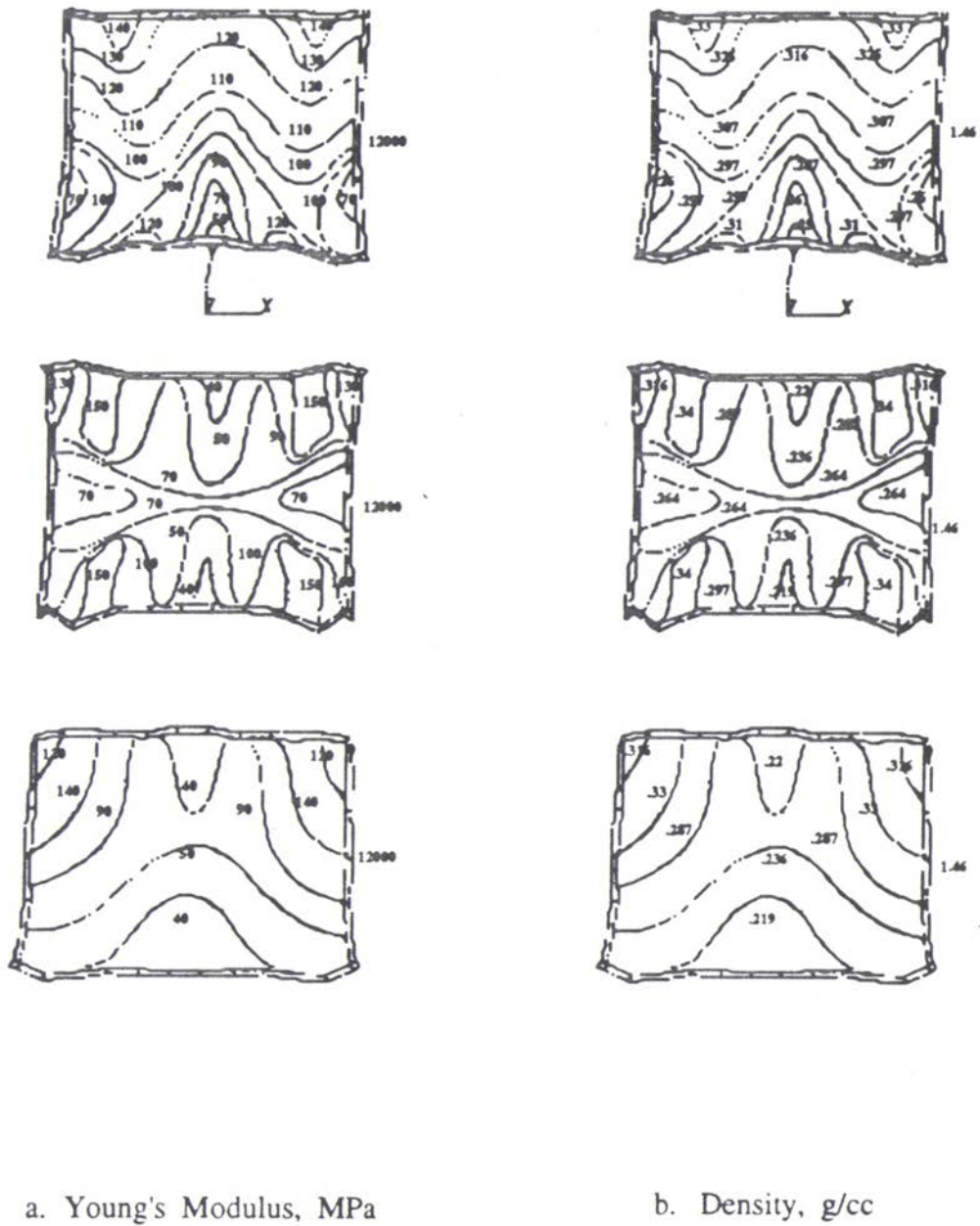
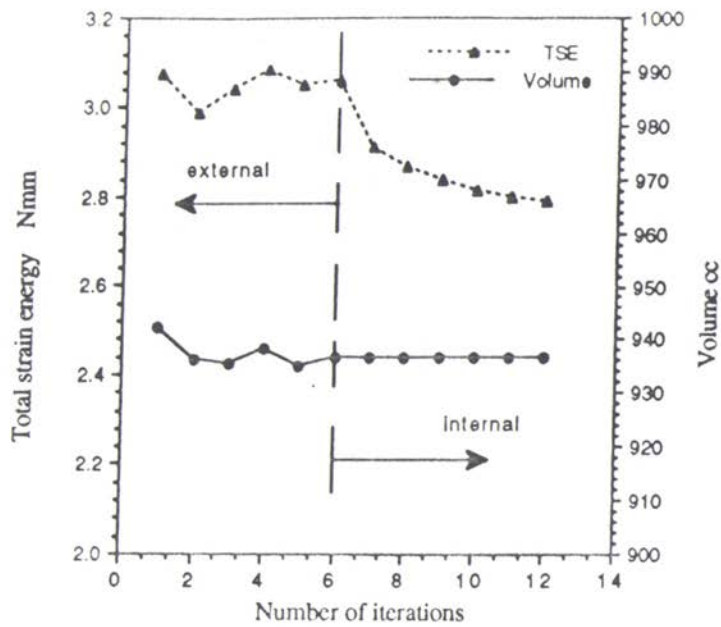
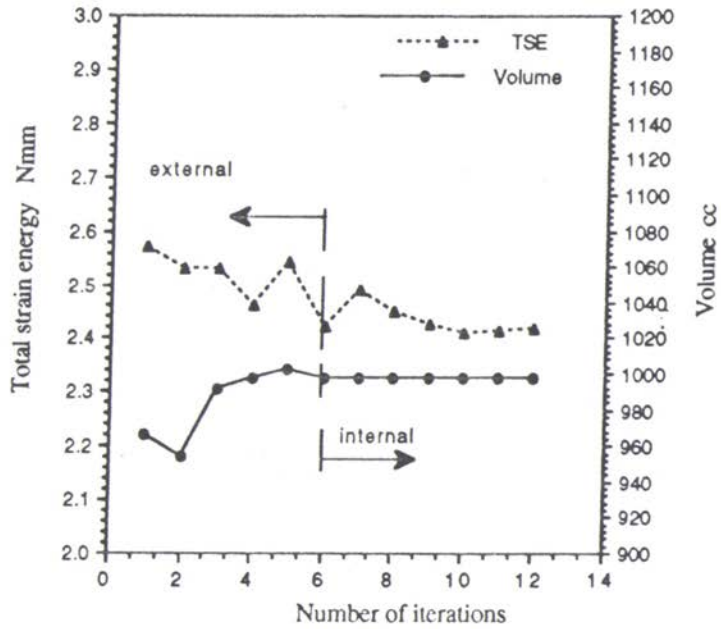


Figure 4-14. Internal remodelling following Nucleotomy of 2D, 2motion segment model: Type II study

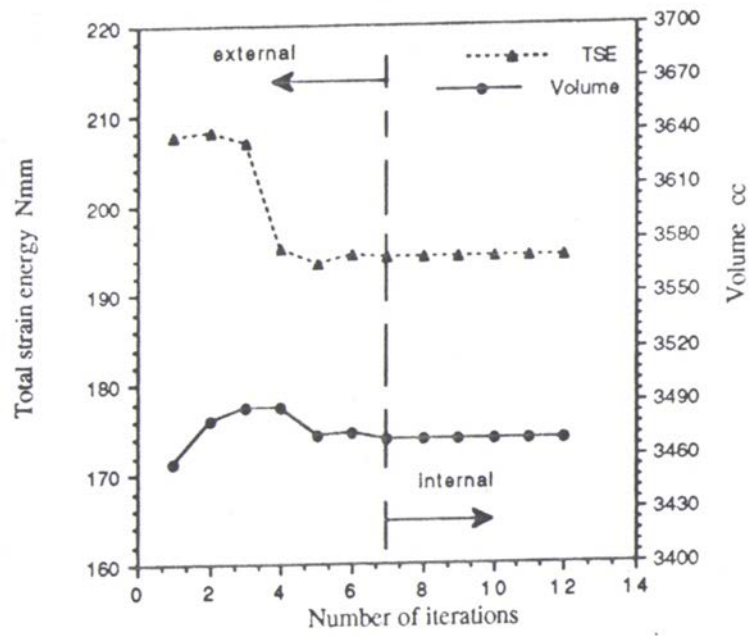


a. Superior vertebra



b. Middle vertebra

Figure 4-15. TSE and Volume of 2D, 2 motion segments model, Type II



c. Full model

Figure 4-15. Continued

4.3.3 Results of 3-Dimensional two motion segments model

In the type II study, the 3-Dimensional two motion segments model with the vertebral bodies having optimal shape and internal structure, obtained through the type I remodelling study, was subjected to partial nucleotomy. A part of the elements representing the nucleus pulposus of superior intervertebral disc(right half of the nucleus as seen in Figure 4-16a was removed) were removed to simulate a partial nucleotomy. The inferior disc was kept intact. Figure 4-16 also shows a cross sectional view of the superior intervertebral disc(cross section created by a horizontal plane passing through of the mid-plane of the superior intervertebral disc). The resulting model was subjected to the same loading conditions as in the case of type I study. Figure 4-16b shows the final shape of the vertebral bodies of 3-Dimensional two motion segments model after the type II remodelling study. Figure 4-16a shows the initial model taken for the study, to facilitate comparison. Figure 4-17a and b show the changes in the total Strain Energy of the superior and middle vertebral bodies and the whole model along the iterative sequence of remodelling.

4.3.3.1 Discussion of results

By comparing the Figures 4-16a and b, it can be observed that there is significant growth of the cortical bone in the superior and middle vertebral segments at the end plate regions adjacent to the nucleotomised disc as shown by Figure 4-16b. There is no significant remodelling in the inferior vertebral body and the lower end plate of the middle vertebra as the disc in-between these vertebral bodies was kept intact. The partial nucleotomy of the superior disc has induced abnormal stresses near the endplate regions adjacent to the disc, of the vertebral bodies and the subsequent external remodelling has caused the osteophytic type growth at the endplate regions. The nature of growth of the superior vertebral body is different from that of the inferior one. The growth of the cortical

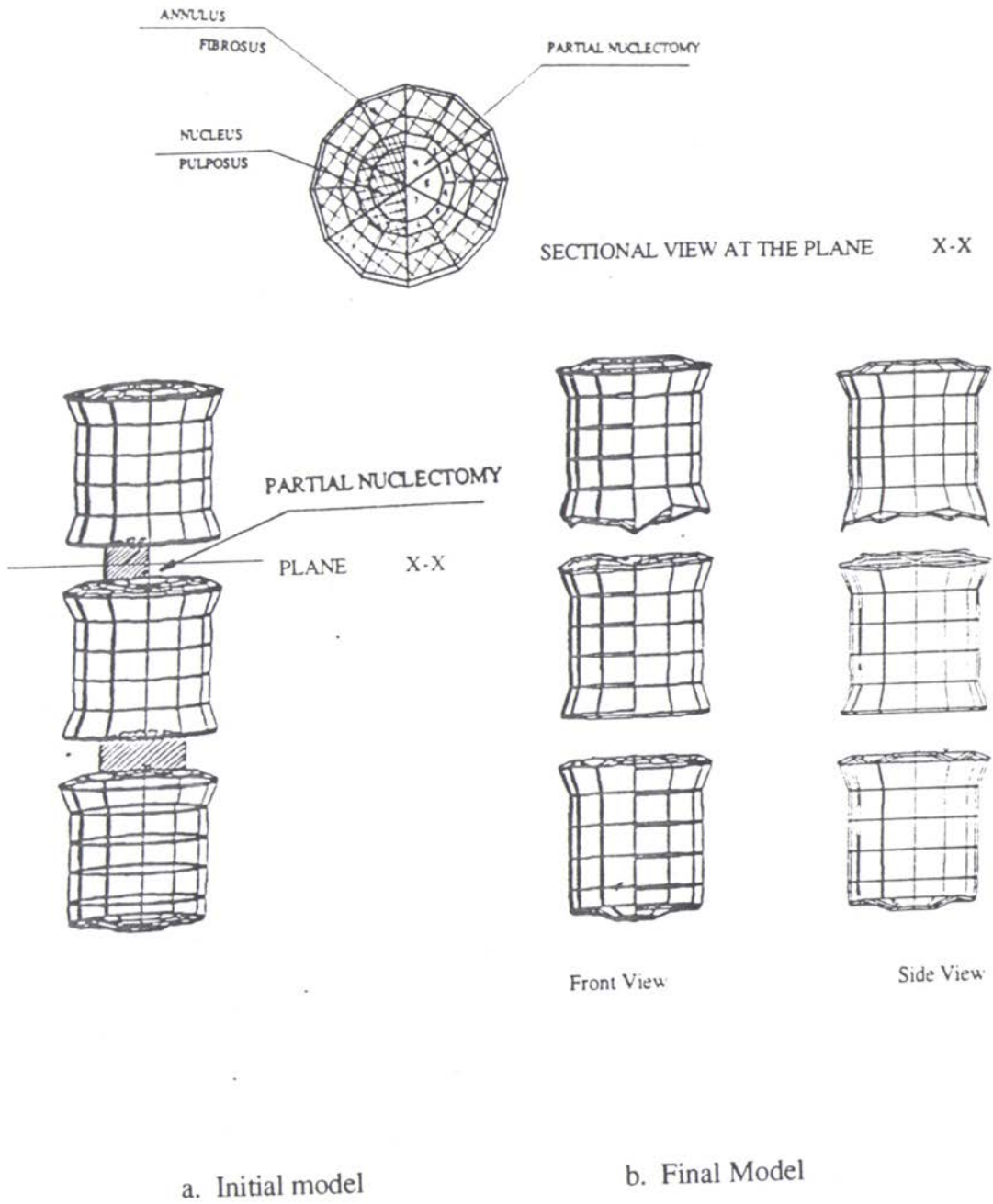
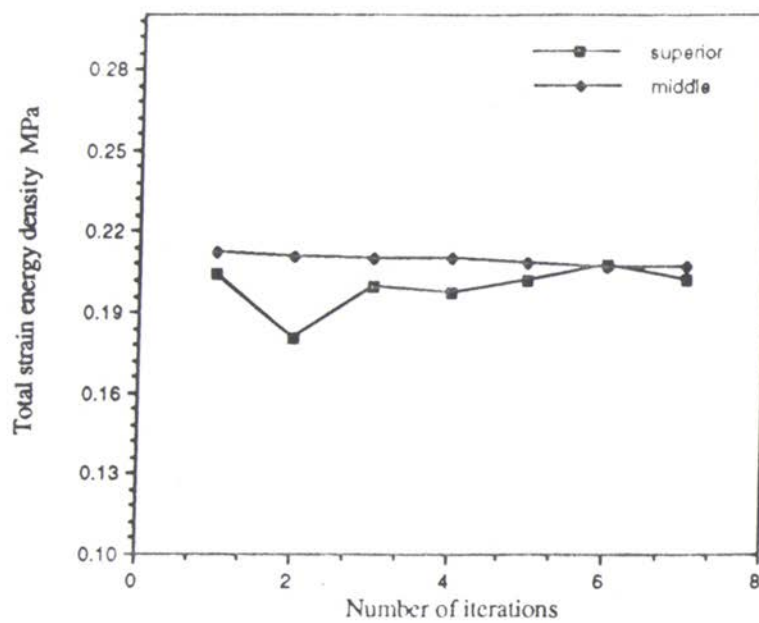
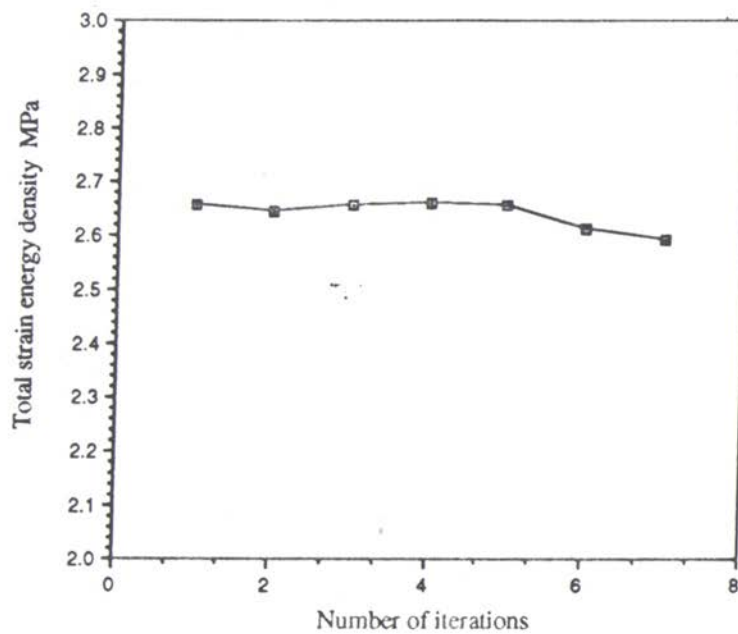


Figure 4-16. External remodelling following partial nucleotomy of 3D, 2motion segment model: Type II study



a. Superior and middle vertebrae



b. Full model

Figure 4-17. Change of TSED with iterations on the 3D model, Type II

bone is at the edges in the superior body where as it is just interior to the edges of the end plate in the middle vertebral body. Secondly the growth of the bone is on the side of the intact part of nucleus for the middle vertebral body where as for the superior vertebral body the growth of the bone is on three regions of its inferior end plate on the side of nucleotomised half of the body, with the major growth in the side opposite to that of the middle body. Thirdly a general observation for all the three cases of the type II study is that the cortical bone of the end plate region grows towards the disc in order to minimize its abnormal increase in strain energy caused by the injury in the disc.

Figure 4-17a shows the gradual reduction in the TSED of the middle vertebral body while the TSED of the superior vertebral body undergoes a oscillative pattern and finally attains a slightly reduced value. Figure 4-17b shows the reduction in the TSED of the whole model as a result of adaptive remodelling.

It is of importance to note here that the nature of growth of the bone may not be the exact representation of one that would occur in the actual vertebral body as the present model is a simplified version of the motion segment. But by observing from the present simplified model the nature of growth patterns due to nucleotomy, the remodelling study can be extended to the more complex model involving all the constituent parts.

4.4 Results of adaptive remodelling study type III

The type III adaptive remodelling study involves the prediction of shape remodelling behaviour of the vertebral bodies of the spinal motion segments, caused by stress shielding following the fixation of a plate connecting two vertebral bodies. This study was conducted on the 3-Dimensional model. The 3-Dimensional two motion segments model with vertebral bodies having the optimal shape and internal structure, obtained through the type I remodelling study, was subjected to partial nucleotomy of the upper intervertebral disc(between the superior and middle vertebral bodies). A plate was

fixed connecting the two adjoining vertebral bodies of the injured disc. The driving force for the remodelling is the deviation of the average nodal SED of the cortical bone of the injured model from the corresponding homostatic SED of the intact model.

The remodelling behaviour was studied by performing the remodelling iterations using FE stress analysis in combination with the application of external remodelling equations using FORT III program. The shape of the vertebral bodies were modified after every iteration using the new nodes obtained through the solution of remodelling equations. The iterations were continued until the total Strain Energy of the vertebral bodies were minimized.

Figure 4-18b shows the final shape of the vertebral bodies of 3-Dimensional two motion segments model after the type III remodelling study. Figure 4-18a shows the initial model taken for the study, to facilitate comparison. Figure 4-19a shows the changes in the total Strain Energy of the superior and middle vertebral bodies and Figure 4-19b of the whole model along the iterative sequence of remodelling.

4.4.1 Discussion of results

The nature of shape remodelling of the vertebral body segments following the fixation of stabilizer plate on partially nucleotomised disc model could be seen from the comparison of Figures 4-18a and b. The first observation would be that the extent of shape change with the plate is less compared to the one with out the plate namely that of the type II study involving only the partial nucleotomy of the disc. The abnormal growth of the cortical bone of the superior vertebral body near the inferior end plate region is minimized to a considerable extent. The superior end plate of the middle vertebral body remodelled by growing in the side opposite to that of the stabilizer plate. Also there is a small resorption in the lower end plate of the middle vertebral body on the side same as that of the fixator plate. Thus fixing a stabilizer plate in fact reduces the abnormality caused by the

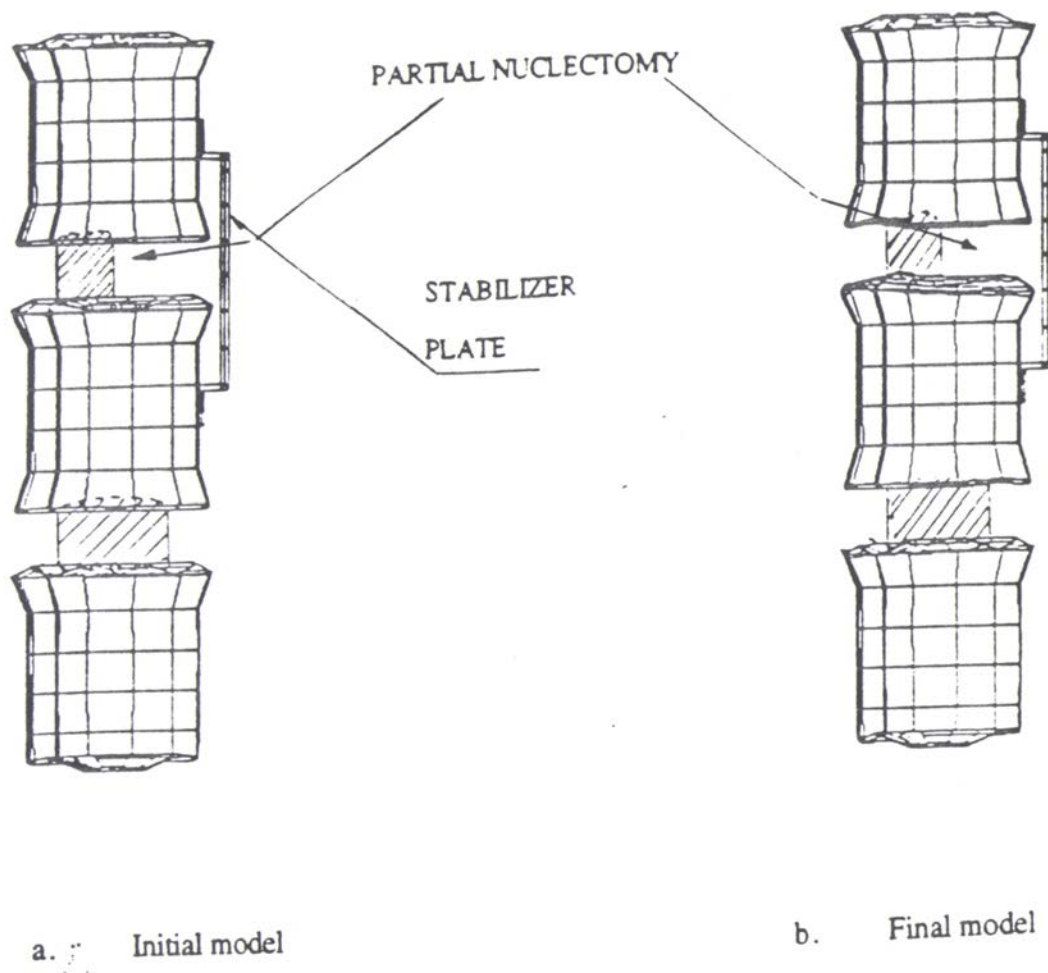
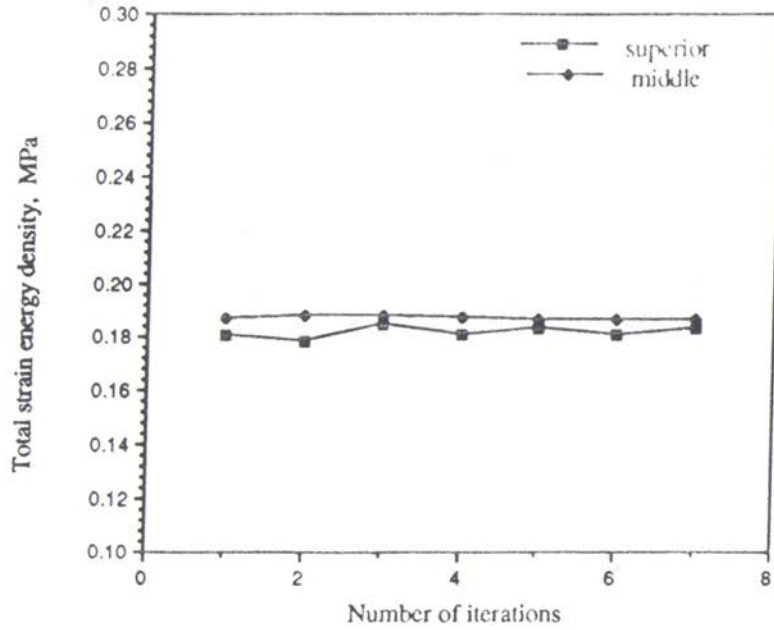
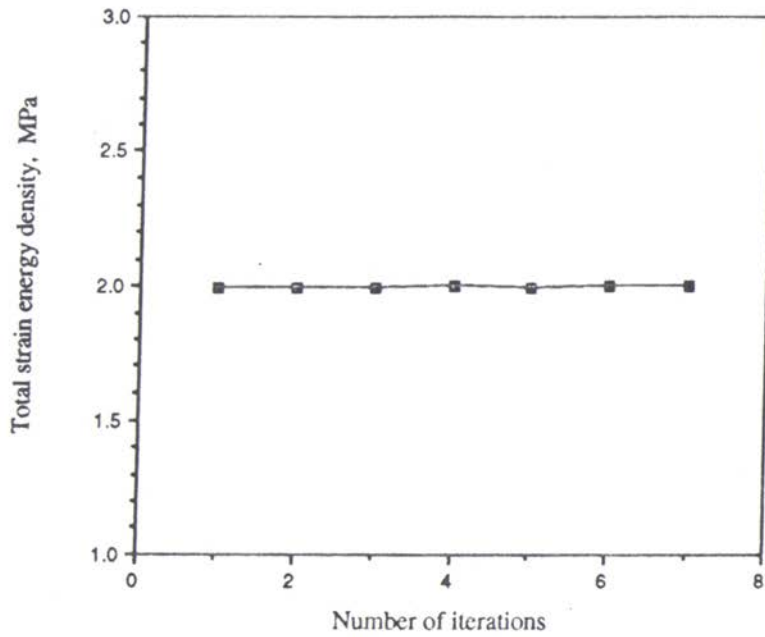


Figure 4-18. External remodelling following fixation of stabilizer plate on the partially nucleotomized 3D, 2 motion segments model: Type II study



a. Superior and middle vertebrae



b. Full model

Figure 4-19. Change of TSED with iterations on 3D model with plate, Type III

injury of the disc. But it is important to note that the stabilizer plate should be placed in the same side as that of the injury in the disc(the side of the part of the nucleus which has been removed) in order to bring the stabilizing effect. Also placing of a plate would not completely get rid of changing of shape of the vertebral body.

Thus it is important with respect to the remodelling of the vertebral body, to take extreme care in placement of the plate or any stabilizing reinforcements in order to avoid abnormal growth of the vertebral bodies or allowing certain degree of growth that would increase the stability of the motion segment.

4.5 General discussion on the studies and the results

The adaptive bone remodelling studies carried out on the vertebral bodies of the spinal motion segments have yielded satisfactory results with reference to the general trends both in the cases of shape(external) and structural(internal) remodelling. The type I study of prediction of normal shape and structure of the vertebral bodies has resulted in the prediction of shapes and structures(in the cases 2 motion segments models) which are in considerably close agreement with the actual vertebral bodies. The boundary conditions found to affect the local remodelling behaviour of the vertebral bodies. This effect of boundary conditions was minimised by using 2 motion segments models where the middle vertebral body was isolated from the boundary effects. The remodelling behaviour following the nucleotomy as predicted by the type II studies has tendencies comparable to that of the actual cases such as formation of osteophytic type of growth. The type III study on the 3D model, remodelling following the fixation of a plate has yielded results which are reasonable but needs to be studied to a great extent as the variability involved in these cases are quite high. The assumption that the bone of the vertebral body, for the present study, considered as isotropic in its properties is to simplify model analysis and the

subsequent remodelling as the study is a first step in the direction of more accurate remodelling predictions.

Also in all the studies conducted the external remodelling preceded the internal remodelling. The argument that which remodelling should precede the other is still not definite. One can separate these two remodelling behaviours and study them as one is occurring after the other choosing one of them to precede the other. Alternately one can study both of them as a simultaneous events and alternate the remodelling iterations accordingly. In any case a great deal of experimental study need to be conducted to arrive at the remodelling coefficients and the rate at which the remodelling proceeds in the actual cases.

4.5.1 Comparison of the three different models

The 2-dimensional one motion segment model was the most simplified model that was employed for the remodelling study. The effect of boundary loading and constraint conditions was the most in this model. As a consequence the remodelling behaviour of this model did not closely resemble that of a real one. The use of 2 motion segments model effectively reduced the influence of boundary conditions. As a result of this the middle vertebral body of the 2 motion segments model remodelled resembling more closely that of a real case. The 2D two motion segments model could effectively predict the external and internal remodelling behaviour of the vertebral body. In any case an actual spine specimen is a 3D structure. So the use of 2D models would have limitations in their ability to represent the actual loading configuration. Thus the 3-dimensional two motion segments model used in the present study was the closest to reality among the selected models. The adaptive remodelling behaviour of the vertebral bodies predicted using the 3D model was in close agreement with the real case. The remodelling behaviour near the end plate regions and the external surfaces very closely resemble that of a real case.

Thus the 3D model used in the present study was the most effective model among the models used. The further improvements such as addition of ligaments and posterior elements have to be done on this model to make a true representation of spinal motion segments.

Having carried out the studies and examined the results it is important to consider the limitations as well as the beneficial aspects of the present study.

4.5.2 Limitations

Even though the trends of the results obtained appear to be towards that of the actual cases there are limitations related to the present studies which need to be discussed here. Firstly the spinal motion segment models considered in the present work are simplified Finite element models of the real ones. The vertebral body of the spinal motion segment considered in the models are without the posterior elements, which are quite intricate in their shape and structure. There are no ligaments incorporated in the models. There are dimensional effects as two of the models studied are 2-dimensional in nature and may not possibly represent the behaviour of the actual motion segments which are 3-dimensional structures.

Secondly, the mathematical representation of the remodelling behaviour of the bone(vertebral body) is dependent on the remodelling coefficient employed. The values of these coefficients are arbitrary in nature and only the final shapes and structures obtained at the end of iterations are valid to be considered for discussion. This is due to the involvement of the time factor in the coefficient, which is eliminated if we consider final remodelled shape or structure is outside the domain of time related change, which is a rational assumption.

Thirdly, only one type of loading is considered for the remodelling behaviour, which is axial compressive load. This could prove insufficient to predict the complete

remodelling behaviour of the vertebral body, under different loading conditions, that a normal actual spine would undergo. Fourthly the boundary loading conditions employed at the vertebral end plates may not be true representation of the actual nature of loading(stress conditions) acting on the actual vertebral body. Finally the studies consider the remodelling behaviour only of bone and not any other part such as disc or ligaments connecting the vertebral bodies which would occur in the real spine.

Having seen the different limitations of the study undertaken it is also important to see the positive and useful aspects of the study carried out.

4.5.3 Usefulness and importance of the present study

The application of theory of adaptive bone remodelling behaviour to the spinal motion segments has several useful consequences. The study has brought out the capability of the concept of application of adaptive bone remodelling theory to predict quite remarkably the optimising tendency of bone, the vertebral body, reacting to the stress field it is subjected to.

Firstly the 2 motion segments models both 2-dimensional and 3-dimensional ones, have closely predicted the actual(real) optimal shape and internal structure of the vertebral bodies under normal(uninjured or intact) conditions, subjected to compressive loading.

Secondly the tendency of the vertebral body to remodel, following a disc injury simulated by nucleotomy, to form osteophytic type of bone growth near the endplate region has been predicted. Also the internal structural property modifications due to internal remodelling following the nucleotomy were in general agreement with the experimental predictions.

Thirdly the effect of plate on the remodelling behaviour of the vertebral body has been predicted and brought out the usefulness of reinforcements in reducing the extent of remodelling leading to osteophytic formations.

The results obtained may not be exact but they have proved to be in the correct domain. The study needs only fine tuning with the respect to more realistic representation of the models and loading conditions in order to achieve more precise results. The results obtained even using the simplified models are encouraging in that they are in agreement with the experimental results available in the literature.

Considering clinical aspects the results of these studies would lead to the proper treatment procedures in the cases on injuries of spine taking into account the subsequent remodelling behaviour of the motion segments. The study would provide useful input to the design of spinal implants in achieving long term success of the related surgical treatment. In any case a huge body of experimental research in the area of bone remodelling of spine should go in parallel rather precede the theoretical adaptive remodelling studies for the comparisons and corrective modifications in this type of study. This would ensure the precision in which the theoretical adaptive remodelling study could predict the remodelling behaviour of spinal motion segments.

Having discussed the results, limitations and usefulness of the present study it is important to mention here that inspite all limitations of the study it has achieved the objectives with which the study was undertaken. For the first time the adaptive bone remodelling has been applied to vertebral bodies of spinal motion segments yielding satisfactory results.

CHAPTER V

CONCLUSIONS

5.1 Present Study

Adaptive remodelling study on the vertebral motion segments have been carried out for the first time. This study has been undertaken in a period where the factors influencing the bone remodelling behaviour in general, for any bony structure, has not been very well established. Nevertheless there has been considerable quantum of research done and being carried out to explore and apply the bone remodelling tendency to different bones and more specifically to simple bone structures such as femur, ulna and radius. Different remodelling theories have been proposed and followed by different researchers in the course of these studies. Considering the importance of spine and its stability for the normal functioning of the human body, study of bone remodelling applied to spinal motion segments is as much urgent as it is necessary in the clinical perspective considering the number of spine related injuries and defects. In the present study the adaptive bone remodelling theory with SED as the stimulus for remodelling was applied to the spinal motion segment models, for the first time, and the remodelling behaviour of the vertebral bodies were studied.

The study has yielded satisfactory results considering the simplified nature of the motion segment models and the loading conditions. The study could effectively predict the optimal normal shape of a vertebral body with the predicted shapes closely resembling the shapes of the actual vertebral bodies. The optimal internal architecture predicted by the

study compares well with experimental findings available in the literature. The adaptive remodelling performed following the nucleotomy on the discs have predicted the shapes which resemble osteophytic type of growth on the endplate regions of the vertebral bodies. The type III study conducted on the 3D model has shown the effect of stabilizer plates in reducing the osteophytic type of growth on the endplate regions of the vertebral bodies.

The different limitations in the present studies have been discussed in the previous chapter on Results. In spite of different limitations, the present study has achieved the set objectives. The use of simplified models of spinal motion segments is justified considering the complex shape and internal structure of actual motion segments for the first time application of adaptive remodelling theory. The study calls for huge computer programs for the application of the theory to the models along with the FE analysis.

5.2 Future work

The satisfactory nature of results obtained in the present remodelling study would be a great stimulus for the future remodelling studies on spinal motion segments. Finite element models of motion segments resembling more closely the actual spine have to be studied as a further step in the direction. Inclusion of posterior elements and following that addition of ligaments on the models would get the models more close to the actual spinal motion segments while easing the difficulties on the related activities such as development of appropriate computer programs for the application of remodelling theory on the models

A parallel experimental investigations on remodelling of spine are essential to give the necessary information and results for comparing with the computer simulated results of remodelling. In the future study the remodelling of other constituent parts of motion segments, such as disc, ligaments and the posterior elements need to be included in order to achieve more realistic remodelling behaviour. The models could also include the muscular forces and other kinds of loading such as bending and torsion for more realistic

representation of the stresses. The employment of remodelling coefficients for each of the parts and the selection of appropriate parameter as the stimuli for remodelling call for tremendous amount of experimental and theoretical investigations on the motion segments. These are the areas towards which future research studies could be pointed for marching forward in the remodelling related studies on the spine.

APPENDIX I
PROGRAM FORT -I

```
DIMENSION SED(200),SEND(600),XN(660),YN(660)
DIMENSION X(660),Y(660),N(660),VOL(200),EN(200),GEL(600)
REAL DELX(600),DELY(600),RCX,RCY,TSED,HSED,SE(200)
REAL DELF(600),DLSEND(600),SENDO(600),FAC(600),RATIO(600)
REAL CTSED,CHSED,EXN(200),EXO(200),DELE(200),RMC,TSE
REAL VOLUME
INTEGER KX(600),MD,NRMN,E,P,Q,R,S,J,W,L,M,V,O,U,T
INTEGER HMT(600),KY(600)
OPEN(7,FILE='STENVOL')
OPEN(8,FILE='Nodes')
OPEN(9,FILE='ALLNEW')
OPEN(10,FILE='REMODNODES')
OPEN(11,FILE='XREMOD1')
OPEN(12,FILE='XREMOD2')
OPEN(13,FILE='YREMOD1')
OPEN(14,FILE='YREMOD2')
OPEN(15,FILE='SED001')
OPEN(16,FILE='OLDSEND')
OPEN(17,FILE='MODK')
```

```

OPEN(18,FILE='REMODNOD2')
OPEN(19,FILE='MODKY')
OPEN(20,FILE='YOUNGOLD')
OPEN(21,FILE='MATSPEC')
OPEN(22,FILE='cancelem')
OPEN(23,FILE='ELSPEC')
OPEN(24,FILE='CANELEM')
do 100, I=1,559
  read(8,*) N(I),X(I),Y(I)
C 41  Format(i9,2f12.5)
      XN(I)=X(I)
      YN(I)=Y(I)
100  continue
      DO 38 J=40,47
      Write(15,37)X(J)
37  Format(F12.5)
38  continue
      dif=-X(42)-14.0
      Dr = (( 1+ ((2*dif*1)/35))**2 )
      CTSED=0
      TSE=0
      VOLUME=0
      do 200 I=1,156
      read(7,*) EN(I),SE(I),VOL(I)
      SE(I)=SE(I)/DR
      SED(I)= SE(I)/VOL(I)

```

```

VOLUME=VOLUME+VOL(I)
TSE=TSE+SE(I)
write(15,*)I,SED(I),VOLUME,TSE

```

```
200 continue
```

```
write(*,*)" give MD value"
```

```
read(*,*)MD
```

```
c UPPER SEGMENT
```

```
c LEFT EX
```

```
SEND( 46 )= (SED( 1 )+sed(2))/2
```

```
SEND( 1 )= ( SED( 1 ) + SED( 15)+sed(19)+sed(2)) / 4
```

```
SEND( 73 )= ( SED( 15 ) + SED(14 )+sed(19)+sed(18)) / 4
```

```
SEND(71 )= ( SED( 14 ) + SED(13 )+sed(18)+sed(17)) / 4
```

```
SEND( 69 )= ( SED(13) + SED( 12)+sed(17)+sed(16)) / 4
```

```
SEND( 67 )= ( SED(12) + SED( 56)+sed(16)+sed(57)) / 4
```

```
SEND(221 )= (SED(56 )+sed(57))/2
```

```
c RIGHT EX
```

```
SEND(24 )=(SED(11)+sed(10))/2
```

```
SEND(22 )= (SED( 11) + SED(23)+sed(24)+sed(10)) / 4
```

```
SEND(91 )= (SED( 23) + SED(22)+sed(24)+sed(25)) / 4
```

```
SEND(93 )= (SED( 22) + SED(21)+sed(25)+sed(26)) / 4
```

```
SEND(95 )= ( SED(21) + SED(20)+sed(26)+sed(27)) / 4
```

```
SEND(97 )= ( SED(20) + SED(66)+sed(27)+sed(65)) / 4
```

```
SEND(199 )= (SED(66)+sed(65))/2
```

```
c TOP UP
```

```
SEND(46 )= SEND( 46 )
```

```
SEND(44 )= (SED( 1) + SED(2)+sed(15)+sed(19)) / 4
```

$$\text{SEND}(42) = (\text{SED}(2) + \text{SED}(3) + \text{sed}(19) + \text{sed}(31)) / 4$$

$$\text{SEND}(40) = (\text{SED}(3) + \text{SED}(4) + \text{sed}(31) + \text{Sed}(40)) / 4$$

$$\text{SEND}(38) = (\text{SED}(4) + \text{SED}(5) + \text{sed}(40) + \text{sed}(39)) / 4$$

$$\text{SEND}(36) = (\text{SED}(5) + \text{SED}(6) + \text{sed}(39) + \text{Sed}(38)) / 4$$

$$\text{SEND}(34) = (\text{SED}(6) + \text{SED}(7) + \text{sed}(38) + \text{sed}(37)) / 4$$

$$\text{SEND}(32) = (\text{SED}(7) + \text{SED}(8) + \text{Sed}(37) + \text{SEd}(36)) / 4$$

$$\text{SEND}(30) = (\text{SED}(8) + \text{SED}(9) + \text{sed}(36) + \text{Sed}(35)) / 4$$

$$\text{SEND}(28) = (\text{SED}(9) + \text{SED}(10) + \text{sed}(35) + \text{sed}(24)) / 4$$

$$\text{SEND}(26) = (\text{SED}(10) + \text{SED}(11) + \text{sed}(24) + \text{Sed}(23)) / 4$$

$$\text{SEND}(24) = \text{SEND}(24)$$

c BOTTOM UNDER

$$\text{SEND}(221) = \text{SEND}(221)$$

$$\text{SEND}(219) = (\text{SED}(56) + \text{SED}(57) + \text{sed}(12) + \text{sed}(16)) / 4$$

$$\text{SEND}(217) = (\text{SED}(57) + \text{SED}(58) + \text{sed}(16) + \text{sed}(28)) / 4$$

$$\text{SEND}(215) = (\text{SED}(58) + \text{SED}(59) + \text{Sed}(28) + \text{sed}(41)) / 4$$

$$\text{SEND}(213) = (\text{SED}(59) + \text{SED}(60) + \text{sed}(41) + \text{sed}(42)) / 4$$

$$\text{SEND}(211) = (\text{SED}(60) + \text{SED}(61) + \text{sed}(42) + \text{sed}(43)) / 4$$

$$\text{SEND}(209) = (\text{SED}(61) + \text{SED}(62) + \text{sed}(43) + \text{sed}(44)) / 4$$

$$\text{SEND}(207) = (\text{SED}(62) + \text{SED}(63) + \text{sed}(44) + \text{sed}(45)) / 4$$

$$\text{SEND}(205) = (\text{SED}(63) + \text{SED}(64) + \text{sed}(45) + \text{sed}(32)) / 4$$

$$\text{SEND}(203) = (\text{SED}(64) + \text{SED}(65) + \text{sed}(32) + \text{sed}(27)) / 4$$

$$\text{SEND}(201) = (\text{SED}(65) + \text{SED}(66) + \text{sed}(27) + \text{sed}(20)) / 4$$

$$\text{SEND}(199) = \text{SEND}(199)$$

c LOWER SEGMENT

c L.OUTER

$$\text{SEND}(264) = (\text{SED}(89) + \text{sed}(88)) / 2.0$$

$$\text{SEND}(278) = (\text{SED}(89) + \text{SED}(121) + \text{sed}(88) + \text{sed}(125)) / 4.0$$

$$\text{SEND}(478) = (\text{SED}(121) + \text{SED}(120) + \text{sed}(124) + \text{sed}(125)) / 4.0$$

$$\text{SEND}(476) = (\text{SED}(120) + \text{SED}(119) + \text{sed}(124) + \text{sed}(123)) / 4$$

$$\text{SEND}(474) = (\text{SED}(119) + \text{SED}(118) + \text{sed}(123) + \text{sed}(122)) / 4$$

$$\text{SEND}(472) = (\text{SED}(134) + \text{SED}(118) + \text{sed}(122) + \text{sed}(135)) / 4$$

$$\text{SEND}(534) = (\text{SED}(134) + \text{sed}(135)) / 2.0$$

c R.OUTER

$$\text{SEND}(275) = (\text{SED}(79) + \text{sed}(80)) / 2$$

$$\text{SEND}(300) = (\text{SED}(79) + \text{SED}(133) + \text{sed}(80) + \text{sed}(129)) / 4$$

$$\text{SEND}(500) = (\text{SED}(133) + \text{SED}(132) + \text{sed}(129) + \text{sed}(128)) / 4$$

$$\text{SEND}(502) = (\text{SED}(131) + \text{SED}(132) + \text{sed}(128) + \text{sed}(127)) / 4$$

$$\text{SEND}(504) = (\text{SED}(130) + \text{SED}(131) + \text{sed}(127) + \text{sed}(126)) / 4$$

$$\text{SEND}(506) = (\text{SED}(130) + \text{SED}(144) + \text{sed}(126) + \text{sed}(143)) / 4$$

$$\text{SEND}(512) = (\text{SED}(144) + \text{sed}(143)) / 2$$

c TOP UP

$$\text{SEND}(264) = \text{SEND}(264)$$

$$\text{SEND}(261) = (\text{SED}(89) + \text{SED}(88) + \text{sed}(125) + \text{sed}(121)) / 4$$

$$\text{SEND}(258) = (\text{SED}(88) + \text{SED}(87) + \text{sed}(125) + \text{sed}(98)) / 4$$

$$\text{SEND}(256) = (\text{SED}(87) + \text{SED}(86) + \text{sed}(98) + \text{Sed}(94)) / 4$$

$$\text{SEND}(309) = (\text{SED}(86) + \text{SED}(85) + \text{sed}(94) + \text{sed}(93)) / 4$$

$$\text{SEND}(307) = (\text{SED}(85) + \text{SED}(84) + \text{sed}(93) + \text{sed}(92)) / 4$$

$$\text{SEND}(305) = (\text{SED}(84) + \text{SED}(83) + \text{sed}(92) + \text{sed}(91)) / 4$$

$$\text{SEND}(303) = (\text{SED}(83) + \text{SED}(82) + \text{sed}(91) + \text{sed}(90)) / 4$$

$$\text{SEND}(269) = (\text{SED}(82) + \text{SED}(81) + \text{sed}(90) + \text{sed}(102)) / 4$$

$$\text{SEND}(267) = (\text{SED}(81) + \text{SED}(80) + \text{sed}(102) + \text{sed}(129)) / 4$$

$$\text{SEND}(272) = (\text{SED}(80) + \text{SED}(79) + \text{sed}(129) + \text{sed}(133)) / 4$$

SEND(275)= SEND(275)

c BOTTOM UNDER

SEND(534)= SEND(534)

SEND(532)= (SED(134) + SED(135)+sed(122)+Sed(118))/ 4

SEND(530)= (SED(135) + SED(136)+sed(122)+sed(95)) / 4

SEND(528)= (SED(136) + SED(137)+sed(95)+Sed(107)) / 4

SEND(526)= (SED(137) + SED(138)+sed(107)+sed(106)) / 4

SEND(524)= (SED(138) + SED(139)+Sed(106)+sed(105))/ 4

SEND(522)= (SED(139) + SED(140)+sed(105)+sed(104))/ 4

SEND(520)= (SED(140) + SED(141)+sed(104)+sed(103))/ 4

SEND(518)= (SED(141) + SED(142)+sed(103)+sed(99)) / 4

SEND(516)= (SED(142) + SED(143)+sed(99)+sed(126)) / 4

SEND(514)= (SED(143) + SED(144)+Sed(126)+sed(130))/ 4

SEND(512)= SEND(512)

DO 905 I=16,19

CTSED= CTSED+SED(I)

READ(20,*)exo(I)

905 CONTINUE

DO 901 I=24,55

CTSED= CTSED+SED(I)

READ(20,*)exo(I)

901 CONTINUE

DO 902 I=90,117

CTSED=CTSED+SED(I)

READ(20,*)exo(I)

902 CONTINUE

```
DO 906 I=122,129
  CTSED= CTSED+SED(I)
  READ(20,*)exo(I)
906 CONTINUE
  CHSED=CTSED/72.0
  Tsed=0
  DO 300 J=1,76
    Read(10,*)NRMN
    I=NRMN
    READ(16,*)SENDO(I)
    TSED=TSED + SEND(I)
    write(*,*)I,TSED,SEND(I)
300 CONTINUE
  Do 1500 J=1,28,1
    READ(17,*)I,KX(I),HMT(I)
1500 CONTINUE
  DO 1550 J=1,48
    READ(19,*)I,KY(I),HMT(I)
1550 CONTINUE
  HSED=(TSED+CTSED)/148
  RCX =300
  RCY =200
  Write(15,*) HSED
c   HSED= 2.7E-03
c   LEFT EX
  DO 350 J=1,14
```

```

READ(11,*)I
DELX(I)= RCX*(SEND(I)-HSED)
Write(15,33) N(I), SEND(I)
33  Format(I4,x,F12.5)
    DELF(I)=(SEND(I)-HSED)
    DLSEND(I)= (SEND(I)- SENDO(I))
    FAC(I)= DLSEND(I)/DELF(I)
    RATIO(I)= DELF(I)/HSED
c   IF (RATIO(I).LT.(-0.25)) GOTO 611
    IF(MD.GT.1) GOTO 511
    GOTO 611
511  CONTINUE
    IF(FAC(I).LT.(0.0)) GOTO 611
    KX(I)= -KX(I)
    HMT(I)=HMT(I)+1
611  CONTINUE
    Delx(i)= - delx(I) * KX(I)
    XN(I) =X(I)+DELX(I)
    WRITE(17,71)I,KX(I),HMT(I)
71  FORMAT(I3,3X,I3,3X,I3)
350  CONTINUE
c   RIGHT EX
    DO 360 J=1,14
    READ(12,*)I
    DELX(I)= RCX*(SEND(I)-HSED)
    Write(15,33) N(I), SEND(I)

```

```

      DELF(I)=(SEND(I)-HSED)
      DLSEND(I)= (SEND(I)- SENDO(I))
      FAC(I)= DLSEND(I)/DELF(I)
      RATIO(I)= DELF(I)/HSED
c     IF (RATIO(I).LT.(-0.25)) GOTO 622
      IF(MD.GT.1) GOTO 522
      GOTO 622
522   CONTINUE
      IF(FAC(I).LT.(0.0)) GOTO 622
      KX(I)= -KX(I)
      HMT(I)=HMT(I)+1
622   CONTINUE
      Delx(i)= delx(I) * KX(I)
      XN(I) =X(I)+DELX(I)
      WRITE(17,71)I,KX(I),HMT(I)
360   CONTINUE
c     TOP OUT
c     LOWER IN
      DO 370 J=1,24
      READ(13,*)I
      DELY(I)= RCY*(SEND(I)-HSED)
      WRITE(15,33) N(I),SEND(I)
      DELF(I)=(SEND(I)-HSED)
      DLSEND(I)= (SEND(I)- SENDO(I))
      FAC(I)= DLSEND(I)/DELF(I)
      RATIO(I)= DELF(I)/HSED

```

```

      GEL(I) = (DLSEND(I))/send(I)
C     IF (RATIO(I).LT.(-0.25)) GOTO 633
c     IF (RATIO(I).GT.(0.5)) GOTO 633
      IF (abs(GEL(I)).lt.(.01)) GOTO 633
      IF(MD.GT.1) GOTO 533
      GOTO 633
533   CONTINUE
      IF(FAC(I).LT.(0.0)) GOTO 633
      KY(I)= -KY(I)
      HMT(I)=HMT(I)+1
633   CONTINUE
      DelY(i)= - delY(I) * KY(I)
      YN(I) =Y(I)+DELY(I)
      WRITE(19,71)I,KY(I),HMT(I)
370   CONTINUE
c     TOP IN
c     LOWER OUT
      DO 380 J=1,24
      READ(14,*)I
      DELY(I)=RCY*(SEND(I)-HSED)
      WRITE(15,33) N(I),SEND(I)
      DELF(I)=(SEND(I)-HSED)
      DLSEND(I)= (SEND(I)- SENDO(I))
      FAC(I)= DLSEND(I)/DELF(I)
      RATIO(I)= DELF(I)/HSED
      GEL(I) = (DLSEND(I))/send(I)

```

```
C    IF (RATIO(I).LT.(-0.25)) GOTO 644
c    IF (RATIO(I).GT.(0.5)) GOTO 644
    IF (abs(GEL(I)).lt.(.01)) GOTO 644
    IF(MD.GT.1) GOTO 544
    GOTO 644
544  CONTINUE
    IF(FAC(I).LT.(0.0)) GOTO 644
    KY(I)= -KY(I)
    HMT(I)=HMT(I)+1
644  CONTINUE
    DelY(i)= delY(I) * KY(I)
    YN(I) =Y(I)+DELY(I)
    WRITE(19,71)I,KY(I),HMT(I)
380  CONTINUE
    DO 500 J=1,76
    READ(18,*)I
    SENDO(I)= SEND(I)
    WRITE(16,*)SENDO(I)
500  CONTINUE
    WRITE(15,*)TSE,VOLUME
    WRITE(*,*)HSED
    XN( 47) = DELX( 46 ) + X(47 )
    XN( 44) = DELX( 46 ) + X(44 )
    XN( 45) = DELX( 46 ) + X(45 )
    XN( 42) = DELX( 46 ) + X(42 )
    XN( 3 ) = DELX( 1 ) + X(3 )
```

```

XN( 2 ) = DELX( 1 ) + X( 2 )
XN( 5 ) = DELX( 1 ) + X( 5 )
XN( 4 ) = DELX( 1 ) + X( 4 )
XN( 76 ) = DELX( 73 ) + X( 76 )
XN( 59 ) = DELX( 73 ) + X( 59 )
XN( 88 ) = DELX( 73 ) + X( 88 )
XN( 79 ) = DELX( 73 ) + X( 79 )
XN( 77 ) = DELX( 71 ) + X( 77 )
XN( 61 ) = DELX( 71 ) + X( 61 )
XN( 89 ) = DELX( 71 ) + X( 89 )
DO 375 I=1,559
X(I)=XN(I)
Y(I)=YN(I)
375 CONTINUE
DO 400 I=1,559
WRITE(9,22)"N,"I,"",X(I),"",Y(I)
22 FORMAT(A3,I3,A1,F10.4,A1,F10.4)
WRITE(8,23)I,X(I),Y(I)
23 FORMAT(I3,6x,F10.4,2x,F10.4)
400 continue
C INTERNAL REMODELLING
RMC=500
CHSED=CTSED/72.0
DO 903 J=1,72
READ(24,*)I
DELE(I) = RMC*(SED(I)-CHSED)

```

```

c      if(dele(I).lt.(0.0))GOTO 88
      EXN(I)= EXO(I)+DELE(I)
      GOTO 89
c 88  EXN(I)=EXO(I)
      89  CONTINUE
      WRITE(21,77)"MP,EX,"I,"",EXN(I)
      write(15,*)I, SED(I)
      77  FORMAT(A6,I3,a1,F10.4)
      EXO(I)= EXN(I)
      903 CONTINUE
      Do 1000 I=1,72
      Read(22,*)e,p,q,r,s,j,W,l,m,V,o,u,t
      WRITE(23,332)"MAT",E
      332 FORMAT(A4,I3)
      write(23,5)"EN","E","",j,"",W,"",l,"",m,"",V,"",o,"",u,"",t
      5  Format(a3,i3,a1,i3,a1,i3,a1,i3,a1,i3,a1,i3,a1,i3,a1,i3)
      WRITE(20,27)exo(e)
      27  format(f12.4)
      1000 CONTINUE
      STOP
      END

```

APPENDIX II
PROGRAM FORT-II

```
DIMENSION SED(400),SEND(1200),XN(1200),YN(1200)
DIMENSION DLSENO(1200)
DIMENSION X(1200),Y(1200),N(1200),VOL(400),EN(400),GEL(1200)
REAL DELX(1200),DELY(1200),RCX,RCY,TSED,HSED
REAL SE(400),Matn
REAL DELF(1200),DLSEND(1200),SENDO(1200)
REAL FAC(1200),RATIO(1200)
REAL CTSED,CHSED,EXN(400),EXO(400),DELE(400)
REAL RMC,TSE,VOLUME
INTEGER KX(1200),MD,NRMN,E,P,Q,R,S,J,W,L,M,V,O,U,T
INTEGER HMT(1200),KY(1200)
OPEN(7,FILE='STENVOL3')
OPEN(8,FILE='Nodes3S')
OPEN(9,FILE='ALLNEW3S')
OPEN(10,FILE='REMODNODE3S')
OPEN(11,FILE='XREMOD13S')
OPEN(12,FILE='XREMOD23S')
OPEN(13,FILE='YREMOD13S')
OPEN(14,FILE='YREMOD23S')
```

```
OPEN(15,FILE='SED0013S')
OPEN(16,FILE='OLDSEND3S')
OPEN(17,FILE='MODK3S')
OPEN(18,FILE='REMODNOD23S')
OPEN(19,FILE='MODKY3S')
OPEN(20,FILE='YOUNGOLD3S')
OPEN(21,FILE='MATSPEC3S')
OPEN(22,FILE='cancelem3S')
OPEN(23,FILE='ELSPEC3S')
OPEN(24,FILE='CANELEM3S')
OPEN(25,FILE='DLSENO3S')
do 100, I=1,1059
read(8,*) N(I),X(I),Y(I)
c 41  Format(i9,2f12.9)
XN(I)=X(I)
YN(I)=Y(I)
100  continue
DO 38 J=40,47
Write(15,37)X(J)
37  Format(F12.5)
38  continue
dif=-X(42)-14.0
Dr = (( 1+ ((2*dif*1)/35))**2 )
CTSED=0
TSE=0
VOLUME=0
```

```

do 200 I=1,156
  read(7,*) EN(I),SE(I),VOL(I)
  SE(I)=SE(I)/DR
  SED(I)= SE(I)/VOL(I)
  VOLUME=VOLUME+VOL(I)
c   write(15,*)I,"",SED(I),"",VOLUME
  TSE=TSE+SE(I)
  write(15,*)I,"",SED(I),"",VOLUME,TSE
c   write(*,*)" The element is" , I
200  continue
  do 201 I=195,284
    read(7,*) EN(I),SE(I),VOL(I)
    SE(I)=SE(I)/DR
    SED(I)= SE(I)/VOL(I)
    VOLUME=VOLUME+VOL(I)
c   write(15,*)I,"",SED(I),"",VOLUME,TSE
    TSE=TSE+SE(I)
    write(15,*)I,"",SED(I),"",VOLUME,TSE
c   write(*,*)" The element is" , I
201  continue
  write(*,*)" give MD value"
  read(*,*)MD
c   UPPER SEGMENT
c   LEFT EX
  SEND( 46 )= (SED( 1 )+sed(2))/2
  SEND( 1 )= (      SED( 1 ) + SED( 15)+sed(19)+sed(2)) / 4

```

$$\text{SEND}(73) = (\text{SED}(15) + \text{SED}(14) + \text{sed}(19) + \text{sed}(18)) / 4$$

$$\text{SEND}(71) = (\text{SED}(14) + \text{SED}(13) + \text{sed}(18) + \text{sed}(17)) / 4$$

$$\text{SEND}(69) = (\text{SED}(13) + \text{SED}(12) + \text{sed}(17) + \text{sed}(16)) / 4$$

$$\text{SEND}(67) = (\text{SED}(12) + \text{SED}(56) + \text{sed}(16) + \text{sed}(57)) / 4$$

$$\text{SEND}(221) = (\text{SED}(56) + \text{sed}(57)) / 2$$

c RIGHT EX

$$\text{SEND}(24) = (\text{SED}(11) + \text{sed}(10)) / 2$$

$$\text{SEND}(22) = (\text{SED}(11) + \text{SED}(23) + \text{sed}(24) + \text{sed}(10)) / 4$$

$$\text{SEND}(91) = (\text{SED}(23) + \text{SED}(22) + \text{sed}(24) + \text{sed}(25)) / 4$$

$$\text{SEND}(93) = (\text{SED}(22) + \text{SED}(21) + \text{sed}(25) + \text{sed}(26)) / 4$$

$$\text{SEND}(95) = (\text{SED}(21) + \text{SED}(20) + \text{sed}(26) + \text{sed}(27)) / 4$$

$$\text{SEND}(97) = (\text{SED}(20) + \text{SED}(66) + \text{sed}(27) + \text{sed}(65)) / 4$$

$$\text{SEND}(199) = (\text{SED}(66) + \text{sed}(65)) / 2$$

c TOP UP

$$\text{SEND}(46) = \text{SEND}(46)$$

$$\text{SEND}(44) = (\text{SED}(1) + \text{SED}(2) + \text{sed}(15) + \text{sed}(19)) / 4$$

$$\text{SEND}(42) = (\text{SED}(2) + \text{SED}(3) + \text{sed}(19) + \text{sed}(31)) / 4$$

$$\text{SEND}(40) = (\text{SED}(3) + \text{SED}(4) + \text{sed}(31) + \text{Sed}(40)) / 4$$

$$\text{SEND}(38) = (\text{SED}(4) + \text{SED}(5) + \text{sed}(40) + \text{sed}(39)) / 4$$

$$\text{SEND}(36) = (\text{SED}(5) + \text{SED}(6) + \text{sed}(39) + \text{Sed}(38)) / 4$$

$$\text{SEND}(34) = (\text{SED}(6) + \text{SED}(7) + \text{sed}(38) + \text{sed}(37)) / 4$$

$$\text{SEND}(32) = (\text{SED}(7) + \text{SED}(8) + \text{Sed}(37) + \text{SEd}(36)) / 4$$

$$\text{SEND}(30) = (\text{SED}(8) + \text{SED}(9) + \text{sed}(36) + \text{Sed}(35)) / 4$$

$$\text{SEND}(28) = (\text{SED}(9) + \text{SED}(10) + \text{sed}(35) + \text{sed}(24)) / 4$$

$$\text{SEND}(26) = (\text{SED}(10) + \text{SED}(11) + \text{sed}(24) + \text{Sed}(23)) / 4$$

$$\text{SEND}(24) = \text{SEND}(24)$$

c BOTTOM UNDER

$$\text{SEND}(221) = \text{SEND}(221)$$

$$\text{SEND}(219) = (\text{SED}(56) + \text{SED}(57) + \text{sed}(12) + \text{sed}(16)) / 4$$

$$\text{SEND}(217) = (\text{SED}(57) + \text{SED}(58) + \text{sed}(16) + \text{sed}(28)) / 4$$

$$\text{SEND}(215) = (\text{SED}(58) + \text{SED}(59) + \text{Sed}(28) + \text{sed}(41)) / 4$$

$$\text{SEND}(213) = (\text{SED}(59) + \text{SED}(60) + \text{sed}(41) + \text{sed}(42)) / 4$$

$$\text{SEND}(211) = (\text{SED}(60) + \text{SED}(61) + \text{sed}(42) + \text{sed}(43)) / 4$$

$$\text{SEND}(209) = (\text{SED}(61) + \text{SED}(62) + \text{sed}(43) + \text{sed}(44)) / 4$$

$$\text{SEND}(207) = (\text{SED}(62) + \text{SED}(63) + \text{sed}(44) + \text{sed}(45)) / 4$$

$$\text{SEND}(205) = (\text{SED}(63) + \text{SED}(64) + \text{sed}(45) + \text{sed}(32)) / 4$$

$$\text{SEND}(203) = (\text{SED}(64) + \text{SED}(65) + \text{sed}(32) + \text{sed}(27)) / 4$$

$$\text{SEND}(201) = (\text{SED}(65) + \text{SED}(66) + \text{sed}(27) + \text{sed}(20)) / 4$$

$$\text{SEND}(199) = \text{SEND}(199)$$

c LOWER SEGMENT

c L.OUTER

$$\text{SEND}(264) = (\text{SED}(89) + \text{sed}(88)) / 2.0$$

$$\text{SEND}(278) = (\text{SED}(89) + \text{SED}(121) + \text{sed}(88) + \text{sed}(125)) / 4.0$$

$$\text{SEND}(478) = (\text{SED}(121) + \text{SED}(120) + \text{sed}(124) + \text{sed}(125)) / 4.0$$

$$\text{SEND}(476) = (\text{SED}(120) + \text{SED}(119) + \text{sed}(124) + \text{sed}(123)) / 4$$

$$\text{SEND}(474) = (\text{SED}(119) + \text{SED}(118) + \text{sed}(123) + \text{sed}(122)) / 4$$

$$\text{SEND}(472) = (\text{SED}(134) + \text{SED}(118) + \text{sed}(122) + \text{sed}(135)) / 4$$

$$\text{SEND}(534) = (\text{SED}(134) + \text{sed}(135)) / 2.0$$

c R.OUTER

$$\text{SEND}(275) = (\text{SED}(79) + \text{sed}(80)) / 2$$

$$\text{SEND}(300) = (\text{SED}(79) + \text{SED}(133) + \text{sed}(80) + \text{sed}(129)) / 4$$

$$\text{SEND}(500) = (\text{SED}(133) + \text{SED}(132) + \text{sed}(129) + \text{sed}(128)) / 4$$

$$\text{SEND}(502) = (\text{SED}(131) + \text{SED}(132) + \text{sed}(128) + \text{sed}(127)) / 4$$

$$\text{SEND}(504) = (\text{SED}(130) + \text{SED}(131) + \text{sed}(127) + \text{sed}(126)) / 4$$

$$\text{SEND}(506) = (\text{SED}(130) + \text{SED}(144) + \text{sed}(126) + \text{sed}(143)) / 4$$

$$\text{SEND}(512) = (\text{SED}(144) + \text{sed}(143)) / 2$$

c TOP UP

$$\text{SEND}(264) = \text{SEND}(264)$$

$$\text{SEND}(261) = (\text{SED}(89) + \text{SED}(88) + \text{sed}(125) + \text{sed}(121)) / 4$$

$$\text{SEND}(258) = (\text{SED}(88) + \text{SED}(87) + \text{sed}(125) + \text{sed}(98)) / 4$$

$$\text{SEND}(256) = (\text{SED}(87) + \text{SED}(86) + \text{sed}(98) + \text{Sed}(94)) / 4$$

$$\text{SEND}(309) = (\text{SED}(86) + \text{SED}(85) + \text{sed}(94) + \text{sed}(93)) / 4$$

$$\text{SEND}(307) = (\text{SED}(85) + \text{SED}(84) + \text{sed}(93) + \text{sed}(92)) / 4$$

$$\text{SEND}(305) = (\text{SED}(84) + \text{SED}(83) + \text{sed}(92) + \text{sed}(91)) / 4$$

$$\text{SEND}(303) = (\text{SED}(83) + \text{SED}(82) + \text{sed}(91) + \text{sed}(90)) / 4$$

$$\text{SEND}(269) = (\text{SED}(82) + \text{SED}(81) + \text{sed}(90) + \text{sed}(102)) / 4$$

$$\text{SEND}(267) = (\text{SED}(81) + \text{SED}(80) + \text{sed}(102) + \text{sed}(129)) / 4$$

$$\text{SEND}(272) = (\text{SED}(80) + \text{SED}(79) + \text{sed}(129) + \text{sed}(133)) / 4$$

$$\text{SEND}(275) = \text{SEND}(275)$$

c BOTTOM UNDER

$$\text{SEND}(534) = \text{SEND}(534)$$

$$\text{SEND}(532) = (\text{SED}(134) + \text{SED}(135) + \text{sed}(122) + \text{Sed}(118)) / 4$$

$$\text{SEND}(530) = (\text{SED}(135) + \text{SED}(136) + \text{sed}(122) + \text{sed}(95)) / 4$$

$$\text{SEND}(528) = (\text{SED}(136) + \text{SED}(137) + \text{sed}(95) + \text{Sed}(107)) / 4$$

$$\text{SEND}(526) = (\text{SED}(137) + \text{SED}(138) + \text{sed}(107) + \text{sed}(106)) / 4$$

$$\text{SEND}(524) = (\text{SED}(138) + \text{SED}(139) + \text{Sed}(106) + \text{sed}(105)) / 4$$

$$\text{SEND}(522) = (\text{SED}(139) + \text{SED}(140) + \text{sed}(105) + \text{sed}(104)) / 4$$

$$\text{SEND}(520) = (\text{SED}(140) + \text{SED}(141) + \text{sed}(104) + \text{sed}(103)) / 4$$

$$\text{SEND}(518) = (\text{SED}(141) + \text{SED}(142) + \text{sed}(103) + \text{sed}(99)) / 4$$

$$\text{SEND}(516) = (\text{SED}(142) + \text{SED}(143) + \text{sed}(99) + \text{sed}(126)) / 4$$

$$\text{SEND}(514) = (\text{SED}(143) + \text{SED}(144) + \text{Sed}(126) + \text{sed}(130)) / 4$$

$$\text{SEND}(512) = \text{SEND}(512)$$

c left ex (3rd segment)

$$\text{SEND}(764) = (\text{SED}(217) + \text{sed}(216)) / 2.0$$

$$\text{SEND}(778) = (\text{SED}(217) + \text{SED}(249) + \text{sed}(216) + \text{sed}(253)) / 4.0$$

$$\text{SEND}(978) = (\text{SED}(249) + \text{SED}(248) + \text{sed}(252) + \text{sed}(253)) / 4.0$$

$$\text{SEND}(976) = (\text{SED}(248) + \text{SED}(247) + \text{sed}(252) + \text{sed}(251)) / 4$$

$$\text{SEND}(974) = (\text{SED}(247) + \text{SED}(246) + \text{sed}(251) + \text{sed}(250)) / 4$$

$$\text{SEND}(972) = (\text{SED}(262) + \text{SED}(246) + \text{sed}(250) + \text{sed}(263)) / 4$$

$$\text{SEND}(1034) = (\text{SED}(262) + \text{sed}(263)) / 2.0$$

c R.OUTER

c $\text{SEND}(775) = (\text{SED}(207) + \text{sed}(208)) / 2$

c $\text{SEND}(800) = (\text{SED}(207) + \text{SED}(261) + \text{sed}(208) + \text{sed}(257)) / 4$

c $\text{SEND}(1000) = (\text{SED}(261) + \text{SED}(260) + \text{sed}(257) + \text{sed}(256)) / 4$

c $\text{SEND}(1002) = (\text{SED}(259) + \text{SED}(260) + \text{sed}(256) + \text{sed}(255)) / 4$

c $\text{SEND}(1004) = (\text{SED}(258) + \text{SED}(259) + \text{sed}(255) + \text{sed}(254)) / 4$

c $\text{SEND}(1006) = (\text{SED}(258) + \text{SED}(272) + \text{sed}(254) + \text{sed}(271)) / 4$

c $\text{SEND}(1012) = (\text{SED}(272) + \text{sed}(271)) / 2$

$$\text{SEND}(775) = \text{SEND}(764)$$

$$\text{SEND}(800) = \text{SEND}(778)$$

$$\text{SEND}(1000) = \text{SEND}(978)$$

$$\text{SEND}(1002) = \text{SEND}(976)$$

$$\text{SEND}(1004) = \text{SEND}(974)$$

$$\text{SEND}(1006) = \text{SEND}(972)$$

SEND(1012)= SEND(1034)

c TOP UP

SEND(764)= SEND(764)

SEND(761)= (SED(217) + SED(216)+sed(253)+sed(249))/4

SEND(758)= (SED(216) + SED(215)+sed(253)+sed(226)) / 4

SEND(756)= (SED(215) + SED(214)+sed(226)+Sed(222)) / 4

SEND(809)= (SED(214) + SED(213)+sed(222)+sed(221)) / 4

SEND(807)= (SED(213) + SED(212)+sed(221)+sed(220)) / 4

c END(805)= (SED(212) + SED(211)+sed(220)+sed(219))/4

c END(803)= (SED(211) + SED(210)+sed(219)+sed(218))/4

c SEND(769)= (SED(210) + SED(209)+sed(218)+sed(230))/4

c SEND(767)= (SED(209) + SED(208)+sed(230)+sed(257))/4

c SEND(772)= (SED(208) + SED(207)+sed(257)+sed(261))/4

c SEND(775)= SEND(775)

SEND(805)=send(807)

SEND(803)=send(809)

SEND(769)=send(756)

SEND(767)=send(758)

SEND(772)=send(761)

SEND(775)=send(764)

c BOTTOM UNDER

SEND(1034)= SEND(1034)

SEND(1032)= (SED(262) + SED(263)+sed(250)+Sed(246))/ 4

SEND(1030)= (SED(263) + SED(264)+sed(250)+sed(223)) / 4

SEND(1028)= (SED(264) + SED(265)+sed(223)+Sed(235)) / 4

SEND(1026)= (SED(265) + SED(266)+sed(235)+sed(234)) / 4

```

SEND(1024)= (SED(266 ) + SED(267 )+Sed(234)+sed(233))/ 4
c SEND(1022)= (SED(267 ) + SED(268 )+sed(233)+sed(232))/ 4
c SEND(1020)= (SED(268 ) + SED(269 )+sed(232)+sed(231))/ 4
c SEND(1018)= (SED(269 ) + SED(270 )+sed(231)+sed(227)) / 4
c SEND(1016)= (SED(270 ) + SED(271 )+sed(227)+sed(254)) / 4
c SEND(1014)= (SED(271 ) + SED(272 )+Sed(254)+sed(258))/ 4
c SEND(1012)= SEND(1012)

SEND(1022)= send(1024)
SEND(1020)= send(1026)
SEND(1018)= send(1028)
SEND(1016)= send(1030)
SEND(1014)= send(1032)
SEND(1012)= send(1034)

DO 905 I=16,19

CTSED= CTSED+SED(I)

READ(20,*)exo(I)

905 CONTINUE

DO 901 I=24,55

CTSED= CTSED+SED(I)

READ(20,*)exo(I)

`901 CONTINUE

DO 902 I=90,117

CTSED=CTSED+SED(I)

READ(20,*)exo(I)

902 CONTINUE

DO 906 I=122,129

```

```
CTSED= CTSED+SED(I)
READ(20,*)exo(I)
906 CONTINUE
DO 907 I=218,245
CTSED= CTSED+SED(I)
READ(20,*)exo(I)
907 CONTINUE
DO 908 I=250,257
CTSED= CTSED+SED(I)
READ(20,*)exo(I)
908 CONTINUE
CHSED=CTSED/108
Tsed=0
DO 300 J=1,114
Read(10,*)NRMN
I=NRMN
READ(16,*)SENDO(I)
TSED=TSED + SEND(I)
write(*,*)I,TSED,SEND(I)
300 CONTINUE
Do 1500 J=1,42,1
READ(17,*)I,KX(I),HMT(I)
1500 CONTINUE
DO 1550 J=1,72,1
READ(19,*)I,KY(I),HMT(I)
1550 CONTINUE
```

```

HSED=(TSED+CTSED)/222
RCX =300
RCY =200
Write(15,*) HSED
c HSED= 2.7E-03
c LEFT EX
DO 350 J=1,21
READ(11,*)I
c write(*,*)"NO PROBLEM HERE"
DELX(I)= RCX*((SEND(I)-HSED)**(2/2) )
Write(15,33) N(I), SEND(I)
33 Format(I4,x,F12.5)
DELF(I)=(SEND(I)-HSED)
DLSEND(I)= (SEND(I)- SENDO(I))
FAC(I)= DLSEND(I)/DELF(I)
RATIO(I)= DELF(I)/HSED
c IF (RATIO(I).LT.(-0.25)) GOTO 611
IF(MD.GT.1) GOTO 511
GOTO 611
511 CONTINUE
IF(FAC(I).LT.(0.0)) GOTO 611
KX(I)= -KX(I)
HMT(I)=HMT(I)+1
611 CONTINUE
Delx(i)= - delx(I) * KX(I)
XN(I) =X(I)+DELX(I)

```

```

WRITE(17,71)I,KX(I),HMT(I)
71  FORMAT(I5,3X,I3,3X,I3)
350  CONTINUE
c    RIGHT EX
      DO 360 J=1,21
      READ(12,*)I
      DELX(I)= RCX*((SEND(I)-HSED)**(2/2) )
      Write(15,33) N(I), SEND(I)
      DELF(I)=(SEND(I)-HSED)
      DLSEND(I)= (SEND(I)- SENDO(I))
      FAC(I)= DLSEND(I)/DELF(I)
      RATIO(I)= DELF(I)/HSED
c    IF (RATIO(I).LT.(-0.25)) GOTO 622
      IF(MD.GT.1) GOTO 522
      GOTO 622
522  CONTINUE
      IF(FAC(I).LT.(0.0)) GOTO 622
      KX(I)= -KX(I)
      HMT(I)=HMT(I)+1
622  CONTINUE
      Delx(i)= delx(I) * KX(I)
      XN(I) =X(I)+DELX(I)
      WRITE(17,71)I,KX(I),HMT(I)
360  CONTINUE
c    TOP OUT
c    LOWER IN

```

```

DO 370 J=1,36
READ(13,*)I
DELY(I)= RCY*((SEND(I)-HSED)**(2/2) )
WRITE(15,33) N(I),SEND(I)
DELF(I)=(SEND(I)-HSED)
DLSEND(I)= (SEND(I)- SENDO(I))
FAC(I)= DLSEND(I)/DELF(I)
RATIO(I)= DELF(I)/HSED
GEL(I) = (DLSEND(I))/send(I)
C   IF (RATIO(I).LT.(-0.25)) GOTO 633
c   IF (RATIO(I).GT.(0.5)) GOTO 633
    IF (abs(GEL(I)).lt.(.01)) GOTO 633
    IF(MD.GT.1) GOTO 533
    GOTO 633
533  CONTINUE
    IF(FAC(I).LT.(0.0)) GOTO 633
    KY(I)= -KY(I)
    HMT(I)=HMT(I)+1
633  CONTINUE
    DelY(i)= - delY(I) * KY(I)
    YN(I) =Y(I)+DELY(I)
    WRITE(19,71)I,KY(I),HMT(I)
370  CONTINUE
c    TOP IN
c    LOWER OUT
DO 380 J=1,36

```

```

READ(14,*)I
DELY(I)=RCY*((SEND(I)-HSED)**(2/2) )
WRITE(15,33) N(I),SEND(I)
DELF(I)=(SEND(I)-HSED)
DLSEND(I)= (SEND(I)- SENDO(I))
FAC(I)= DLSEND(I)/DELF(I)
RATIO(I)= DELF(I)/HSED
GEL(I) = (DLSEND(I))/send(I)
C   IF (RATIO(I).LT.(-0.25)) GOTO 644
c   IF (RATIO(I).GT.(0.5)) GOTO 644
    IF (abs(GEL(I)).lt.(.01)) GOTO 644
    IF(MD.GT.1) GOTO 544
    GOTO 644
544  CONTINUE
    IF(FAC(I).LT.(0.0)) GOTO 644
    KY(I)= -KY(I)
    HMT(I)=HMT(I)+1
644  CONTINUE
    DeLY(i)= delY(I) * KY(I)
    YN(I) =Y(I)+DELY(I)
    WRITE(19,71)I,KY(I),HMT(I)
380  CONTINUE
    DO 500 J=1,114
    READ(18,*)I
    SENDO(I)= SEND(I)
    WRITE(16,*)SEUDO(I)

```

```

500  CONTINUE
      WRITE(15,*)TSE,VOLUME
      WRITE(*,*)HSED
      XN( 47) = DELX( 46 ) + X(47 )
      XN( 44) = DELX( 46 ) + X(44 )
      XN( 45) = DELX( 46 ) + X(45 )
      XN( 42) = DELX( 46 ) + X(42 )
      XN( 3 ) = DELX( 1 ) + X(3 )
      XN( 2 ) = DELX( 1 ) + X( 2 )
      XN( 5 ) = DELX( 1 ) + X( 5 )
      XN( 4 ) = DELX( 1 ) + X( 4 )
      XN( 76) = DELX( 73 ) + X(76 )
      XN( 59) = DELX( 73 ) + X(59 )
      XN( 88) = DELX( 73 ) + X(88 )
      XN( 79) = DELX( 73 ) + X(79 )
      DO 375 I=1,1059
        X(I)=XN(I)
        Y(I)=YN(I)
375  CONTINUE
      DO 400 I=1,1059
        WRITE(9,22)"N,"I,"",X(I),"",Y(I)
22   FORMAT(A3,I5,A1,F12.5,A1,F12.5)
        WRITE(8,23)I,"",X(I),"",Y(I)
23   FORMAT(I5,a1,6x,F12.5,a1,2x,F12.5)
400  continue
C    Internal Remodelling

```

```

RMC=5000
CHSED=CTSED/108
DO 903 J=1,108
READ(24,*)I
DELE(I) = RMC*(SED(I)-CHSED)
c   if(dele(I).lt.(0.0))GOTO 88
EXN(I)= EXO(I)+DELE(I)
MATN= EXO(I)/10.0
GOTO 89
c 88 EXN(I)=EXO(I)
89  CONTINUE
WRITE(21,77)"MP,EX,"NINT(MATN),"",EXO(I)
c  WRITE(21,77)"MP,EX,"I,"",EXN(I)
write(15,*)I, SED(I)
77  FORMAT(A6,I3,a1,F10.4)
CC  EXO(I)= EXN(I)
903 CONTINUE
Do 1000 I=1,108
Read(22,*)e,p,q,r,s,j,W,l,m,V,o,u,t
MATN=EXO(e)/10.0
c  write(23,*)"MAT",E
WRITE(23,332)"MAT",NINT(MATN)
332 FORMAT(A4,I3)
write(23,5)"EN,"E,"",j,"",W,"",l,"",m,"",V,"",o,"",u,"",t
5  Format(a3,i3,a1,i3,a1,i3,a1,i3,a1,i3,a1,i3,a1,i3,a1,i3)
WRITE(20,27)exo(e)

```

```
27  format(f12.4)
1000 CONTINUE
      STOP
      END
```

APPENDIX III
PROGRAM FORT-III

```
DIMENSION SED(3000),SEN2(3000),SEND(3000),DELZ(3000)
DIMENSION DELR(3000)
DIMENSION ZN(3000),RN(3000),R(3000),Z(3000),T(3000)
INTEGER N(3000)
REAL DELF(3000),DLSEND(3000),SENDO(3000),FAC(3000)
REAL CTSED,CHSED,SEN1(3000)
REAL SEN3(3000),EY(2000)
REAL RMC,TSE,VOLUME,TSED,HSED,DELZ1
REAL DELZ2,DELEY,RCXC
INTEGER KR(3000),KZ(3000),KC(3000),HMTR(3000),HMTZ(3000)
INTEGER JR,JC,JZ,MON1,MON2,NUMB
OPEN(7,FILE='STENEND3D')
OPEN(8,FILE='NODES3D')
OPEN(9,FILE='ALLNEW3D')
OPEN(16,FILE='OLDSEND3D')
OPEN(17,FILE='MODKR3D')
OPEN(18,FILE='MODKR3DW')
OPEN(19,FILE='MODKZ3D')
OPEN(20,FILE='MODKZ3DW')
```

```

OPEN(21,FILE='MODKC3D')
OPEN(22,FILE='MODKC3DW')
OPEN(24,FILE='SED3d')
OPEN(25,FILE='MATDESC')
OPEN(26,FILE='OLDYOUNG3D')
OPEN(27,FILE='NEWYOUNG3D')
OPEN(28,FILE='CANCSSED')
DO 210 I=1,1586
READ(8,*)J,R(J),T(J),Z(J)
RN(J)=R(J)
ZN(J)=Z(J)
N(I)=J
210 CONTINUE
write(*,*)"ok here after nodes"
DR=((R(2701)/17.5)**2)**2
write(*,*)"give MD"
read(*,*)md
TSE=0
TSED=0
DO 100 i=1,1278
c   K=1+(J-1)*500
c   M=414+(J-1)*500
c   DO 200 I=K,M
READ(7,*)J,SED(J)
SED(j)=SED(j)/DR
TSED=TSED+SED(j)

```

```
c 200 CONTINUE
100 CONTINUE
    write(*,*)"ok here after seds",SED(J),DR
    HSED=TSED/1242.0
    do 124 j=1,3
    do 125 i=1,5
    DO 126 L=1,4
    M=73+(I-1)*60+(J-1)*500+(L-1)*12
    CTSED=CTSED+SED(M)
    WRITE(28,*)M,SED(M)
126 CONTINUE
125 CONTINUE
124 CONTINUE
    CHSED=CTSED/60
    WRITE(28,*)CTSED,CHSED
    RCXC=16000
    do 121 j=1,3
    do 122 i=1,5
    DO 123 L=1,4
    M=73+(I-1)*60+(J-1)*500+(L-1)*12
    READ(26,*)EY(M)
    DELEY=RCXC*(SED(M)-CHSED)
    EY(M)=EY(M)+DELEY
    If(EY(M).GT.175) GOTO 107
    goto 109
107 EY(M)=175
```

```

109  NUMB=121+(L-1)+(I-1)*10+(J-1)*100
      WRITE(25,87)"*MATERIAL,NAME=CAMAT",NUMB
87   format(a20,i3)
      WRITE(25,88)"*ELASTIC"
      WRITE(25,*)EY(M),"0.3"
88   format(a8)
      WRITE(27,*)EY(M)

123  CONTINUE
122  CONTINUE
121  CONTINUE

C   CIRCUMFRENTIAL CORTICAL ELEMENTS

SEND( 2)=(SED( 2)+SED( 1)+SED( 14)+SED( 13 ) ) /4
SEND( 3)=(SED( 3)+SED( 2)+SED( 15)+SED( 14 ) ) /4
SEND( 4)=(SED( 4)+SED( 3)+SED( 16)+SED( 15 ) ) /4
SEND( 5)=(SED( 5)+SED( 4)+SED( 17)+SED( 16 ) ) /4
SEND( 6)=(SED( 6)+SED( 5)+SED( 18)+SED( 17 ) ) /4
SEND( 7)=(SED( 7)+SED( 6)+SED( 19)+SED( 18 ) ) /4
SEND( 8)=(SED( 8)+SED( 7)+SED( 20)+SED( 19 ) ) /4
SEND( 9)=(SED( 9)+SED( 8)+SED( 21)+SED( 20 ) ) /4
SEND( 10)=(SED( 10)+SED( 9)+SED( 22)+SED( 21 ) ) /4
SEND( 11)=(SED( 11)+SED( 10)+SED( 23)+SED( 22 ) ) /4
SEND( 12)=(SED( 12)+SED( 11)+SED( 24)+SED( 23 ) ) /4
SEND( 102)=SED( 62)+SED( 61)+SED( 74)+SED( 73 )
SEN2( 102)=SED( 2)+SED( 1)+SED( 14)+SED( 13 )
SEND( 102)=(SEND( 102)+SEN2( 102 ) )/8.0
SEND( 103)=SED( 63)+SED( 62)+SED( 75)+SED( 74 )

```

$SEN2(103) = SED(3) + SED(2) + SED(15) + SED(14)$
 $SEND(103) = (SEND(103) + SEN2(103)) / 8.0$
 $SEND(104) = SED(64) + SED(63) + SED(76) + SED(75)$
 $SEN2(104) = SED(4) + SED(3) + SED(16) + SED(15)$
 $SEND(104) = (SEND(104) + SEN2(104)) / 8.0$
 $SEND(105) = SED(65) + SED(64) + SED(77) + SED(76)$
 $SEN2(105) = SED(5) + SED(4) + SED(17) + SED(16)$
 $SEND(105) = (SEND(105) + SEN2(105)) / 8.0$
 $SEND(106) = SED(66) + SED(65) + SED(78) + SED(77)$
 $SEN2(106) = SED(6) + SED(5) + SED(18) + SED(17)$
 $SEND(106) = (SEND(106) + SEN2(106)) / 8.0$
 $SEND(107) = SED(67) + SED(66) + SED(79) + SED(78)$
 $SEN2(107) = SED(7) + SED(6) + SED(19) + SED(18)$
 $SEND(107) = (SEND(107) + SEN2(107)) / 8.0$
 $SEND(108) = SED(68) + SED(67) + SED(80) + SED(79)$
 $SEN2(108) = SED(8) + SED(7) + SED(20) + SED(19)$
 $SEND(108) = (SEND(108) + SEN2(108)) / 8.0$
 $SEND(109) = SED(69) + SED(68) + SED(81) + SED(80)$
 $SEN2(109) = SED(9) + SED(8) + SED(21) + SED(20)$
 $SEND(109) = (SEND(109) + SEN2(109)) / 8.0$
 $SEND(110) = SED(70) + SED(69) + SED(82) + SED(81)$
 $SEN2(110) = SED(10) + SED(9) + SED(22) + SED(21)$
 $SEND(110) = (SEND(110) + SEN2(110)) / 8.0$
 $SEND(111) = SED(71) + SED(70) + SED(83) + SED(82)$
 $SEN2(111) = SED(11) + SED(10) + SED(23) + SED(22)$
 $SEND(111) = (SEND(111) + SEN2(111)) / 8.0$

```

SEND( 112)=SED( 72)+SED( 71)+SED( 84)+SED( 83)
SEN2( 112)=SED( 12)+SED( 11)+SED( 24)+SED( 23 )
SEND( 112)= (SEND( 112)+SEN2( 112) )/8.0
SEND( 202)=SED( 122)+SED( 121)+SED( 134)+SED( 133 )
SEN2( 202)=SED( 62)+SED( 61)+SED( 74)+SED( 73 )
SEND( 202)= (SEND( 202)+SEN2( 202) )/8.0
SEND( 203)=SED( 123)+SED( 122)+SED( 135)+SED( 134)
SEN2( 203)=SED( 63)+SED( 62)+SED( 75)+SED( 74 )
SEND( 203)= (SEND( 203)+SEN2( 203) )/8.0
SEND( 204)=SED( 124)+SED( 123)+SED( 136)+SED( 135 )
SEN2( 204)=SED( 64)+SED( 63)+SED( 76)+SED( 75 )
SEND( 204)= (SEND( 204)+SEN2( 204) )/8.0
SEND( 205)=SED( 125)+SED( 124)+SED( 137)+SED( 136 )
SEN2( 205)=SED( 65)+SED( 64)+SED( 77)+SED( 76 )
SEND( 205)= (SEND( 205)+SEN2( 205) )/8.0
SEND( 206)=SED( 126)+SED( 125)+SED( 138)+SED( 137 )
SEN2( 206)=SED( 66)+SED( 65)+SED( 78)+SED( 77 )

```

C REMODELLING NODES CIRCUMFERENCE

```

RCR=0.0
DO 150 J=1,3
DO 175 L=1,8
K=1+(L-1)*100+(J-1)*1000
M=11+K
DO 250 I=K,M
READ(17,*)JR,KR(I),HMTR(I)
write(*,*)"ok here after KR"

```

```
DEL R(I)=RCR*(SEND(I)-SENDO(I))
DEL F(I)=(SEND(I)-HSED)
DLSEND(I)=(SEND(I)-SENDO(I))
FAC(I)=DLSEND(I)/DEL F(I)
IF(MD.GT.1) GOTO 522
GOTO 622
522 CONTINUE
IF(FAC(I).LT.(0.0)) GOTO 622
IF(ABS(FAC(I)).LT.(0.1)) GOTO 622
KR(I)= -KR(I)
HMTR(I)=HMTR(I)+1
622 CONTINUE
DEL R(I)=DEL R(I)*KR(I)
WRITE(18,71)I,KR(I),HMTR(I)
71 FORMAT(I6,3X,I4,3X,I4)
250 CONTINUE
175 CONTINUE
150 CONTINUE
C REMODELLING NODES END PLATES
RCZ=1500
DO 300 J=1,3
DO 375 L=1,5
K=1+(L-1)*20+(J-1)*1000
M=11+K
DO 450 I=K,M
READ(19,*)JZ,KZ(I),HMTZ(I)
```

```
write(*,*)"ok here after kzs"  
DELZ(I)=RCZ*(SEND(I)-SENDO(I))  
DELF(I)=(SEND(I)-HSED)  
DLSEND(I)=(SEND(I)-SENDO(I))  
FAC(I)=DLSEND(I)/DELF(I)  
IF(MD.GT.1) GOTO 532  
GOTO 632  
532 CONTINUE  
IF(FAC(I).LT.(0.0)) GOTO 632  
IF(ABS(FAC(I)).lt.(0.1)) GOTO 632  
KZ(I)= -KZ(I)  
HMTZ(I)=HMTZ(I)+1  
632 CONTINUE  
DELZ(I)=DELZ(I)*KZ(I)  
IF(L.EQ.5) GOTO 697  
WRITE(20,71)I,KZ(I),HMTZ(I)  
MON1=0  
GOTO 450  
697 MON1=MON1+1  
IF(MON1.EQ.1)GOTO 696  
DELZ(I)=DELZ1  
WRITE(20,71)I,KZ(I),HMTZ(I)  
GOTO 450  
696 DELZ1=DELZ(I)  
WRITE(20,71)I,KZ(I),HMTZ(I)  
450 CONTINUE
```

```
375 CONTINUE
300 CONTINUE
    DO 301 J=1,3
    DO 376 L=1,5
    K=1+(L-1)*20+(J-1)*1000+700
    M=11+K
    DO 451 I=K,M
    READ(19,*)JZ,KZ(I),HMTZ(I)
    write(*,*)"ok here after kzs"
    DELZ(I)=RCZ*(SEND(I)-SEND0(I))
    DELF(I)=(SEND(I)-HSED)
    DLSEND(I)=(SEND(I)-SEND0(I))
    FAC(I)=DLSEND(I)/DELF(I)
    IF(MD.GT.1) GOTO 533
    GOTO 633
533 CONTINUE
    IF(FAC(I).LT.(0.0)) GOTO 633
    IF(ABS(FAC(I)).lt.(0.1)) GOTO 633
    KZ(I)= -KZ(I)
    HMTZ(I)=HMTZ(I)+1
    633 CONTINUE
    DELZ(I)=DELZ(I)*KZ(I)
    IF(L.EQ.5) GOTO 699
    WRITE(20,71)I,KZ(I),HMTZ(I)
    MON2=0
    GOTO 451
```

```
699  MON2=MON2+1
      IF(MON2.EQ.1)GOTO 698
      DELZ(I)=DELZ2
      WRITE(20,71)I,KZ(I),HMTZ(I)
      GOTO 451
698  DELZ2=DELZ(I)
      WRITE(20,71)I,KZ(I),HMTZ(I)
451  CONTINUE
376  CONTINUE
301  CONTINUE
C    EX REMODELLING OF ENDPLATES CENTRAL NODES
      Do 600 J=1, 3,1
      DO 650 K=1, 2,1
      I=99+(K-1)*700+(J-1)*1000
      READ(21,*)JC,KZ(I),HMTZ(I)
      write(*,*)"ok here after kc"
      DELZ(I)=RCZ*(SEND(I)-SENDO(I))
      DELF(I)=(SEND(I)-HSED)
      DLSEND(I)=(SEND(I)-SENDO(I))
      FAC(I)=DLSEND(I)/DELF(I)
      IF(MD.GT.1) GOTO 542
      GOTO 642
542  CONTINUE
      IF(FAC(I).LT.(0.0)) GOTO 642
      KZ(I)= -KZ(I)
      HMTZ(I)=HMTZ(I)+1
```

```

642 CONTINUE
      DELZ(I)=DELZ(I)*KZ(I)
      WRITE(22,71)I,KZ(I),HMTZ(I)
650 CONTINUE
600 CONTINUE
      DO 800 I=1,1586
        write(*,*)"ok here in writing send"
        j=N(I)
        Write(16,46)j," ",SEND(J)
46  FORMAT(I5,A1,5X,F14.10)
800 CONTINUE
      ZN( 2687) =DELZ( 2787)+ Z( 2687)
      ZN( 2788) =DELZ( 2788)+ Z( 2788)
      ZN( 2688) =DELZ( 2788)+ Z( 2688)
      ZN( 2789) =DELZ( 2789)+ Z( 2789)
      ZN( 2689) =DELZ( 2789)+ Z( 2689)
      ZN( 2790) =DELZ( 2790)+ Z( 2790)
      ZN( 2690) =DELZ( 2790)+ Z( 2690)
      ZN( 2791) =DELZ( 2791)+ Z( 2791)
      ZN( 2691) =DELZ( 2791)+ Z( 2691)
      ZN( 2792) =DELZ( 2792)+ Z( 2792)
      ZN( 2692) =DELZ( 2792)+ Z( 2692)
        write(*,*)"OK after Zn"
      DO 900 I=1,1586
        J=N(I)
        WRITE(8,45)J," ",RN(J)," ",T(J)," ",ZN(J)

```

```
45  Format(I5,A1,3X,F12.4,A1,3X,F10.4,A1,3X,F12.4)
    write(*,*)"ok after new nodes"
900  CONTINUE
    DO 901 j=1,3
        K=1+(J-1)*500
        M=486+(J-1)*500
        DO 902 I=K,M
            TSE=TSE+SED(I)
            write(24,*)I, " ",SED(I), " ",TSE
902  CONTINUE
901  CONTINUE
    write(24,*)HSED,DR
    STOP
    END
```

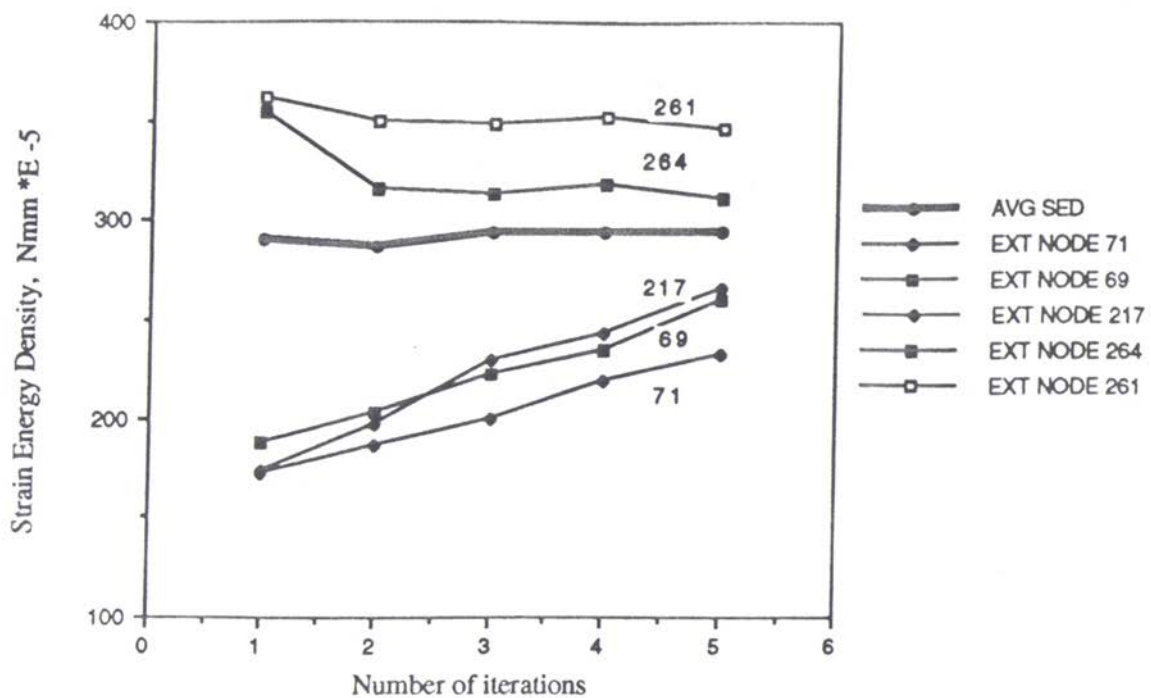


Figure A-1. The local changes in SED at surface nodes

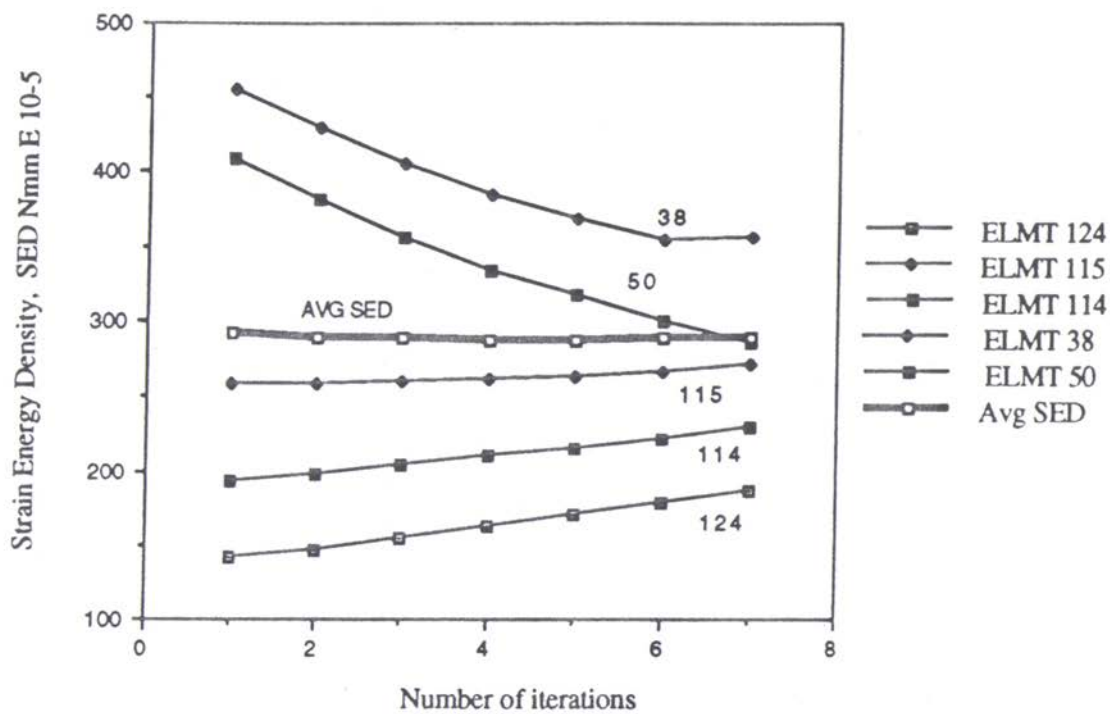


Figure A-2. The local changes in SED of cancellous elements

REFERENCES

1. Anderson, J.E., "Grants atlas of Anatomy", eighth edition, Williams & Wilkins, 1983.
2. Blunn, G. W., Wait, M.E., "Remodelling of bone around intramedullary stems in growing patients", *Journal of Orthopaedic Research*, 809-819, 1991.
3. Brown T.D., Pedersen, D.R., Gray, M.L., Brand, R.A., Rubin, C.T., "Toward an identification of mechanical parameters initiating periosteal remodelling: A combined experimental and analytic approach", *Journal of Biomechanics*, Vol. 23., No. 9, 893-905, 1990.
4. Carter, D.R., Orr, T.E., Fyhrie, D.P., "Relationships between loading history and femoral cancellous bone architecture", *Journal of Biomechanics* Vol. 22., No. 3, 231-244, 1989.
5. Carter, D.R., Whalen, R.T., "Trabecular bone density and loading history: Regulation of connective tissue biology by mechanical energy", *Journal of Biomechanics*, Vol. 20, 785-794, 1987.
6. Cheal, E.J., Snyder, B.D., Nunamaker, D.M., Hayes, W.C., "Trabecular bone remodelling around smooth and porous implants in an equine patellar model", *Journal of Biomechanics*, Vol. 20. No. 11/12, 1121-1134, 1987.
7. Cowin, S.C., Hegedus, D.H., "Bone remodelling I: theory of adaptive elasticity", *Journal of Elasticity*, Vol. 6, No. 3, 313-326, 1976.
8. Cowin, S.C., Firoozbakhsh., "Bone remodelling of diaphysial surfaces under constant load: Theoretical predictions", *Journal of Biomechanics*, Vol.7, 471-484, 1981.
9. Cowin, S.C., Firoozbakhsh, K., "An analytical model of Pauwel's functional adaptation mechanics in bone", *Journal of Biomechanical engineering*, Vol. 103, 246-252, 1981.
10. Cowin, S.C., Hart, R.T., Balsler, J.R., Kohn, D.H., "Functional adaptation in long bones: Establishing in vivo values for surface remodelling rate coefficients", *Journal of Biomechanics*, 665-684, 1985.

11. Fyhrie, D.P., Carter, D.R., "A unifying principle relating stress to trabecular bone morphology", *Journal of Orthopaedic Research*, Vol. 4., 304-317, 1986.
12. Goel, V.K., Kim, Y.E., Lim.T.H., Weinstein.J.N., "An analytical investigation of the mechanics of spinal instrumentation", *Spine* 13, 1003-1011, 1988.
13. Hart, R.T., Davy, D.T., Heiple., K.G., " A computational method for solution of adaptive elasticity problems", *Advances in Bio engineering*, American Society of Mechanical Engineers, 123-126., 1982.
14. Hart, R.T., Davy, D.T., Heiple, K.G., "A computational method for stress analysis of adaptive elastic materials with a view toward applications", *Journal of Biomechanical Engineering*, 106, 342-350, 1984.
15. Huiskes, R., Weinans, H., Grootenboer, H.J., Dalstra, M., Fudala, B., and Sloof, T.J., "Adaptive bone remodelling theory applied to prosthetic-design analysis ", *Journal of Biomechanics*, Vol.20.,No. 11/12, 1135-1150, 1987.
16. Huiskes, R. Weinans, H., Rietbegen, B.V., Turner, T.M., "Simulation and validation of bone remodelling around unbonded, Press-fitted hip stems", 38th Annual meeting, Orthopaedic Research Society, 304-305, 1992.
17. Jaworski., Z.G.F., Liskova-Kiar, M. and Uthoff, H.K., "Effect of long term immobilization on the pattern of bone remodelling", *Journal of bone joint surgery*, 62-B, 104-110, 1980.
18. Keller, T.S., Hansson, T.H., Abram, A.C., Spengler, D.M., and Punjabi, M.M., "Regional variations in the compressive properties of lumbar vertebral trabeculae: effects of disc degeneration", *Spine*, 14, 1012, 1989.
19. Lanyon, L.E., Goodship, A.E., and McFie, J.H., " Functional adaptation of bone to increased stress", *Journal of Biomechanics*, 15, 141-154, 1982.
20. Lee, C.K., Vuono-Hawkins, M., Langrana, N.A., Zimmerman, M.C., Parsons, J.R., " Vertebral Osteophytes: An experimental animal model", *ISSLS*, 36-37, 1992.
21. Lavaste, F., Skalli, W., Robin, S., Roy-Camille, R., Mazel, C., " Three dimensional geometrical and mechanical modelling of the lumbar spine", *Journal of Biomechanics*, Vol. 25, No. 10, 1153-1164, 1992.
22. Levenston, M.E., Beaupre, G.S., D.R.Carter and Schurman, D.J., " Skeletogenesis and bone remodelling theory applied to the peri-acetabular Region", 38th Annual meeteing, Orthopaedic Research Society, 536, 1992.
23. Mattheck, C., Burkhardt, S., "A new method of structural shape optimization based on biological growth", *International Journal of Fatigue*, Vol.12, No. 3, 185-190, 1990.

24. Mattheck, C., Bethge, K., Erb, D., Blomer, W., "Successful shape optimization of a pedicular screw", *Medical & Biological Engineering & computing*, 446-448, 1992.
25. McNamara, B.P., Prendergast, P.J., Taylor, D., "Prediction of bone adaptation in the ulnar-osteotomized sheep's forelimb using an anatomical finite element model", *Journal of Biomechanics*, 1992.
26. Mizrahi, J., Silva, M.J., Hayes, W.C., "Finite element stress analysis of simulated metastatic lesions in the lumbar vertebral body", *Journal of Biomedical Engineering*, Vol. 14, 467-474, 1992.
27. Woo, S.L.Y., Kuci, S.C., Dillon, W.A., Amiet, White, F.L., Akeson, W.H., "The effect of Prolonged physical training on the properties of bone", *Journal of bone joint surgery*, 63A, 780-787, 1981.
28. Wolff, J. "Ueber die Bedeutung der Architektur der spongiosen Substanz", *Zent bl. med. Wiss.* VI, 223-234., 1869.